PROCESSING AND MANUFACTURE OF SOYBEAN AND WHEAT STRAW MEDIUM DENSITY FIBERBOARD UTILIZING EPOXIDIZED SUCROSE SOYATE RESIN

A Thesis
Submitted to the Graduate Faculty
of the
North Dakota State University
of Agriculture and Applied Science

By

Evan Donald Sitz

In Partial Fulfillment of the Requirements
for the Degree of
MASTER OF SCIENCE

Major Department:
Mechanical Engineering

April 2016

Fargo, North Dakota

North Dakota State University
Graduate School

Title

Processing and Manufacture of Soybean and Wheat Straw Medium Density Fiberboard Utilizing Epoxidized Sucrose Soyate Resin

By

Evan Donald Sitz

The Supervisory Committee certifies that this ***disquisition*** complies with North Dakota State University's regulations and meets the accepted standards for the degree of

MASTER OF SCIENCE

SUPERVISORY COMMITTEE:

Dr. Dilpreet Bajwa
Chair

Dr. Sreekala Bajwa

Dr. Dennis Wiesenborn

Dr. Long Jiang

Approved:

4/15/2016
Date

Dr. Alan Kallmeyer
Department Chair

ABSTRACT

Soybean straw and wheat straw show promise as annually renewable alternative to traditional wood sources for fiberboard. Epoxidized sucrose soyate has shown high performance as a thermosetting resin and could be adapted for use in fiberboard. This research evaluated the physical and mechanical properties of medium density fiberboard using wheat and soy straw while using various binders, including epoxidized sucrose soyate. Additionally, several experiments were conducted to evaluate optimal process conditions for hammer milling of soy and wheat straw to reduce fines and maximize viable fiber content for fiberboard manufacture. Test results indicate that soy straw boards were not able to meet the properties of wheat straw boards on all levels. Epoxidized sucrose soyate was not effective as the sole binder but had similar properties when blended with MDI resin. Optimal conditions were identified to reduce fines and maximize the viable fiber fraction produced for both wheat and soy straw.

ACKNOWLEDGEMENTS

I would like to thank the North Dakota Soybean Council and the North Dakota Industrial Commission for providing funding for this thesis project; without your investment, this research would not be possible. I would also like to thank Masonite Primeboard, Inc. for providing testing materials as well as all of the processed and unprocessed straw fibers used in this project. I would like to especially thank my adviser Dr. Dilpreet Bajwa for providing me an opportunity to work within his research group for the last four years and for the guidance he has shown me along the way. Thank you to my committee members as well, Dr. Sreekala Bajwa, Dr. Dennis Wiesenborn, and Dr. Long Jiang, for their time and direction on this project.

I would like to acknowledge several other members of the North Dakota State University team for their assistance in this project: Dr. Dean Webster, Adlina Paramarta, David Sundquist, Ryan Dumont, Tyler Loll, Glenn Peterson, Darrin Haagenson, and Ewumbua Monono. Thank you for assistance in completing this project and helping me to learn a variety of testing techniques and research practices which have formed the basis for my research career.

TABLE OF CONTENTS

LIST OF TABLES

LIST OF FIGURES

LIST OF APPENDIX TABLES

1. INTRODUCTION

This chapter introduces background information on lignocellulosic board products, including definitions, applications, and manufacture. This chapter will also cover issues with currently used resin binder systems utilized in lignocellulosic boards as well as issues with processing various types of lignocellulosic fibers used in board products.

1.1. Fiberboard and Particleboard Definitions and Demand

Conventional fiberboard is a composite board that is composed of wood particles that have been pressed together under high temperature and pressure with a resin binder to form a homogeneous board [1]. The fibers themselves are defined as slender, threadlike elements of cellulosic materials [1]. Particleboard is a generic term for a composite panel composed of cellulosic particles and some sort of binder, where the particles are discrete pieces as distinguished from fibers [1]. The differentiation between a fiber and a particle then is defined more by a slenderness ratio or aspect ratio of the fiber length to its diameter, with fibers having a larger ratio [1]. Fiberboard and particleboard have traditionally been made with wood particles and refuse from lumber processing, however considerable research has also been devoted to producing fiberboard from alternative lignocellulosic materials, with successful commercial operations utilizing crop residuals to make boards. Regardless of the material used to make the boards, fiberboard and particleboard have gained popularity in construction and consumer applications due to being economical as well as providing desirable properties such as dimensional stability and isotropic strength. The demand for wood panel products and fiberboard in general can be seen through Figure 1 which shows the current usage and projected demand for wood-based panel products.

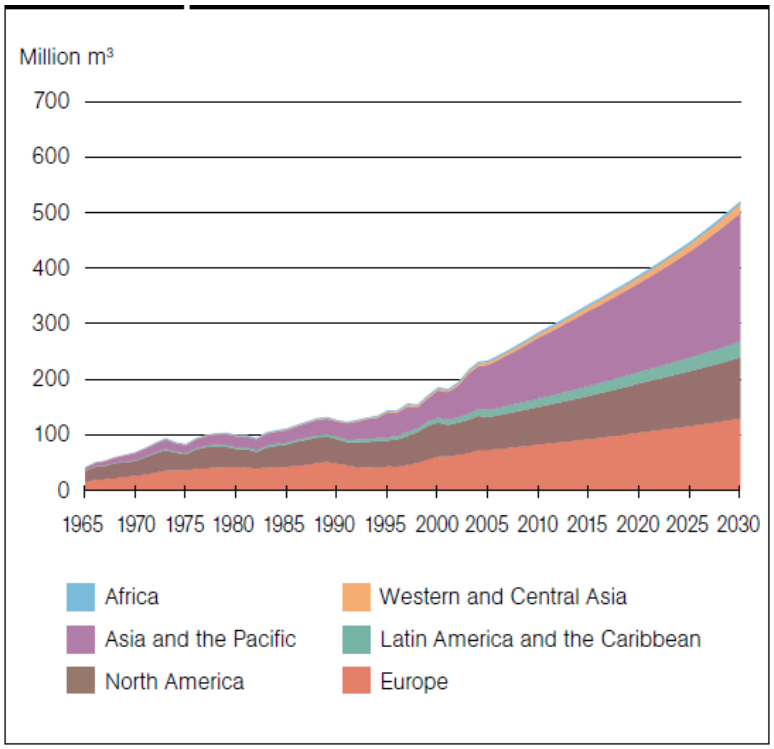

Figure 1. Demand for Wood-Based Panel Production [2]

The figure shows the demand for products such as plywood, veneer sheets, particleboard, and fiberboard is projected to increase significantly, with projected growth in Asian markets supplying the most demand [2].

1.2. Board Manufacture and Classifications

Several classifications for cellulosic boards exist, but of interest for this research is medium density fiberboard and particleboard. Medium density fiberboard can be defined as any composite panel product that is composed chiefly of cellulosic fibers and a resin bonding system that cures under heat and pressure, just like other fiberboards, but has a density between 500 kg/m^3 and 1000 kg/m^3 [3]. Medium density particleboard can be defined as any composite panel

composed of cellulosic particles and some sort of binder, where the particles are discrete pieces as distinguished from fibers, but with a density between 640 kg/m^3 and 800 kg/m^3 [4].

There are several processing methods used to produce fiberboard, with the most common methods being designated as a wet process or dry process. The wet process is defined by using steam to pulp fibers, refining the fibers through separation by fiber size, then pressing and drying the fibers into boards [5]. Additional resin is typically not needed for this process, as the steam and pulping process allows the lignin present in the fibers to repolymerize and create a bond to hold the board together [5]. The dry process of producing fiberboard involves processing natural fibers to an optimal fiber length through milling, refining by fiber size, adding additional resin and other additives, then forming a mat of fibers and pressing the mat into a board under high heat and pressure [5].

1.3. Resin Binder

The main binding component needed in dry process fiberboard production is a suitable resin binder that maintains the board's integrity and improves moisture resistance [5]. The fiberboard industry currently uses many petroleum-based resins due to superior water resistance properties and the low cost of resin. The most commonly used resins used in the modern fiberboard industry in dry process fiberboard production include phenol formaldehyde (PF), urea formaldehyde (UF), and methylene diphenyl diisocyanate (MDI) [6]. These resins provide excellent adhesion properties and improve the moisture resistance of the boards produced as well as being economical to use [7]. The main disadvantage with these resins is the health hazards that they pose to both production of the fiberboard industry and end use consumers. Formaldehyde is a known carcinogen and fiberboard made with UF and PF produce volatile

emissions after production, while MDI has been designated as a potential carcinogen and irritant that can potentially cause asthma and dermatitis [6]. This health hazard, along with the California Air and Resources Board (CARB) phase 2 [8] changes to composite board standards motivates research into alternative resins. To comply with this standard several manufacturers have started to convert the binder system to purely MDI resin, or have started to use melamine urea formaldehyde (MUF) resin, which has shown to have similar properties to UF resin with lower formaldehyde emissions [9].

1.4. Fibers

Two factors that affect the quality of the processed fibers used in fiberboard applications; the fines content and the aspect ratio of the fibers used. Fines are a residual product of fiber milling that is simply fibers or particles that have been reduced to an 80 mesh size or smaller [10]. These particles reduce the quality of the fiberboard produced and represent a loss in usable fiber and milling efficiency [11]. Although it is desirable to reduce the total amount of fines generated through the milling process, fines can be refined from the fiber stream and be used to make products such as fuel pellets and animal bedding [12]. This does provide a secondary use for this waste stream, but it is limited and the benefits of reducing fines produced to make a more consistent fiberboard outweigh the revenue of producing secondary products from fines. Moreover, generated fines appear to cause more wear of tooling used to mill the fibers [13]. Figure 2 shows the general size and appearance of fines sifted from milling wheat straw fibers.

Figure 2. Wheat Straw Fines Generated from Milling

The general size and aspect ratio of the fibers also affects the fiber strength and the ability of the fibers to bond with the resin binder [13]. Another property that affects the quality of the fibers used to make the fiberboard is the constituent makeup of the fibers. Plant matter is composed of three main structures that provide strength and integrity of the fibers: cellulose, hemicellulose, and lignin. Cellulose is a semi-crystalline polysaccharide composed of glucose chains and provides strength to the fibers. Hemicellulose is a polysaccharide with considerably shorter sugar chains. Lignin is a cross-linked phenolic polymer and holds the cellulose and hemicellulose molecules of the fiber together while protecting them from microbial attacks. The fraction of cellulose, hemicellulose, and lignin varies significantly between different types of wood species as well as between different agricultural residuals. Table 1 shows the content of cellulose, hemicellulose, lignin, and ash content of wheat straw, soy straw, and common wood sources.

Table 1. Cellulose, Hemicellulose, Lignin, and Ash Composition of Silver Birch, Spruce, Wheat Straw and Soy Straw

	Silver Birch [14]	Spruce [14]	Wheat Straw [15]	Soy Straw [16]
Cellulose	41.0%	39.5%	33-38%	44.0%
Hemicellulose	32.4%	30.6%	26-32%	29.3%
Lignin	22.0%	27.7%	17-19%	24.1%
Ash	4.6%	2.2%	6-8%	2.6%

2. LITERATURE REVIEW

Several sources of lignocellulosic materials have been identified and implemented into fiberboard production as an alternative to wood fibers. Research has been conducted testing the viability of corn, rice, wheat, bagasse, deoiled sunflower cake, and soybean fibers for use in fiberboard [13] [17] [18] [19] [20]. Wheat fibers have been used by several manufacturers to produce fiberboard products, including the Masonite Corporation's Wahpeton, North Dakota plant where door cores are manufactured. This model works due to the abundance of wheat grown in the North Dakota and Minnesota area [21]. Though wheat has been utilized as a fiber source for several years, another abundant fiber source, soybean, has been identified and is currently being used to produce fiberboard on a commercial scale by Agristrand Mankato [12]. The production of fiberboard using soybean straw by Agristrand shows the commercial viability of fiberboard produced using this fiber source. Straw is used in other industries, primarily agricultural, where both wheat straw and soybean straw are utilized as feedstock for livestock, with soybean straw having higher protein content than wheat straw making it a useful feedstock for livestock [22]. However, it should only acts as a supplement to grain and hay sources and only when proper additives have been introduced [22]. Moreover, fibers that would be viable for use in fiberboard are often chopped and left in the field rather than being utilized for feed or other purposes [12]. This makes soybean straw viable for use in fiberboard as its use would not be deducting from other markets but would instead be an additional income source for agricultural operations from an underutilized resource.

2.1. Materials and Processing of Boards

The main motivation behind current research in fiberboard production is finding alternative sources of lignocellulosic materials to replace slow growth wood sources and to optimize current manufacturing conditions to produce boards with optimal physical and mechanical properties. Literature review was conducted to evaluate current research on the effects of board press processing conditions, resin binders used, and processing of fibers used in board pressing.

2.1.1. Board Press Process Conditions

Several processing factors during board pressing affect the final properties of a fiberboard, including the press temperature [19] [23], cycle time [19] [24], fiber moisture content [25], and the fiber distribution, particularly the fines content [11]. For all settings selected, the main goal for processing of boards is to minimize the cycle time to produce boards as quickly and economically as possible. In order to minimize cycle time, the press temperature must be maximized to induce faster curing rates of the resin binder. This poses problems for the degree of cure for the resin, but more importantly, it creates the potential for the hemicellulose of the fibers to become degraded [26] and significantly reduce both bonding of the resin and fiber [25] and overall strength bearing properties of the fibers [27]. In light of this degradation effect, optimal board pressing temperatures should not exceed 200 °C for the dry process pressing.

2.1.2. Resin Binder System

Alternatives to traditionally used resin binders in wood panel products have been investigated extensively with several novel binder systems being found. Most of these

alternatives are based on utilizing renewable sources for the binder. Some of the alternative resin choices that have been investigated include Soy protein [28], soybean oil based adhesives [29], and dried distiller's grains with solubles (DDGS) derived proteins [30].

Several resins have also been synthesized by epoxidizing vegetable oils derived from linseed, safflower, and soybean which have the general designation of an epoxidized sucrose ester of fatty acids (ESEFAs) [31] [32] . One resin produced that is of interest is epoxidized sucrose soyate (ESS), which is an ESEFA derived from soybean oil and has shown promise as a renewable resin source. ESS has epoxide groups, which are reactive intermediates that can produce functional groups and promote bonding and crosslinking between other appropriate functional groups [32]. The difference between ESS resin and more traditional epoxidized vegetable oils (EVO) is the level of functionality of the two resins, which has also shown to directly affect the mechanical and physical properties of the resin [33]. A fully substituted molecule of ESS resin is composed of a sucrose molecule that has substituted the glycerol molecule in a vegetable oil molecule and then has its eight functional hydroxyl groups substituted with fatty acids from vegetable oil [33]. The full substitution of all eight of the hydroxyl groups which had previously been unachievable allows for a high functionality and subsequently a high degree of crosslinking and mechanical performance when the resin is properly cured [31] [32] [33]. Figure 3 shows an ESS molecule that has full substitution of the hydroxyl groups of the core sucrose molecule.

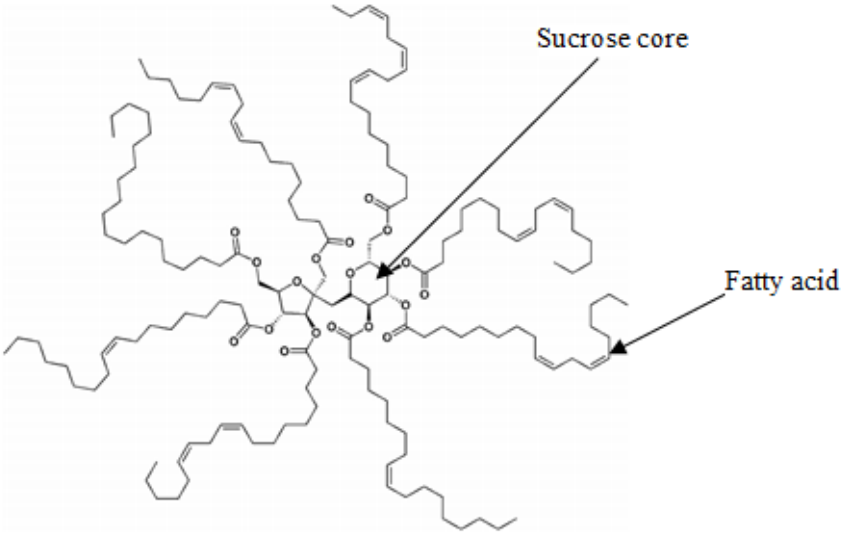

Figure 3. Epoxidized Sucrose Soyate Molecule with All Hydroxyl Groups of the Sucrose Molecule Substituted with a Fatty Acid [32]

It is noteworthy that epoxide groups can react with the functional isocyanate group present in MDI to create an oxazolidone ring [34] [35]; this reaction allows for the mixture of both ESS and MDI resins to potentially create a high-performance resin that utilizes a readily available renewable resource.

The reactions between isocyanate and epoxide groups have two competitive reactions that form two potential products; oxazolidone rings and isocyanurate. Oxazolidone is a heterocyclic ring with that produces improvements in both thermal stability and mechanical properties [35]. A model of the reaction that produces oxazolidone rings can be seen in Figure 4.

Figure 4. Reaction between Isocyanate (R'NCO) and Epoxide Ring (CH_2CHR'') to Form an Oxazolidone Ring [34]

Isocyanurate is a compound that is created when three functional isocyanate groups react with each other Figure 5. The interlaced network that forms from the formation of both oxazolidone and isocyanurate can be seen in Figure 6.

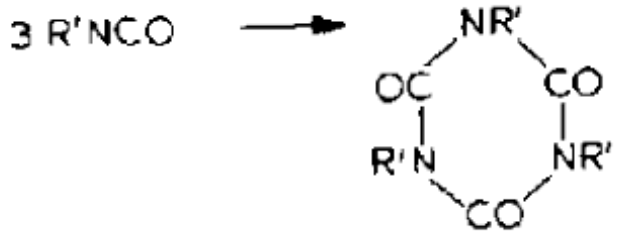

Figure 5. Trimerisation between Three Isocyanate (R'NCO) Molecules to Form Isocyanurate [34]

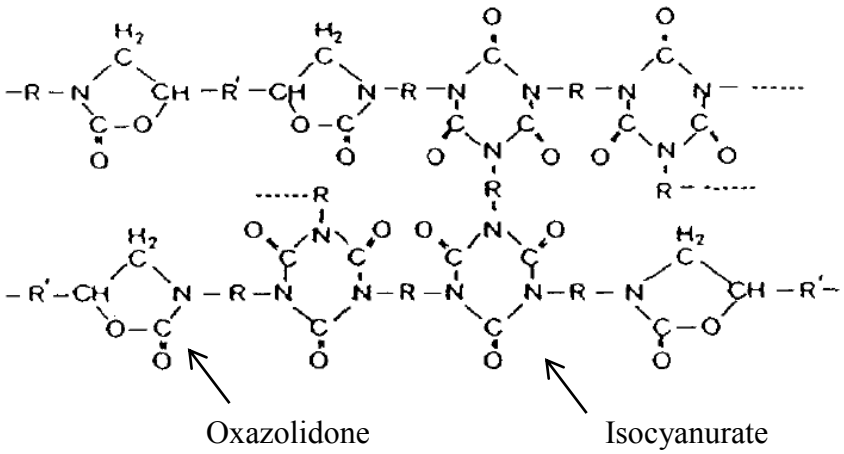

Figure 6. Network of Copolymerized Oxazolidone and Isocyanurate Rings [35]

A theoretical ideal ratio of ESS resin to MDI resin is one in which the ratio of isocyanate to epoxide molecules is 1:1, such that an oxazolidone ring can be formed for each isocyanate and epoxide molecule. With MDI having an equivalent weight of isocyanate of 125 g/mol and ESS having an equivalent weight of epoxide groups of ~251 g/mol [31], the ratio by weight for an ideal formulation of ESS and MDI resin would be approximately 1:2 MDI-ESS. This means for every gram of MDI there should be two grams of ESS used to allow a 1:1 ratio of isocyanate to epoxide molecules. It should be noted that this ratio does not account for trimerisation of isocyanate into isocyanurate or formation of urea groups with H_2O and MDI reactions. In order to allow for these more established reactions to occur while still having enough isocyanate groups to react with epoxides in the ESS, a 2:1 ratio by weight for MDI-ESS mixtures will be implemented and evaluated based on observed mechanical properties.

There is also potential to use ESS resin as the sole binder, as it has been shown to increase its crosslinking and bonding strength considerably when an epoxy-anhydride curing system has been implemented [31] [32] and through lap shear testing performed in previous experimentation. The anhydride system implemented utilizes 4-Methyl-1,2-cyclohexaneedicarboxylic anhydride (MHHPA) which acts a cycloaliphatic anhydride cross-linker, and 1,8-diazabicyclo[5.4.0]undec-7-end (DBU) which acts as a tertiary amine catalyst [31]. This epoxy-anhydride system takes advantage of the high degree of substitution present within the ESS and allows for significant crosslinking to occur [31]. Research has also been conducted to on the viability of producing ESS resin on an industrial scale, with improved scalability and efficiency being reported [36]. ESS is promising as a resin for panel production in that it has the potential to meet CARB standards while still providing excellent properties as an adhesive.

2.1.3. Processing of Wheat and Soy Straw Fibers

Fines generation is of considerable concern when processing fibers for hammer milling. Fines wear milling tooling and degrade the mechanical properties observed in the boards [13]. A higher resin fraction is also required to maintain panel properties as fines have a high surface area to volume ratio and also have poor strength properties due to low aspect ratios [13]. Fines specified as particles smaller than 80 mesh have been specifically identified as being a significant effect on mechanical property loss of agricultural-fiber based composites [37]. Screening is a necessary step to reducing fines content in the final boards and to exclude excessively large fibers [5], but processing conditions can be set to produce a more optimal fiber distribution during fiber milling.

Both wheat straw and soy straw have varying properties that affect how they are milled and what fiber distribution they produce. Wheat straw has high levels of ash content as well as high silica content that can cause tool wear and produce higher fines content [13]. Wheat straw also has a waxy cutin and epicuticular wax layer and a cuticle silica layer that acts as a protective layer from microbial attacks but can also prevent good bonding of the fibers and resin [13] [38]. Chemical treatment of fibers with NaOH can bring better resin wetting and bonding and improve mechanical properties of the boards made from them by removing the waxy outer layer of the fibers, but it adds an additional and somewhat costly processing step [39]. The main purpose of removing the outer layer is to make the hydroxyl groups in the fibers available for chemical reaction with the resins, which makes MDI resin an attractive choice when using wheat fibers. MDI can bond with straw particles without the cutin removed, but the cutin prevents urea formaldehyde or phenyl formaldehyde resins from bonding effectively [20]. MDI resin can bond with hydroxyl groups within the cellulose of the fibers as well as moisture within and on the

fibers to form carbon dioxide and amines. The amines will react with the remaining functional isocyanate molecules to form urea [40]. Soybean straw has similar issues to wheat straw in that it has a waxy cutin layer and has pithy composition in comparison to wood fibers [20]. In general, fibers that are ideal for fiberboard production should have a good aspect ratio, have a thick cell wall, and rich in cellulose; wood fibers are superior to both wheat and soy straw in those regards but can still be effectively utilized in fiberboard [20].

3. THESIS OBJECTIVES

There were three overarching goals for this project; evaluate the properties of fiberboard made with wheat and soybean fibers with various binders, evaluate ESS as a resin for use in fiberboards, and determine optimal milling conditions to reduce the production of fines and maximize the production of viable fibers for board production. In order to adequately evaluate these goals, boards were made using wheat and soy straw fibers using both epoxidized sucrose soyate and methylene diphenyl diisocyanate resin binders. The curing of epoxidized sucrose soyate and potential chemical reactions between epoxidized sucrose soyate and methylene diphenyl diisocyanate were also investigated. Hammer milling of both wheat and soy straw fibers were also conducted for various levels of fiber moisture content, milling speeds, and screen sizes in order to find optimal conditions to produce viable fibers for fiberboards. This thesis evaluated the previously stated goals with the following hypotheses:

H1: Medium density boards made from soy straw fibers have equivalent physical and mechanical properties compared to medium density boards made using wheat straw fibers

H2: Medium density boards can be made using epoxidized sucrose soyate resin system as the only binder and perform similarly to boards produced using only methylene diphenyl diisocyanate binder

H3: Epoxidized sucrose soyate can bond with methylene diphenyl diisocyanate and produce boards with equivalent properties to that of boards produced using only methylene diphenyl diisocyanate binder

H4: Wheat straw fibers content and viable fraction after hammer milling are affected by the fiber's moisture content, the screen's hole sizes, and hammer tip speeds

H5: Soybean fiber's fines content and viable fraction after hammer milling are affected by the fiber's moisture content, the screen's hole sizes, and hammer tip speeds

4. MATERIALS AND METHODS

This chapter details the materials used to create the fiberboard panels as well as the material used in the hammer mill processing study. Standard testing methodology and analytical methods used to characterize the properties of the resin, boards, and fiber distribution achieved through hammer milling are also detailed in this chapter.

4.1. Materials

Two primary biomass materials were utilized during this thesis study: soybean fiber and wheat fibers. Processed and unprocessed fibers were provided by the Primeboard Masonite Corporation (Wahpeton, ND). The unprocessed straw was received as harvested and delivered in bales. The fiber distribution as it was received of both the processed wheat and soybean fibers used to press the test boards are shown in Figure 7 and Figure 8, respectively.

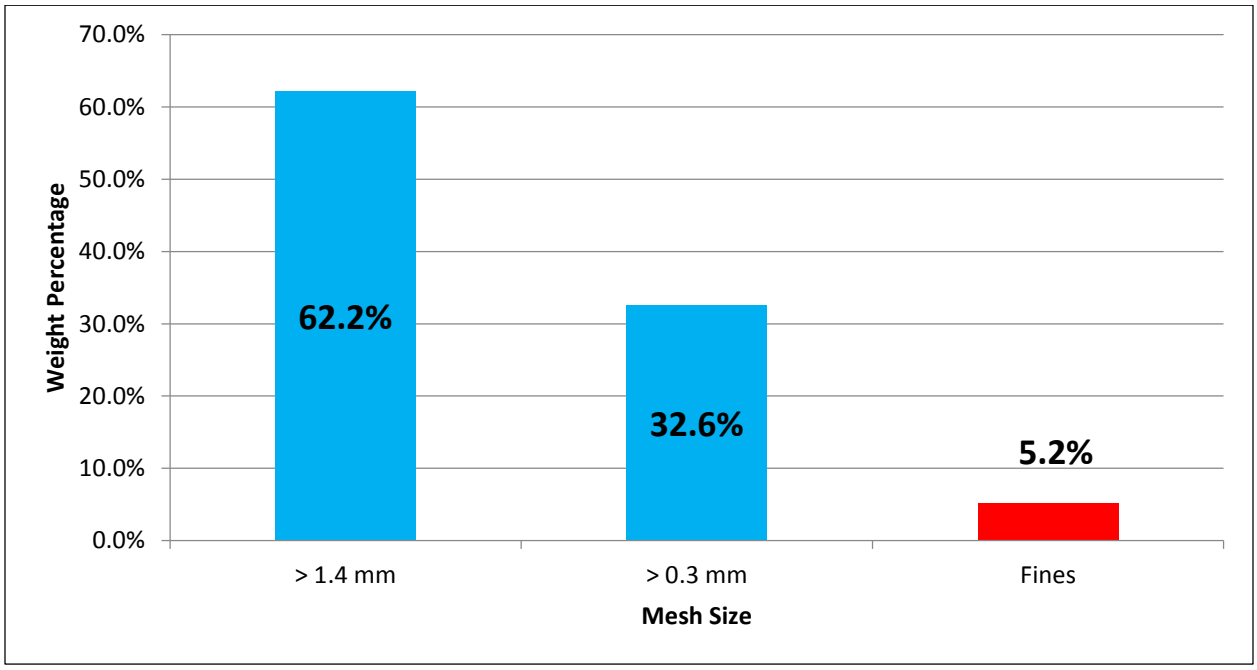

Figure 7. Provided Wheat Straw Fiber Distribution by Weight Percentage

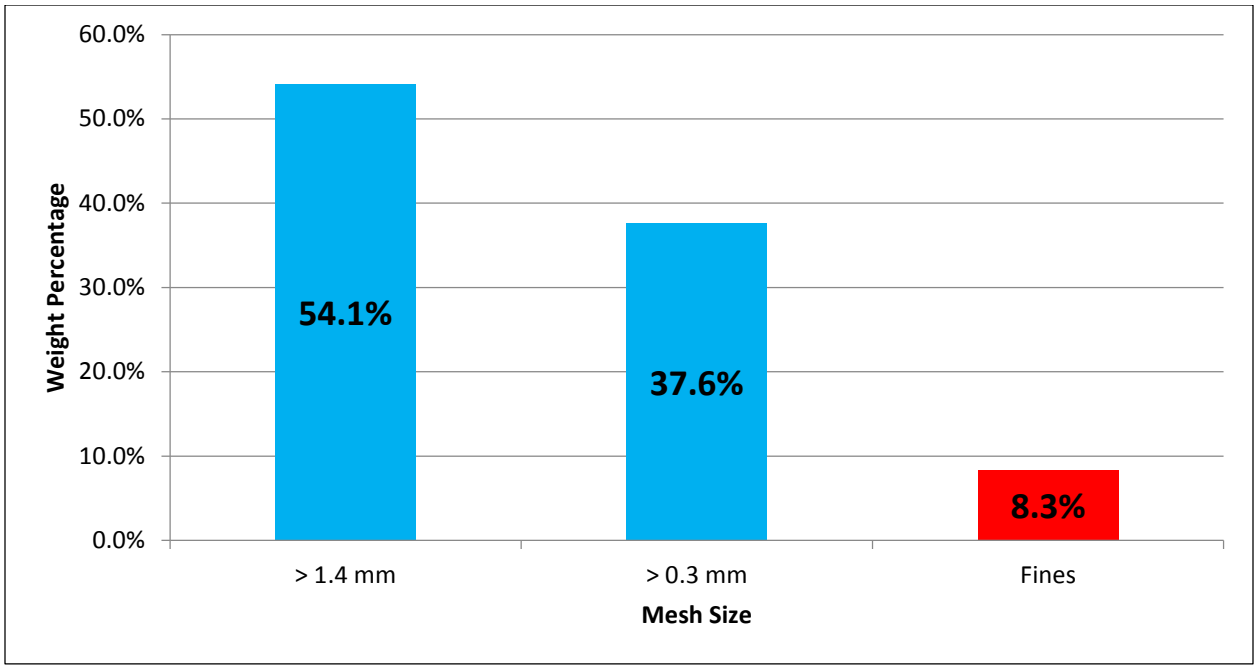

Figure 8. Provided Soy Straw Fiber Distribution by Weight Percentage

The included mesh sizes fall under the ISO sieve sizes scale. The equivalent Tyler Standard Mesh scale for 1.4 mm is 12 mesh and for 0.3 mm is 48 mesh, with the fines accounting for all of the fibers that passed through the 0.3 mm sieve.

The fibers were conditioned to have moisture content between 8-12% before pressing of the boards so as best to simulate the condition of the fiber as it is received at the Masonite location in Wahpeton. Two different resin types were used as binders to create the boards: a pure 4,4'-methylene diphenyl diisocyanate (MDI) resin that was provided by the Primeboard Masonite Corporation; and epoxidized sucrose soyate (ESS) which was provided through the Agricultural and Biosystems Engineering department at North Dakota State University by Monono Ewumbua and Dr. Dennis Wiesenborn . One of the resin curing systems to be tested requires an anhydride and catalyst to be used in conjunction with the ESS resin. The anhydride used was 4-Methyl-1,2-cyclohexaneedicarboxylic anhydride (MHHPA) which was graciously

provided by Dixie Chemical, Inc. (Pasadena, TX) and the catalyst used was 1,8-diazabicyclo[5.4.0]undec-7-end (DBU) which was purchased through Sigma-Aldrich (St. Louis, MO). It is notable that when a mixture of ESS-MHHPA-DBU is called out within this paper, it is referring to a mixture of the three components with a ratio of 67.5:31.0:1.5 by wt%, which has been identified as being an optimal formulation through research conducted at North Dakota State University [31] [32].

4.2. Resin Characterization

Several tests were conducted to characterize the performance and curing characteristics of the MDI resin, ESS resin, and the various interactions with the epoxy-anhydride and MDI-ESS mixtures. Lap shear testing was performed to initially evaluate the adhesive performance of the resin systems considered to be used as binders within the fiberboard. Thermogravimetric analysis and differential scanning calorimetry were used to determine viable press temperatures as well as to identify potential bonding effects from the ESS-MDI mixtures. Fourier transform infrared spectroscopy was used to identify possible changes in the chemical makeup of the MDI-ESS resin systems and to verify if isocyanate-epoxy reactions did indeed occur. Soxhlet extraction was used as a method to determine sol content and a general degree of stable curing within ESS-MDI mixtures.

4.2.1. Lap Shear Testing

Initial Lap Shear testing was performed in accordance with ASTM D2339-2011 – Standard Test Method for Strength Properties of Adhesives in Two-Ply Wood Construction in Shear by Tension Loading [41] as a preliminary evaluator of resin bonding strength and as a way

to evaluate the effects of mixing ESS and MDI resin. Lap shear samples were created by first cutting out samples of 25mm x 85 mm x 3 mm from panels of sliced veneer of yellow birch. Two strips are used to create a sample that can be tested by bonding a 25 mm x 25 mm portion of each strip with the adhesive whose shear strength is to be tested. The strips had approximately 1 gram of adhesive placed of the marked 25 mm x 25 mm portion, then were pressed together and held in place using a pressure clamp that was clamped to "hand tightness." The sample and the clamp were then placed into an oven for the sample to cure. Once the sample had been cured for the allotted time, it was removed and allowed to sit in open lab conditions (20±3˚C and 50±10 % relative humidity) for a minimum of 24 hours before further testing. Once ready to be tested, the samples could be tested by being clamped into testing grips and then pulled apart until adhesive failure of the bonded portion. Figure 9 shows the testing apparatus and a sample being tested.

Figure 9. Lap Shear Testing Apparatus and Loaded Sample

The testing rate was set such that the crosshead rate was 1 mm/min, as opposed to using a load control as suggested in the standard. The sample was tested until adhesive failure, where the maximum load was recorded and could be used to calculate the adhesive shear strength of the resin. The adhesive shear strength can be calculated by using the following equation

$$\tau = \frac{F}{ab} \qquad \text{(Equation 1)}$$

Where τ is the adhesive shear strength of the adhesive, F is the maximum load applied to the lap shear sample at failure, a is the width of the bonded area of the lap shear samples, and b is the length of the bonded area of the sample. Five different resin formulations were tested to evaluate the relative strength of each adhesive considered for use as a binder, with pure MDI, ESS-MHHPA-DBU, and mixtures of ESS-MDI at 25:75 wt%, 50:50 wt%, and 75:25 wt% being tested. Each formulation aside from the ESS-MHHPA-DBU was tested at cure temperatures of 140˚ C and 160˚ C with cure times at 20 minutes, 45 minutes, and 60 minutes to ensure high degree of cure. The ESS-MHHPA-DBU samples were cured at 165˚ C for 45 minutes and 150˚ C for 60 minutes to be more in line with results observed from differential scanning calorimetry performed by Pan, Sengupta, and Webster [31].

4.2.2. Thermogravimetric Analysis

Thermogravimetric analysis was used as a way to evaluate thermal degradation of the uncured resin to determine a maximum allowable curing temperature and as a way to evaluate if intermediary products were being formed through the mixture and subsequent curing of ESS-MDI mixtures at higher degradation temperatures. The analysis was performed using a TA

Instruments Q500 TGA (New Castle, DE). The temperature range tested was set from 25 ˚C to 1000 ˚C using a temperature ramp of 20 ˚C/min. Nitrogen was used as the flow gas to prevent oxidation of the samples, with the flow rate set at 20 mL/min. Samples tested included cured MDI resin, ESS resin, and ESS-MHHPA-DBU resin as well as ESS-MDI resin mixtures with ratios of 75:25 wt%, 50:50 wt%, and 25:75 wt%.

4.2.3. Differential Scanning Calorimetry

Differential Scanning Calorimetry was performed using a TA Instruments Q20 Differential Scanning Calorimeter (New Castle, DE). A heat-cool-heat cycle was implemented to determine the degree of curing. Several temperature ranges were utilized; one of the tests performed for each formulation was from 25 ˚C to 300 ˚C at 10 ˚C/min to determine when a curing reaction occurred within the resin system. A second range was tested from 25 ˚C to 190 ˚C at 10 ˚C/min with a 5 minute hold at 190 ˚C to determine the degree of curing observed for the expected press temperatures. Both test ranges included the heat-coo-heat cycle. The testing chamber was purged with nitrogen gas at a rate of 50 mL/min. Two different resin formulations were tested, a pure MDI resin sample and a mixture of ESS and MDI at an equivalent ratio of 1:1 or 1:2 by wt%.

4.2.4. Fourier Transform Infrared Spectroscopy

Fourier Transform Infrared Spectroscopy or more specifically Attenuated Total Reflection Fourier Transform Infrared Spectroscopy (ATR-FTIR) was performed on samples using a Thermo Scientific Nicolet 6700 FTIR spectrometer with a germanium crystal as the attenuating crystal in a plain air atmosphere. A total of 32 scans with a resolution of 4 cm^{-1} was

used to generate spectra. Samples of uncured MDI and ESS were created and tested using the FTIR. Samples of ESS-MDI were also cured to determine any interaction effects, with samples of ESS-MDI being made with ratios of 75:25 wt%, 50:50 wt%, and 25:75 wt%. The general purpose of FTIR analysis is to identify and changes in the functionality or chemical composition within a tested material.

4.2.5. Soxhlet Extraction

Soxhlet extraction is a method of determining the general degree of stable curing and or crosslinking within a cured resin. The method works primarily by using a heated solvent to dissolve the portion of the cured resin that has minimal bonding to other molecules within the sample. The extraction was carried out by using hexane (C_6H_{14}) as the solvent. The hexane was heated to 75 ºC, with the total extraction time totaling 24 hours. Once completed, the samples were removed and then oven dried again. There are two components that are of interest in a Soxhlet extraction: the sol and gel portions. The sol portion refers to the soluble portion of the samples, which is the portion that has been extracted by the solvent. The gel refers to the portion of the sample that remained as a solid after extraction and can be considered to be fully cured. The sum of these two values should be equal to the original mass of the sample before extraction was initiated. The following equation can be used to determine the sol content after extraction

$$\%_{sol} = 100\left(\frac{w_t - w_{gel}}{w_t}\right) \qquad \text{(Equation 2)}$$

Where $\%_{sol}$ is the percentage of the sol content, w_t is the initial oven dry weight of the sample, and w_{gel} is the oven dry weight of the solid portion left after extraction, or the gel.

Soxhlet extraction was performed for two resin formulations, MDI and MDI-ESS mixed at a 1:1 equivalent ratio or 2:1 ratio by wt%. Three repetitions were performed for each formulation. FTIR was also performed on the sol extracted from the ESS-MDI samples to evaluate what parts of the sample were soluble.

4.3. Board Manufacture

Once the soybean straw fibers, wheat straw fibers, and resins had been obtained the materials were ready to be pressed into a testable board. The fibers were analyzed for moisture content using an Arizona Instrument LLC Computrac® Max® 4000XLMoisture Analyzer (Chandler, AZ). If the moisture content was below the desired 8-12 wt%, then water was sprayed directly onto the fibers to reach a target of 10 wt%, with the assumption that the excess water would account for reactions with the resin. The water was sprayed using an atomizing spray gun, with the fibers themselves being continually agitated in a cement mixer, shown in Figure 10. The figure also shows how the mixed fibers were removed after sufficient resin spraying so they could be placed into the press.

Figure 10. Cement Mixer used to Agitate Fibers During Spraying

Resin was added to the fiber mixture with the atomizing sprayer in batches of 1 kg of fiber such that the resin would account for 4 wt% of the total mixture. This was kept consistent throughout each formulation. After sufficient spraying of the resin, the mixture of resin and fibers were laid into a custom produced aluminum mold that would press 305 mm x 305 mm panels. Fibers were added to the mold such that a target density of 640 kg/m^3 would be reached and a target board thickness of 7.5 mm would be achieved. Sheets of Teflon were also used on the two halves of the mold to prevent fibers sticking to the mold surface during pressing. The mold used for this process can be seen in Figure 11. The apparatus used to evenly disperse the fibers throughout the mold can be seen in Figure 12.

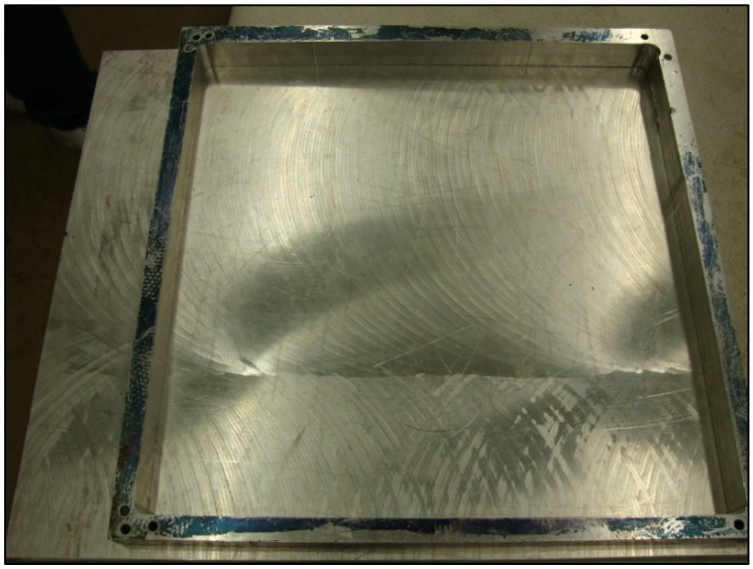

Figure 11. Aluminum Mold Used for Board Pressing

Figure 12. Guide Used to Disperse Fibers Evenly Through Mold

Once the fibers had been laid out, a second, the top half of the mold with a Teflon sheet between it and the fibers was laid onto the top half using guide pins. The two halves of the mold were then placed into a preheated Carver Hot Press Model 4122 (Wabash, IN). Once placed into the hot press, the mold was pressed together by the top and bottom heated platens of the press, with time allowed for degassing. Once the final press load had been achieved, the mold was held together for 5 minutes, with the load applied to the boards being equivalent to 2117 kPa of pressure on the surface of the pressed board. Once the desired cycle time had passed, the pressure was released and the mold was removed and immediately separated to remove the pressed board. The board was then allowed to cool in standard lab conditions for 24 hours until it could be cut into viable testing samples on a band saw. The Carver Hot Press Model 4122 used for pressing can be seen in Figure 13. The board as it came out of the mold can be seen in Figure 14, while the final cooled board can be seen in Figure 15. A summary of the test conditions used to create the boards can be viewed in Table 2.

Figure 13. Carver Hot Press with Mold Being Pressed Between the Heated Platens

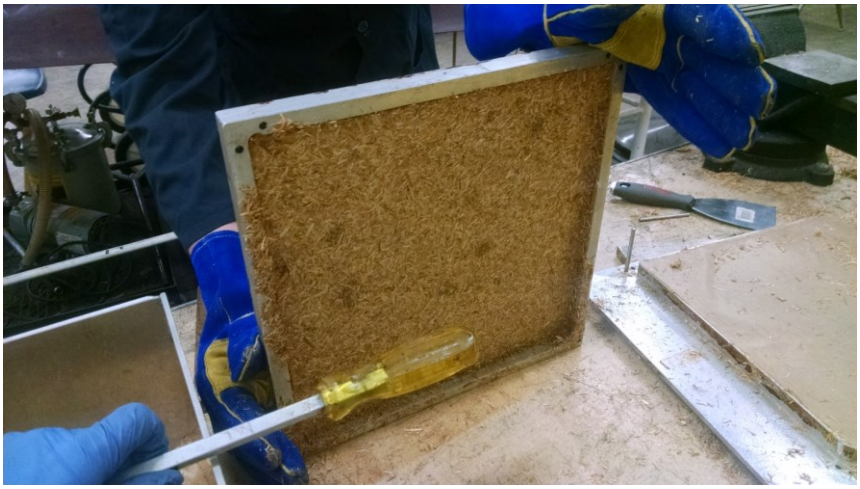

Figure 14. Pressed Board being Removed from Mold

Figure 15. Cooled Board after Being Removed from the Mold

Table 2. Press Conditions Used for all Formulations

Upper and Lower Platen Temperatures	190 ˚C
Degassing Cycle Time	Two 20 second intervals at 7 metric tons and 14 metric tons
Final Press Load	20 metric tons (2117 kPa equivalent)
Press Cycle Time	5 minutes

4.4. Design of Experiment

Two distinct designs of experiment were required to evaluate the properties of the pressed boards as well as the effects of the processing conditions for hammer milling. Both designs were full factorial designs to obtain comprehensive overviews of which factors and corresponding levels were optimal for the board properties as well as the reduction of fines and maximization of the viable fraction content.

4.4.1. Design of Experiment for Testing of Boards

A full factorial design was implemented to test two factors, the effect of the component fiber on the board and the effect of resin binder selected. The component straw factor had two levels represented by two different fiber choices, wheat straw and soybean straw. The resin binder factor had three levels of testing: a pure 4,4'-methylene diphenyl diisocyanate (MDI) resin being one binder system; an epoxy-anhydride system composed of epoxidized sucrose soyate, and anhydride of 4-Methyl-1,2-cyclohexaneedicarboxylic anhydride (MHHPA) a catalyst of 1,8-diazabicyclo[5.4.0]undec-7-end (DBU) being used as another resin system, with mixtures being at a ratio of ESS:MHHPA:DBU being at 67.5:31.0:1.5 by wt%; the final resin system used was a mixture of MDI and ESS resins mixed at a ratio of ESS-MDI 1:1 by equivalent weight of epoxide to isocyanate, and a ratio of ESS-MDI of 1:2 by wt%. Factors such as the press cycle time, press temperature, press pressure, and resin wt% of the pressed boards were kept constant so as not to be influencing factors in the analysis of significant factors and to reduce the total number of formulations to accommodate for the amount of straw fiber available for pressing. In total, six unique formulations were created for testing of the varied factor levels. Four replicate boards with target dimensions of 305 mm x 305 mm x 7.5 mm with target densities of 640 kg/m^3 were created for each formulation for testing of physical properties, resulting in 24 total boards being pressed. All samples used for testing as detailed in Section 4.5 were cut from these boards. Table 3 shows a summary of the experimental design implemented.

Table 3. Board Testing Summary Table with Replication Counts at Each Level

	Fiber Type	
Resin Binder System	Wheat Straw	Soybean Straw
MDI Resin	4	4
ESS-MHHPA-DBU Resin	4	4
ESS-MDI resin	4	4

4.4.2. Design of Experiment for Hammer Milling Process Effects

A full factorial design was implemented for the hammer milling of straw fibers to test four factor effects; the effect of different straw types, the effect of different screen hole size, the effect of different hammer tip speed, and the effect of varying moisture content of the milled fibers. Two types of straw were used in this experimentation, wheat straw and soybean straw. Two different screen sizes were used, with the shapes of the holes being circular, and the two screens having 3/8" diameter holes and 1" diameter holes. The tip speed of the hammers in the hammer mill were varied using a variable frequency motor in the W-6-H Model Hammer Mill (Schutte Buffalo, Buffalo, NY), with the equivalent tip speeds set to 26.9 m/s, 35.9 m/s, and 44.9 m/s. The final factor to be tested was the moisture content of the fibers before milling, with moisture levels set for 5 wt%, 15 wt%, and 25 wt%, with a margin of error ±2.5 wt%. The factor of the rate of feeding into the hammer mill was kept constant to mitigate clogging and blinding effects. The fibers for each formulation then had their distributions characterized by determining fines content and the viable fraction. There were 36 unique formulations were tested, with three replications made for each formulations, resulting in 108 samples that required distribution analysis. Table 4 shows a summary of the experimental design implemented.

Table 4. Hammer Milling Summary Table with Total Replication Count

Factor	Factor Level
Natural Straw Fibers	Wheat and Soybean
Hammer Tip Speed	26.9 m/s, 35.9 m/s, 44.9 m/s
Fiber Moisture Content	5 wt%, 15 wt%, 25 wt%
Screen Size	3/8” round holes, 1” round holes
Unique Formulations	36
Replications	3
Total Samples	**108**

4.5. Mechanical and Physical Testing of Processed Boards

Testing of the mechanical properties of the pressed boards were conducted in accordance with ASTM D1037-12 – Standard Test Methods for Evaluating Properties of Wood-Base Fiber and Particle Panel Materials [42], which has been shown to be a useful measurement of physical properties of traditional wood-based panels as well as non-traditional panels composed of alternative biomass sources. Tests of the panel properties were conducted using the sections for static bending, tension perpendicular to surface (internal bond), direct screw withdrawal, hardness, water absorption and thickness swelling, and linear expansion and change in moisture content. Due to limitations of the board geometry that could be pressed on the available Carver Press Model 4122, adaptations to the cut geometry were made to obtain a suitable number of samples for each test from the four pressed boards. Figure 16 shows the initial cut patterns used for the four boards to obtain samples for static bending, linear expansion, water absorption, density, and internal bond testing.

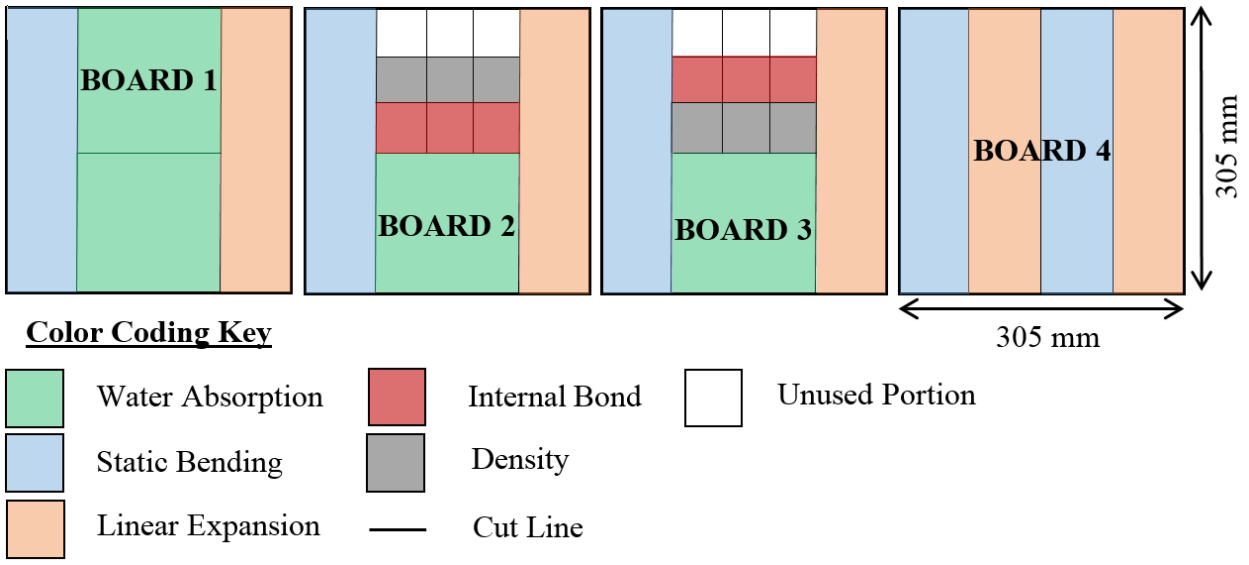

Figure 16. Cut Pattern for Pressed Boards Used in Mechanical and Physical Testing

In order to complete testing for the direct screw withdrawal and hardness tests, additional cuts were made to the static bending samples after they had been tested. The samples were cut in such a way as to not include the fractured portion of the static bending samples, with the cut pattern shown in Figure 17.

Figure 17. Cut Pattern for Post Static Bending Test Samples

The samples for the screw withdrawal testing had to be modified in order to achieve the desired engagement length required to complete testing. Two 76 mm x 127 mm sections from the same flexure testing sample were stacked together creating a thicker board required for this testing as required by ASTM D1037. This did not create the 1" thick sample as prescribed in the

standard; however, the screw did not engage a third panel when drilled to the prescribed 17 mm engagement length, thus the test was conducted as such. The layup of boards used for this testing is shown in Figure 18.

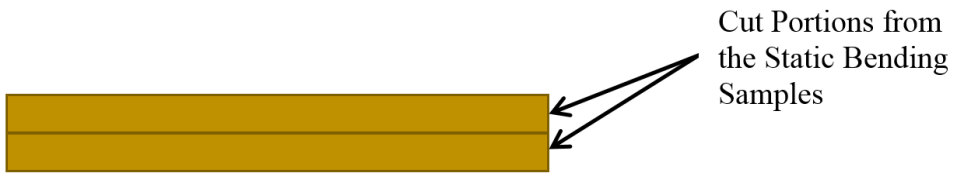

Figure 18. Layup for Direct Screw Withdrawal Samples

A similar multi-panel sample was created for the hardness testing, with four 76 mm x 127 mm panels used to create the suggested 25 mm thick sample panel for the testing. The samples were oriented in such a way that the top surface of the top panel was facing upward and the bottom surface of the bottom panel was facing downward, such that the top and bottom surfaces of each board could be tested in accordance to ASTM D1037. The orientation of the top and bottom in relation to how the board was pressed is illustrated in Figure 19. The layup used to create the hardness samples is illustrated in Figure 20.

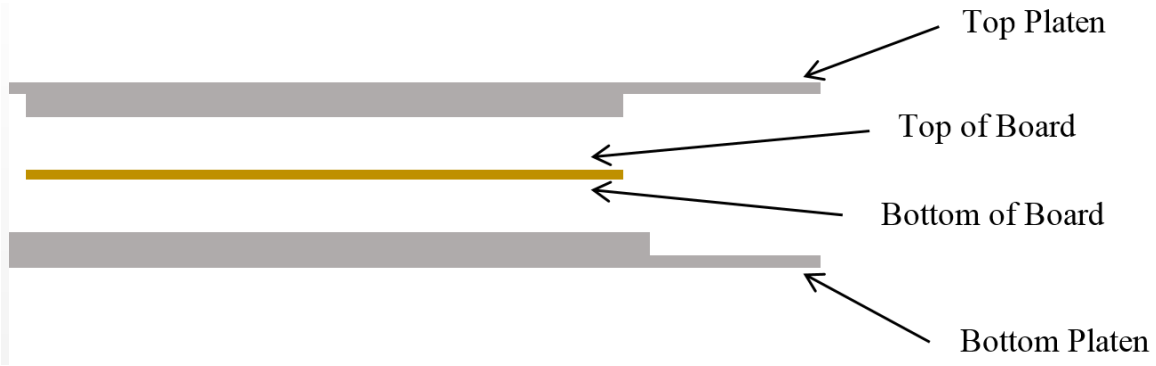

Figure 19. Top and Bottom Orientation of Boards

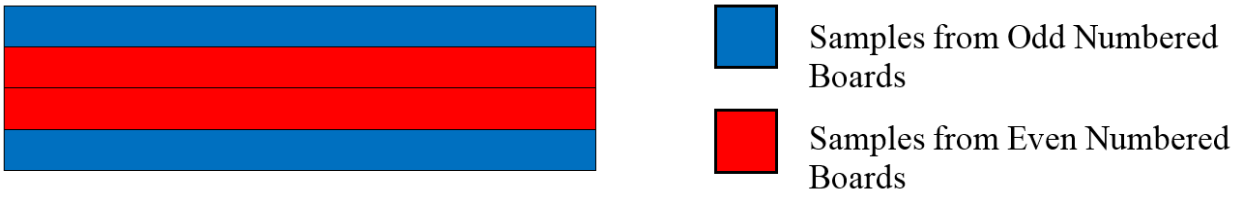

Figure 20. Layup for Hardness Samples

In order to obtain a greater number of samples for the static bending testing, screw withdrawal, and hardness value testing, some of the samples that had gone through the linear expansion testing were allowed to reach a lab condition temperature and humidity and then tested again. In order to remove the effects of the linear expansion testing, blocking was used during ANOVA analysis to determine if the previously used samples were viable. If the blocking factor was significant at a 95% confidence level, then the tested samples' values were removed when calculating averages and other significant factor effects. All mechanical testing of the samples were conducted using an Instron Load Frame model 5567 unless otherwise specified in the relevant section.

4.5.1. Density Measurement

ASTM D1037-12 Section 8 specifies that ASTM D2395 Method A [43] be followed to obtain the specific gravity of the fiberboard samples. This standard was not followed, however, due to limitations with the cage used in the available testing apparatus; instead, a simple density measurement was obtained. An apparent density was measured by first measuring the mass of a sample of fiberboard with a minimum surface area of 58 cm^2 in accordance with the standard (51 mm x 51 mm x board thickness samples in this case) at the "dry" condition to ±0.1 grams as specified by ASTM D1037. The sample volume was then found through a water displacement

measurement using a graduated cylinder within ±0.5 mL. The apparent density was then calculated by using the following equation

$$\rho = \frac{m}{V} \qquad \text{(Equation 3)}$$

Where ρ is the apparent density, m is the sample mass, and V is the measured displaced volume. Six (6) samples were tested for each formulation, three from board 2 and three from board 3.

4.5.2. Water Absorption

ASTM D1037-12 Section 23 was followed to obtain the results of the water absorption by mass of the fiberboard and to evaluate the thickness swelling of the boards. For the water absorption measurement, Method A was utilized to evaluate the absorption, which stipulates that the mass of the sample as well as the geometry of the samples be measured at a 2 hour interval after submersion and a 24 hour interval after submersion. Samples for the water absorption test were cut from the originally pressed board into 152 mm x 152 mm samples and were squared and trimmed to remove errant fibers. Samples were conditioned for a minimum of 48 hours by being placed in a Binder Humidity Chamber model KBF 115 – UL at the "dry" conditioned state at 20 ± 3 ˚C and 65 ± 5 % relative humidity. After conditioning, the samples were then weighed again and the sample thickness measured immediately before placing the samples in a water bath. The water bath was maintained at 20 ± 1 ˚C, and the samples were submerged horizontally underneath a minimum of 1 inch of water with the help of a plastic cage. Multiple samples were tested in the same bath and fresh tap water was used after each test. Samples were submerged

for 2 hours, then removed and suspended above the bath for 10 minutes to drain and surface water removed before measurement of the sample mass and width, length, and thickness was taken. The same method of removal, suspension, and measurements were repeated at the 24 hour mark. The dry weight of the samples was immediately obtained afterward by drying each sample in an oven for 24 hours at a temperature of 103 ± 2 ˚C and then measuring the sample mass. The moisture content at each stage was measured using the following equation

$$\%MC = 100\left(\frac{w_2 - w_1}{w_1}\right) \qquad \text{(Equation 4)}$$

Where %*MC* represents the percent moisture content of each sample, w_1 represents the initial dry weight in grams, and w_2 represents the mass of the sample at a conditioned or post-submersion state in grams. The increase in thickness due to moisture absorption was also calculated using the following equation

$$\%T = 100\left(\frac{t_2 - t_1}{t_1}\right) \qquad \text{(Equation 5)}$$

Where *%T* represents the percent increase in thickness, t_1 represents the initial thickness of the board at the conditioned state in mm, and t_2 represents the thickness of the board post-submersion in mm. Four (4) samples were created and tested both for the thickness swelling and water absorption measurements for each formulation.

4.5.3. Linear Expansion

ASTM D1037-12 Section 24 was followed to complete the testing of linear expansion with change in moisture content testing. This line of testing evaluates the boards for dimensional

stability as the ambient moisture content changes. The samples used for this testing were 76 mm x 305 mm x as pressed thickness. The linear expansion testing was completed using a Binder Humidity Chamber model KBF 115 – UL. Samples were first conditioned to an equilibrium weight with the conditioning chamber that was set for 20 ˚C and 50% relative humidity, with each sample weighed once every 24 hours to determine when an equilibrium weight had been reached. When an equilibrium weight had been attained, the length of each sample was obtained within an accuracy of 0.02 mm, then the samples were placed back into the chamber and the chamber conditions were set to 20 ± 3 ˚C and 80% relative humidity (the maximum humidity attainable with the device). The samples were then weighed again once every 24 hours to determine when an equilibrium weight had been achieved. Once the equilibrium condition was satisfied, the samples were removed from the chamber and the lengths of each sample were immediately obtained. The linear expansion of each board was calculated using the following equation

$$\%LC = \frac{L_1 - L_0}{L_0} \qquad \text{(Equation 6)}$$

Where *%LC* is the linear expansion along the length of the sample going from 50% relative humidity to 80% relative humidity, L_1 is the new length measured at 90% relative humidity, and L_0 is the length measured 50% relative humidity. Five (5) samples for each formulation were tested for linear expansion. A picture of the weathering chamber used and the placement of the samples within can be seen in Figure 21.

Figure 21. Linear Expansion Samples as Placed into the Conditioning Chamber

4.5.4. Static Bending

Static bending tests were conducted on samples in accordance with ASTM D1037-12 Section 9. The test involves utilizing a three-point bending test to obtain the modulus of elasticity (MOE) and the modulus of rupture (MOR) for the fiberboards. A picture of the test as it was conducted is shown in Figure 22.

Figure 22. Three Point Static Bending Test

Samples were cut from the originally pressed fiberboard into 76 mm x 305 mm x as pressed thickness. Each sample was loaded with a central loading nose and two support noses, each having a radius of 25.4 mm. The two support noses were placed such that the span between them was as suggested in the ASTM D1037, 24 times the nominal board thickness, with the span being adjusted for the variance in thickness in each sample. Loading of the samples was achieved by lowering the central loading nose at a constant crosshead rate determined by the sample geometry, given by the following equation

$$N = \frac{zL^2}{6d} \qquad \text{(Equation 7)}$$

Where N represents the crosshead rate in mm/min, z represents the unit rate of fiber strain of outer fiber length per minute (z = 0.005 according to ASTM D1037), L represents the support span in mm, and d represents the specimen thickness in mm. During sample testing, the maximum load achieved during the test and the corresponding vertical deflection were recorded in order to calculate the MOE and MOR of the samples. The MOR was calculated using the following equation

$$R_b = \frac{3P_{max}L}{2bd^2} \qquad \text{(Equation 8)}$$

Where R_b is the MOR in MPa, P_{max} is the maximum recorded load in Newtons, L is the length of the span in mm, b is the width of the specimen in mm, and d is the thickness of the specimen in mm. The MOE was calculated using the following equation

$$E = \frac{L^3}{4bd^3}\left(\frac{\Delta P}{\Delta y}\right) \qquad \text{(Equation 9)}$$

Where L is the span of the sample in mm, b is the width of the specimen in mm, d is the thickness of the specimen in mm, and $\Delta P/\Delta y$ is the slope of the straight line portion of the load-deflection curve in N/mm (slope between 10% of P_{max} and 40% of P_{max} as suggested in Note 16 of ASTM D1037). Ten (10) static bending samples were tested for each formulation of fiberboard when the linear expansion samples could be repurposed.

4.5.5. Tension Perpendicular to Surface (Internal Bond)

Internal bond strength tests were performed in accordance with ASTM D1037 – 12 Section 11. Samples were cut from the originally pressed boards to be 51 x 51 mm samples as specified in ASTM D1037. Samples were adhered to the faces of aluminum loading blocks by first heating the loading blocks and melting a hot melt adhesive provided by Primeboard Masonite in Wahpeton North Dakota on the face, then placing individual samples between two loading blocks and letting the adhesive set in room temperature with no pressure applied to the samples. A minimum of 6 hours was allowed to pass after adhering to the loading blocks before samples were tested to allow the adhesive to set. Each sample was loaded into the testing fixture by placing the loading blocks such that the slots in each block made sufficient contact with the fixture arms. Samples were loaded perpendicular to the panel face until specimen failure occurred. A picture of the testing fixture and loading blocks can be observed in Figure 23.

Figure 23. Internal Bond Testing Fixture with Loaded Sample

The rate of loading was kept at a constant 1 mm/min rather than keeping the speed of testing at a rate of 0.08 cm/cm as was specified in ASTM D1037. A constant crosshead rate was chosen as opposed to a constant strain because of the unavailability of a suitable extensometer to measure and maintain strain rate. The maximum load achieved during the test after specimen failure occurred was recorded and used to calculate the internal bond strength, where the internal bond strength is given by the following equation

$$I = \frac{P_{max}}{ab} \qquad \text{(Equation 10)}$$

Where I represents the internal bond strength in MPa, P_{max} represents the maximum load applied to the sample before failure in N, a represents the sample width in mm, and b represents the sample length in mm. Six (6) internal bond samples were tested for each fiberboard formulation.

4.5.6. Direct Screw Withdrawal

Section 16 of ASTM D1037-12 was utilized as the guide for this test. Samples were cut from the ends of previously tested flexural samples and from the originally pressed boards into 76 mm x 127 mm samples, with two samples stacked together accommodate for the 17 mm engagement length of the screw for testing. The screws used during the screw withdrawal test were pan head #10 screws, 38.1 mm long. A guide hole was made using a 3.2 mm drill bit as specified in the standard. Specimens were loaded in the testing fixture as recommended in the

standard, with the screw inserted into the fixture slot and the panel face flush to the bottom fixture. A picture of the loaded specimens and the testing fixture can be seen in Figure 24.

Figure 24. Screw Withdrawal Testing Fixture and Loaded Sample

Each specimen was loaded by separation of the top and bottom test fixtures at a constant rate of 1.5 mm/min until the screw was fully withdrawn from each sample. The maximum load required to remove the screw from the panel face was recorded for each sample. Ten (10) samples were tested for each formulation when samples from the linear expansion testing could be appropriately repurposed.

4.5.7. Hardness

Hardness testing was conducted in accordance with Section 17 of ASTM D1037. Hardness testing of the panels shows the ability of the surface of the panels to resist local deformations and scratches. The hardness testing was performed using four 76 mm x 127 mm stacked on top of each other to form a minimum thickness of 25.4 mm as suggested in the standard. The Janka ball method of testing was used, with an 11.3 mm diameter ball depressed

into the surface of the composite sample one-half the diameter of the ball (5.65 mm in this case), with the load required to depress the ball to this distance being recorded as the hardness value. The rate of loading used was 6 mm/min in accordance with the standard. Two hardness measurements were taken on the top and bottom surfaces of each sample in accordance with the standard, with 8 total hardness values obtained for each formulation. A picture of the testing apparatus and the composite sample can be seen in Figure 25.

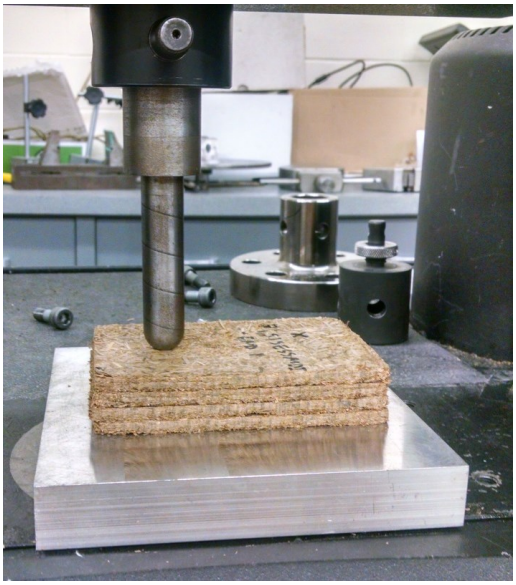

Figure 25. Surface Hardness Testing of the Stacked Boards using the Janka Ball Method

4.6. Hammer Milling of Straw Fibers

Both wheat and soybean straw fibers were milled using a W-6-H Model Hammer Mill (Schutte Buffalo, Buffalo, NY). A picture of the hammer mill used can be seen in Figure 26.

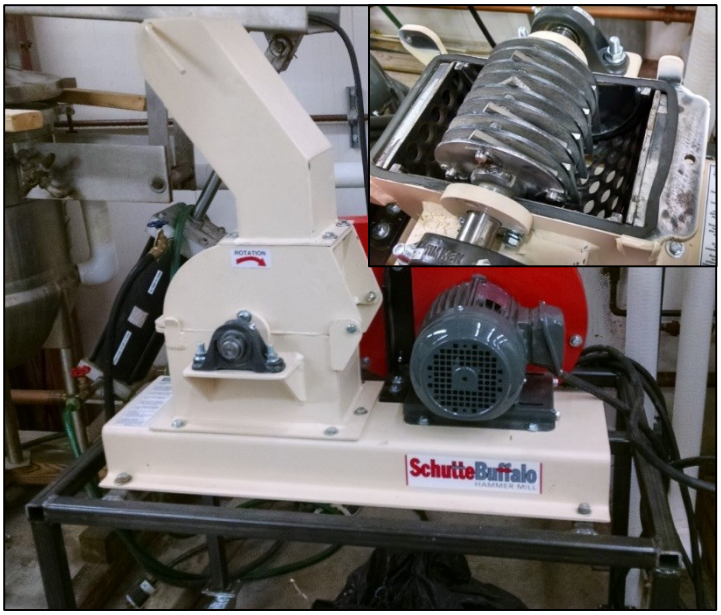

Figure 26. Schutte Buffalo Hammer Mill with Inset Showing Hammers

Two different screen sizes (round holes; 3/8” and 1” holes), three different milling speeds as controlled by the variable frequency drive (equivalent hammer tip speed; 26.9 m/s, 35.9 m/s, 44.9 m/s), and three different fiber moisture contents (5 wt%, 15 wt%, 25 wt%) were tested in accordance with the design of experiment detailed in Section 4.4.2. The Straw was first allowed to reach the desired moisture content by adding water to bags of straw then allowing straw to sit for a minimum of 72 hours before the moisture content of the straw was measured using an Arizona Instrument LLC Computrac® Max® 4000XLMoisture Analyzer (Chandler, AZ) at intervals of 12 hours. Once the straw had reached the desired moisture content ±2.5 wt%, it was taken to be milled by the hammer mill. Straw was hand-fed into the mill input opening at an approximate rate of 150 grams/minute with a desired total mass of fibers for each formulation set at 1 kg. Three replications for each formulation were performed. The milled fibers were collected using a trash bag, with the opening of the trash bag and the output chute sealed such that no fibers could be lost during operation of the mill. The fibers were then allowed to be

exposed to labs conditions (20±3˚C and 50±10% relative humidity) for a minimum of 48 hours before any further testing was completed.

4.6.1. Characterization of Fiber Distribution

Once the hammer milling of all wheat and soybean fibers at each condition were completed, the fines content, and viable fraction for each sample set needed to be obtained. The fiber distribution was found by using a Humboldt H-4325 Series Sieve Shaker to separate the different fiber sizes from the milled samples. A picture of the sieve shaker used for this step can be observed in Figure 27.

Figure 27. Humboldt H-4325 Series Sieve Shaker with Sieves and Fiber

The samples were first prepared by following ASTM E1757-01 – Standard Practice for Preparation of Biomass for Compositional Analysis Method A [10], which details that the fibers first be conditioned and tested at a temperature of 20 to 30 ˚C and relative humidity of 50% or less, which was achieved by allowing the fibers to reach an equilibrium while exposed to a

standard lab atmosphere. Once conditioned, the fibers were laid out onto a mat and then spread and separated in a method adapted from ASTM D75/75M-14 – Standard Practice for Sampling Aggregates [44] in such a way that a portion sample obtained from the 1 kg sample would be representative of the distribution of the entire sample. Figure 28 shows a picture of the fibers as they were laid out before testing.

Figure 28. Fibers Laid Out as Described in ASTM D75/75M

Once laid out, a sample of 40 grams was taken from one of the four quartered portions and then placed into the top sieve contained in the sieve shaker. Four different sizes of sieves were used as an adaptation of ASTM E1757: a 20 mesh sieve, a 40 mesh sieve, a 60 mesh sieve, an 80 mesh sieve, and a final catch pan to catch particles finer than 80 mesh. It should be noted that the mesh size refers to the Tyler Standard mesh scale. The sieve shaker was run for 15 minutes for each sample as suggested in the manufactures manual of the sieve shaker. Once completed, the sieves were removed from the shaker and the material contained within each sieve pan was taken and then weighed. Fiber distribution charts could then be constructed from this data. This data would also show several useful parameters, such as the fines content, which

is defined as fibers that are smaller than 80 mesh and whose fraction can be calculated using the following equation

$$\%F_{80+} = 100\left(\frac{wt_{80+}}{wt_{total}}\right) \qquad \text{(Equation 11)}$$

Where $\%F_{80+}$ is the weight fraction of the particles captured in the catch pan as a percentage defined as fines, wt_{80+} is the weight of the particles in the catch pan after sieving, and wt_{total} is the sum of the weights of all of the particles in each pan after sieving is completed. A second parameter that can be calculated is the viable fraction, which is defined as fibers that fall in the range between the 20 mesh and 80 mesh size, which have been shown to be useful in the production of fiberboard in terms of processability and physical properties of the manufactured board. The viable fraction can be calculated using the following equation

$$\%F_{viable} = 100\left(\frac{wt_{20-80}}{wt_{total}}\right) \qquad \text{(Equation 12)}$$

Where $\%F_{viable}$ is the weight fraction of the particles that can be used in fiberboard manufacture without further processing, wt_{20-80} is the weight of the particles that are smaller than 20 mesh and larger than 80 mesh, and wt_{total} is the sum of the weights of all of the particles in each pan after sieving is completed. The viable fraction is a useful parameter in determining how much additional refinement is needed for fiber to be useful in the board manufacturing process.

4.7. Statistical Analysis

Statistical analysis was conducted on the data obtained in this research to gain objective results on the effect that each variable had on the response values considered to evaluate the hypotheses statements presented in Chapter 3. The following methods were used to determine if the change in fiber and resin in the boards affected physical and mechanical properties at a significant statistical level. The analysis was also implemented to determine if the fiber choice, moisture content, screen size, or hammer tip speed had a significant effect on the fiber distribution obtained from hammer milling straw. All statistical analyses were performed using a statistical software package known as Minitab.

4.7.1. Boxplots of Data

Boxplots are a graphical representation of data that shows several useful pieces of information that similar graphs like bar charts cannot show. A boxplot gives a mean and median value for a data set and shows the general spread of data by finding quartile values and the maximum and minimum response values observed within a data set. A diagram of a boxplot can be seen in Figure 29.

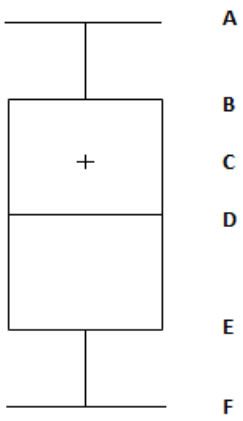

Figure 29. Diagram of a General Boxplot

In the diagram, point A is the maximum value observed in the data set, point B is a value known as the 3rd Quartile, point C is the mean of the data set, point D is the median of the data set, point E is a value known as the 1st Quartile, and point F is the minimum value observed in the data set. The 1st Quartile is a value that is in the data set that is greater than 25% of the smallest valued data and less than 75% of the largest valued data, or in other words it is the median of the lesser half of the data set when then initial data set is divided between values that are greater than the full data set's median and less than the full data set's median. The 3rd Quartile value is a value within the data set that is greater than 75% of the smallest valued data but less than 25% of the largest valued data, meaning it is the median of the greater half of the data sets when then initial data set is divided between values that are greater than the full data set's median and less than the full data set's median.

4.7.2. ANOVA of a Factorial Design

Analysis of Variance or ANOVA is statistical model that can be used to estimate experimental errors and the effect of changing variables within a design on a single response

value for a specified confidence level. For this thesis paper, the commonly used 95% confidence interval was implemented for all ANOVA analyses, which indicates that the estimated bounds of data for a particular set of variables includes 95% of the data that would be produced looking at the entire population of data for that set of variables.

ANOVA models can be broken down into several estimated effect factors; main effects, interaction effects, and error effects, all of which are used to estimate how much of the provided variables account for the variability of the responses. Main effects estimate the amount of response change that is due solely to the level of the a single variable changing, interaction effects account for the effect of the response from a combination of changes in variable levels, and the error effect accounts for randomness of the provided response values and also accounts for a possible lack of relevant variables that are included within the model. For a general factorial design, an algorithm is needed to calculate the main effects, interaction effects, and error effects. General factorial designs with multiple factors and mixed levels for each variable were used in the design of most experiments conducted in this thesis project, making an explanation of the general ANOVA procedure tedious and in need of several robust chapters of explanation that would not be within an appropriate scope of this paper. However, in order to give you, the reader, an idea of what type of analysis was used as the criterion for evaluating the hypothesis within this test, an explanation of the ANOVA for a two-factor design will be provided. An more robust explanation of mixed factor and factor level full factorial designs can be read in several experimental design textbooks, once such textbook being *Design and Analysis of Experiments* by Douglas C. Montgomery [45].

For a two-factor design, assume two variables can be represented as A and B. To compute the sum of squares due to changes in the level of variable A, the following equation can be used

$$SS_A = \frac{1}{bn}\sum_{i=1}^{a} y_{i..}^2 - \frac{y_{...}^2}{abn} \qquad \text{(Equation 13)}$$

Where SS_A is a term known as the sum of squares for factor A, *b* is the number of factor levels in factor B, *n* is the number of replications for each combination of A and B, *a* represents the total number of factor levels in factor A, $y_{i..}$ represents the sum of all data points for each level of factor A at level *i* of factor B, and $y_{...}$ represents the sum of all data points in the design. To compute the sum of squares due to changes in the level of variable B, the following equation can be used

$$SS_B = \frac{1}{an}\sum_{j=1}^{b} y_{.j.}^2 - \frac{y_{...}^2}{abn} \qquad \text{(Equation 14)}$$

Where SS_B is a term known as the sum of squares for factor B, $y_{.j.}$ represents the sum of all data points for each level of factor B at level *j* of factor A, and the other variables are the same as in the equation for the calculation of SS_A. The interaction effect between factors A and B can be accounted for by using the following equation to first calculate an intermediary value

$$SS_{Sub} = \frac{1}{n}\sum_{i=1}^{a}\sum_{j=1}^{b} y_{ij.}^2 - \frac{y_{...}^2}{abn} \qquad \text{(Equation 15)}$$

Where SS_{Sub} is an intermediary value known as the sum of squares subtotal, $y_{ij.}^2$ is the sum of all of the replicates in a single combination of factors A and B for all factor levels, and the other variables are the same as stated in the previous equations. Once SS_{Sub} has been calculated, the sum of squares of the interaction effect can be calculated using the following equation

$$SS_{AB} = SS_{Sub} - SS_A - SS_B \qquad \text{(Equation 16)}$$

Where SS_{AB} is the sum of squares for factors A and B and the other variables are the same as stated in the previous equations. Another sum of squares value is needed for the ANOVA algorithm which is known as the total sum of squares and can be found using the following equation

$$SS_T = \sum_{i=1}^{a}\sum_{j=1}^{b}\sum_{k=1}^{n} y_{ijk}^2 - \frac{y_{...}^2}{abn} \qquad \text{(Equation 17)}$$

Where SS_T is the total sum of squares, y_{ijk} represents replication *k* at the level *i* of factor A and level *j* of factor B, and the other variables represent the same terms as stated in the previous equations. With the SS_T calculated, a sum of squares for the error can be found using the following equation

$$SS_E = SS_T - SS_{Sub} \qquad \text{(Equation 18)}$$

Once all of the sum of squares values have been found, a mean sum of squares value must calculated to account for the degrees of freedom of the system. The mean square of factor A can be found using the following equation

$$MS_A = \frac{SS_A}{a-1} \qquad \text{(Equation 19)}$$

The mean square of factor B can be found as

$$MS_B = \frac{SS_B}{b-1} \qquad \text{(Equation 20)}$$

The mean square of the interaction effect can be found as

$$MS_{AB} = \frac{SS_{AB}}{(a-1)(b-1)} \qquad \text{(Equation 21)}$$

And the mean square of the error effect can be found as

$$MS_E = \frac{SS_E}{ab(n-1)} \qquad \text{(Equation 22)}$$

Once the mean square values have been found for all pertinent factors, a value as the F statistic can be found and an F-test comparison to the F-distribution can be performed. The F statistic can be found by using the following equation for all of the factor effects previously stated

$$F = \frac{MS_{factor}}{MS_E} \qquad \text{(Equation 23)}$$

Where F is the F statistic, MS_{factor} represents the mean square for the pertinent factor A, B, or the interaction of A and B, and MS_E represents the mean squared error value. The F statistic works in much the same way that the t statistic does, in that if the F value is greater than a characteristic F value based on the desired confidence level and degrees of freedom in the considered system there is a statistically significant difference between data sets. For the application in ANOVA, an F statistic for a specific factor that is greater than the characteristic F value means the factor has a statistically significant effect on the variation observed within the response values. The confidence level used for this thesis testing was set at the commonly accepted 95% confidence level. It should be noted that many statistical software packages, Minitab included, use an equivalent p statistic in place of the F statistic when creating ANOVA tables. The only difference with this statistic is that if a calculated p statistic for a certain factor is less than 1-α, where α is the confidence level, then the factor has a significant effect on the response variation.

In order to determine the adequacy of the ANOVA model in determining the significant factors affecting variance of data, the R^2 and Adjusted R^2 statistics will be used. The R^2 statistic is overall measure of the variance that can be attributed to the factors included in the model. The R^2 statistic can be calculated by using the following equation

$$R^2 = \frac{SS_{Model}}{SS_T} \qquad \text{(Equation 24)}$$

Where R^2 is the model adequacy statistic, SS_T is the total sum of squares as calculated previously, and SS_{Model} is the sum of all of the factor sum of squares, which can be written as

$$SS_{Model} = SS_A + SS_B + SS_{AB} \qquad \text{(Equation 25)}$$

Where SS_{Model} is the sum of squares of the model, SS_A is the sum of squares for factor A, SS_B is the sum of squares for the factor B, and SS_{AB} is the sum of squares for the interaction effect between factors A and B.

The R^2 statistic is a useful measure of the variability due to the variance within factors, but it has the inherent flaw of increasing as more factors are added to the model even if the models do not have statistical significance. There are several ways to combat this issue. One such way is to calculated an Adjusted R^2 statistic, which is given by the following equation

$$R^2_{adj} = 1 - \frac{SS_E/df_E}{SS_T/df_T} \qquad \text{(Equation 26)}$$

Where R^2_{adj} is the adjusted model adequacy statistic, SS_E is the sum of squares for the error component as previously described, df_E is the degrees of freedom for the error component, SS_T is the sum of squares for the total component, and df_T is the degrees of freedom for the total component. The R^2_{adj} statistic takes into account the variance that is due only to the significant factors within the model. If the R^2 and R^2_{adj} values are nearly equal, then it indicates that all included factors are significant to some degree. The R^2 and R^2_{adj} should be as close as possible to 1, indicating all variability within a model is due to changes from the included factors.

Typically a model that has an R^2 between 0.8 – 0.9 is considered to be a model that adequately describes the variance in a system.

One other method of obtaining a more accurate R^2 value is to remove insignificant high level interactions between factors. Typically interactions that are high than a second level interaction are not significant and are difficult to account for in designs, thus all ANOVA within this paper will include only those two level interactions or lower unless the high level interactions are statistically significant.

4.7.3. Comparison of Means Testing

While an ANOVA can show statistically significant differences between pairs of means and effects of factors, it does not show how a group of data sets compares to each other in terms of all possible comparisons. For many hypothesis tests, an answer to the hypothesis $H_0 : u_i = u_j \; for \; all \; i \neq j$ is desired. Two common methods used to answer this question after statistically significant difference has been established are Tukey's Test and Fisher's Least Significant Difference Method. Tukey's Test uses the t-distribution to compare all possible pairs of data sets within a group of data sets by first calculating a characteristic difference value which can be calculated by using the following equation

$$T_\alpha = q(a,f)\sqrt{\frac{MS_E}{n}} \qquad \text{(Equation 27)}$$

Where T_α is the characteristic Tukey's difference value, *q(a,f)* is a test statistic value based on the t-distribution, *a* is the number of factors or data sets considered in the comparison, *f*

is the number of degrees of freedom of the MS_E, MS_E is the mean squared error as described in Section 4.7.3, and n is the number of replications for each data set. Once a T_α values has been established, the difference of each pair of data sets can be compared for all data sets, or put mathematically, $T_\alpha < \bar{y}_i - \bar{y}_j$ for all $i \neq j$, where $\bar{y}$ represents the sample mean of a data set. If the inequality is shown to be true, then the two data sets are considered to be different and can be denoted as such.

Fisher's Least Significant Difference method works in much the same way that Tukey's Test does. The characteristic difference value for this method is given by the following equation

$$LSD = t_{\frac{\alpha}{2},N-a}\sqrt{\frac{2MS_E}{n}} \qquad \text{(Equation 28)}$$

Where *LSD* is the characteristic Fisher's difference value, $t_{\frac{\alpha}{2},N-a}$ is a t-distribution value determined from the desired confidence level and degrees of freedom of the considered group, a is the desired significance level, N is the total number of samples in all data sets, a is the total number of factors or data sets in the group, MS_E is the mean squared error value as described in Section 4.7.3, and n is the number of replications in each data set. The method works in the same way as Tukey's Test, where once a *LSD* value has been established, the difference of each pair of data sets can be compared for all data sets where $LSD < \bar{y}_i - \bar{y}_j$ for all $i \neq j$, where $\bar{y}$ represents the sample mean of a data set. If the inequality is shown to be true, then the two data sets are considered to be different and can be denoted as such.

Tukey's and Fisher's methods both yield similar results but should be implemented in differing situations. Tukey's test is best used for a larger number of data points and can control

for the overall error rate and is thus a good general application of the comparison of means test. It is also useful in cases where an unbalanced design has been implemented. Fisher's test is an exact test, meaning it can calculate the significance of the deviation from a null hypothesis exactly, making it useful in applications where there are a limited number of data points available. For this paper, Fisher's test will be applied when the number of data points in a data set being considered is less than five, while Tukey's Test will be implemented in all other cases. The comparison of means process can be used for all pairs of data and can create an arbitrarily labeled grouping system that is easy to show in graphical form such as in a boxplot by placing the labels of each group near the respective data set boxplot. This gives any easy to interpret comparison piece of information about the data sets such that the boxplot not only shows the mean and general spread of data, but also allows the reader to quickly differentiate between different groups of data in terms of their statistically significant differences.

4.7.4. Main Effects Plots and Interaction Plots

Main effect plots are graphical representations of data that show the average response value at each level of a factor, with plots being generated for all factors within a design. Main effect plots are useful in showing the general relation between the change in factor level and how it affects the response value, and is especially useful as an estimator for response values for a given factor level input and as a way to observe nonlinear relationships between factor levels and response values. Figure 30 shows a general main effects plot for a two-factor design with two levels, where the graphs plot the average response level versus the corresponding factor level.

Figure 30. General Main Effects Plot Example

Occasionally several factor interactions significantly contribute to the system variability within the ANOVA analysis and must be accounted for when selecting factor levels for optimal response performance. One way to account for this interaction is to create an interaction plot. The plot shows how the levels of each factor affect the mean response value, giving a good idea which factor level will create ideal conditions for optimizing the response value. Figure 31 shows a general interaction plot for a three factor design.

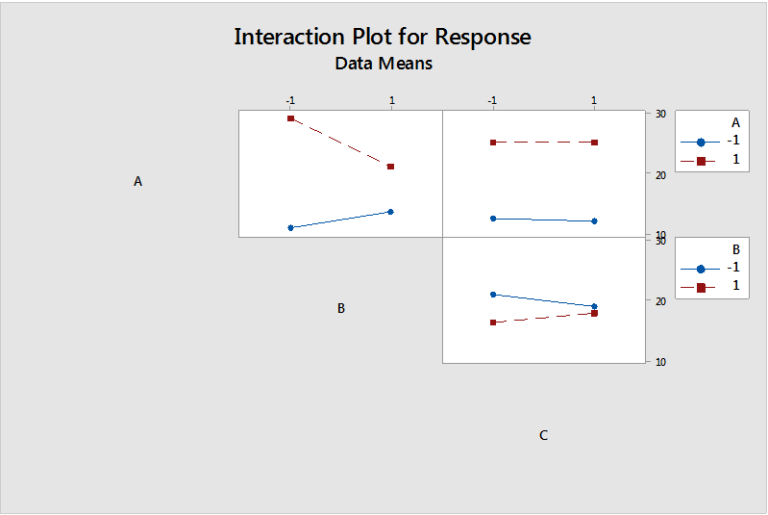

Figure 31. General Interaction Effects Plot Example

5. RESULTS AND DISCUSSION

This chapter covers the experimental results observed during the duration of this thesis project. There are three distinct sections that the results can be divided into: resin characterization results; physical and mechanical board testing results; and hammer milling of straw fibers results.

5.1. Resin Characterization Testing Results

This section contains the results from the lap shear testing, thermogravimetric analysis, differential scanning calorimetry, Fourier transform infrared spectroscopy, and soxhlet extraction.

5.1.1. Lap Shear Testing Results

Lap shear testing was performed as an initial study to preliminarily evaluate resin mixtures and curing times and temperatures to be used in the final fiberboard making process. The adhesive shear strength was measured for each formulation in accordance with ASTM D2339, with five repetitions performed for each cure temperature, cure time, and resin formulation combination. The adhesive shear stress observed for the ESS-MHHPA-DBU samples can be seen in Table 5 where the uncertainty values in the table for the shear stress is the standard deviation.

Table 5. Lap Shear Testing Results for ESS-MHHPA-DBU Formulations

Cure Temperature [°C]	Cure Time	Average Adhesive Shear Stress [MPa]
150	60 minutes	4.277 ± 0.215
165	45 minutes	4.192 ± 0.162

From the results it can be seen that minor changes in strength occurred between the two settings for the cure time and temperature, but no clear relationship between the two factors and the shear strength could be established. From these results it was concluded that the ESS-MHHPA-DBU formulations could produce good bonding between fibers even at short cure times. The testing results for the ESS-MDI resin lap shear testing can be seen in Figure 32. It should be noted that the ratio of ESS to MDI resin is called out as a percentage of the total weight rather than an equivalent ratio.

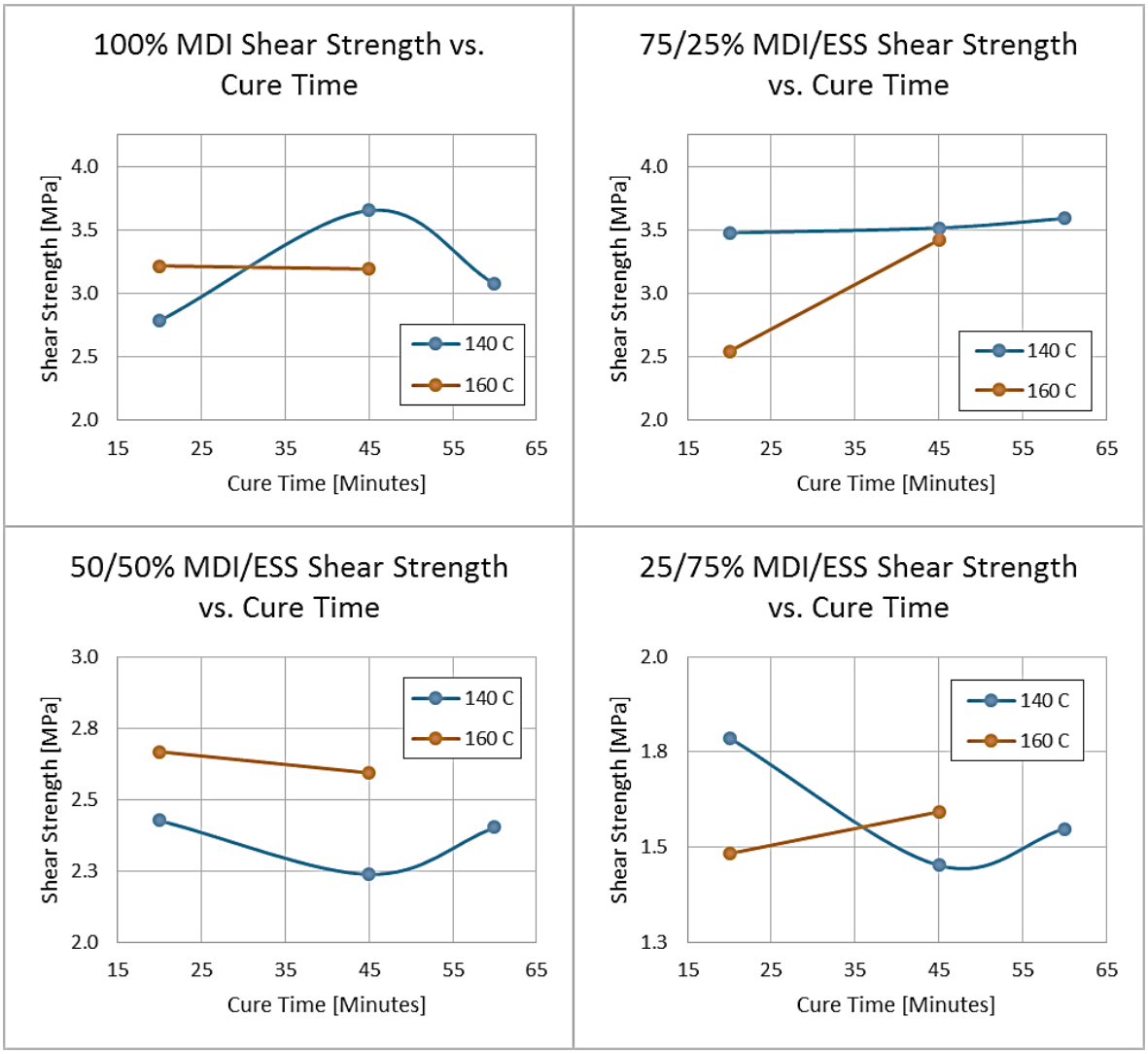

Figure 32. Lap Shear Testing Results for ESS-MDI Resin Systems

The results from the testing show that the pure MDI resin has somewhat similar performance to that of the ESS-MHHPA-DBU as the highest adhesive shear strength observed for pure MDI was 3.65 MPa. The combinations of ESS and MDI resins also had similar performance to the ESS-MHHPA-DBU and pure MDI resins, with the highest shear strength of the mixtures observed to be 3.56 MPa for the 25:75 ESS-MDI ratio. This gives some evidence that the proposed ideal ratio of 2:1 by wt% between MDI and ESS should produce an ideal amount of oxazolidone and isocyanurate without having excessive unreacted reagents. The relatively high adhesive strength indicates that good interfacial bonding between fibers in the boards can be achieved, yielding higher board performance.

No clear relationship was found for the curing temperature or the cure time for ESS-MDI mixtures, thus a proposed temperature of 190 ºC and 5 minutes of curing temperature was considered to be the starting point for board curing for all resin formulations to minimize the cycle time while remaining under the degradation temperature of cellulose within the straw fibers.

5.1.2. Thermogravimetric Analysis Results

Thermogravimetric analysis (TGA) was conducted for six samples, including MDI resin, ESS resin, and ESS-MHHPA-DBU resin as well as ESS-MDI resin mixtures with ratios of 75:25 wt%, 50:50 wt%, and 25:75 wt%. The results shows the change in weight percentage with the change in temperature and show the degradation temperatures of the resin as well as possible multi-step degradation. Figure 33 shows the results of the TGA testing.

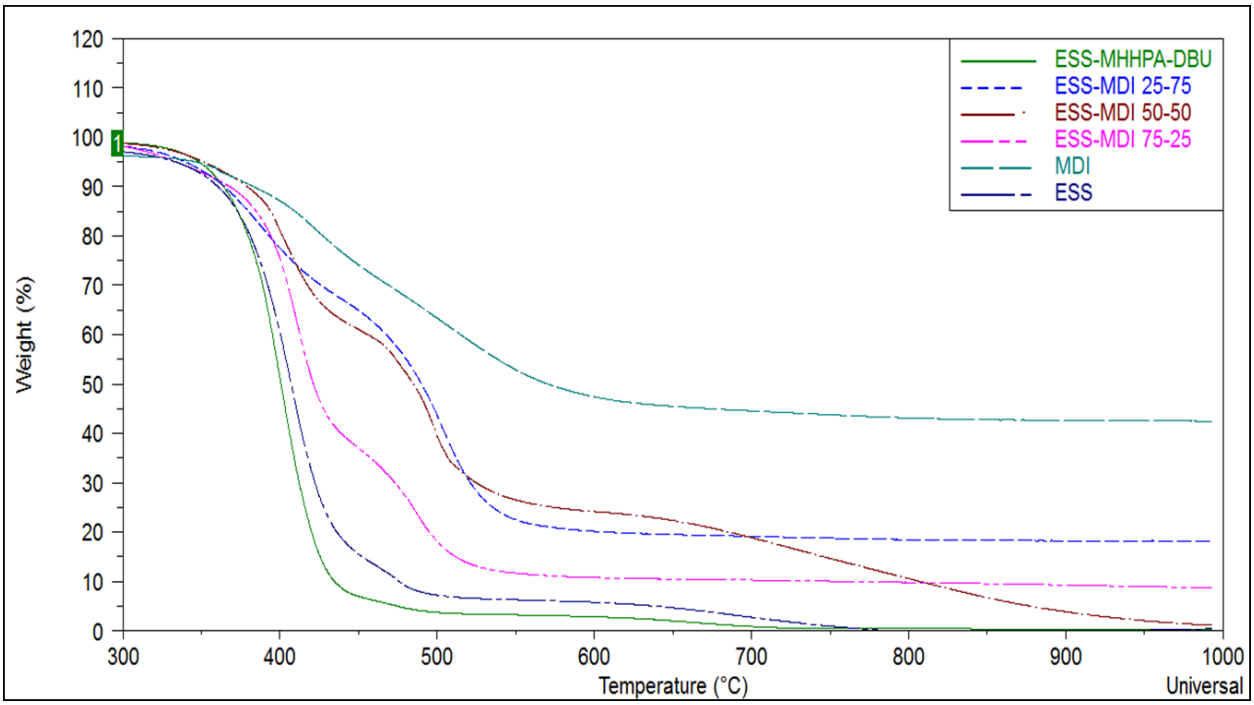

Figure 33. Results from Thermogravimetric Analysis

From the thermal curve the initial degradation onset point for all of the materials occurred at 350 °C, well above operation temperatures expected for fiberboard operations. Of note for this research is the plateau regions observed for all of the ESS-MDI mixtures with an onset temperature of 430 ºC and an ending temperature of 540 °C. These plateaus indicate that an intermediary product was possibly formed between the ESS and MDI that provides a distinctly different curve than those found for the MDI, ESS, and ESS-MHHPA-DBU formulations. However, the presence of these plateaus is not significant enough to identify or characterize what sort of reaction or product formed for the ESS-MDI mixtures.

5.1.3. Differential Scanning Calorimetry Results

In order to characterize the reaction temperatures and to determine if characteristic heat of reactions were observed differential scanning calorimetry (DSC) was performed. DSC curves were generated for samples of MDI and samples of ESS-MDI mixed at a ratio of 1:2 by wt%. Figure 34 shows the thermogram for MDI resin for both the 1st heat and 2nd heat cycles when the temperature range was set for 25 ºC to 190 ºC.

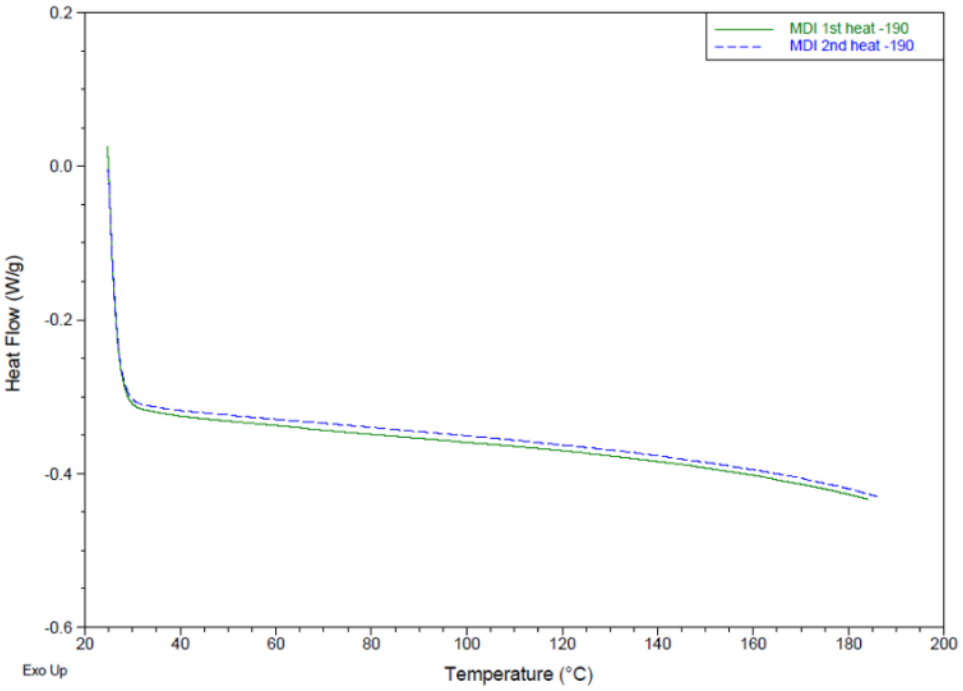

Figure 34. DSC Thermogram for MDI up to 190 ˚C

From the thermogram it can be seen that there was not a peak heat flow observed in either the 1st or 2nd heating cycles, indicating that the optimal curing temperature for MDI should be above 190 ºC. Heat flow did steadily increase from 25 ºC to 190 ºC indicating that some curing is occuring. The thermogram in Figure 35 shows the 1st heat and 2nd heat for MDI when using the 25 ºC to 300 ºC temperature range.

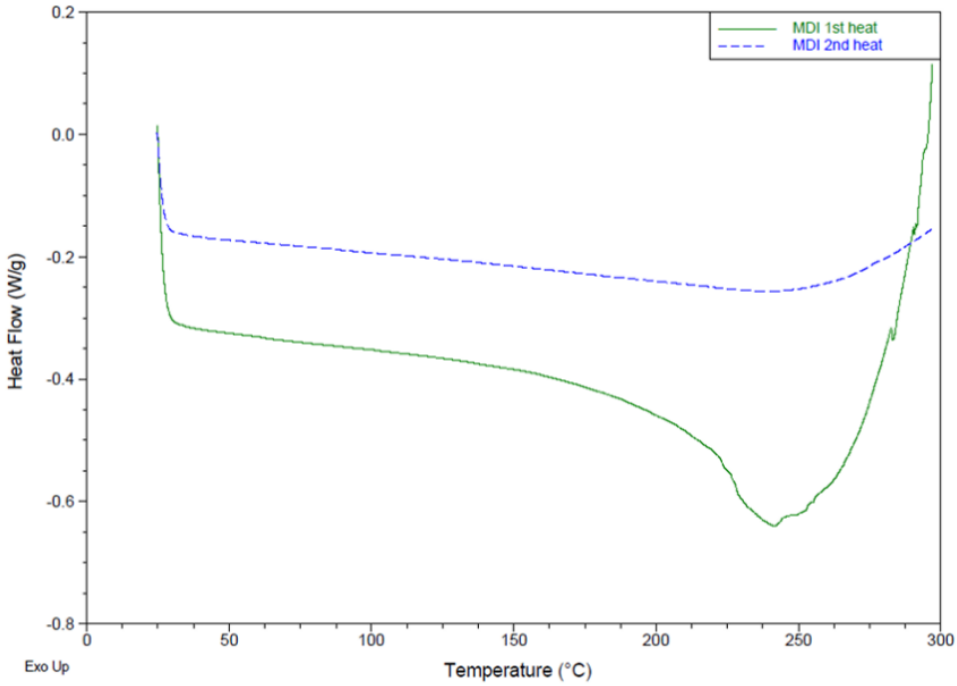

Figure 35. DSC Thermogram for MDI up to 300 ˚C

From the thermogram it can be seen that there was a peak endothermic heat flow observed in the 1st heating cycle, with an onset temperature of 158 ºC and a peak termperature at 241 ºC. The 2nd heat cycle had limited heat flow indicating that most of the sample was cured during the 1st heat cycle and that 241 ºC is an optimal heating level to induce curing. The thermogram in Figure 36 shows the 1st heat and 2nd heat for ESS-MDI when using the 25 ºC to 190 ºC temperature range.

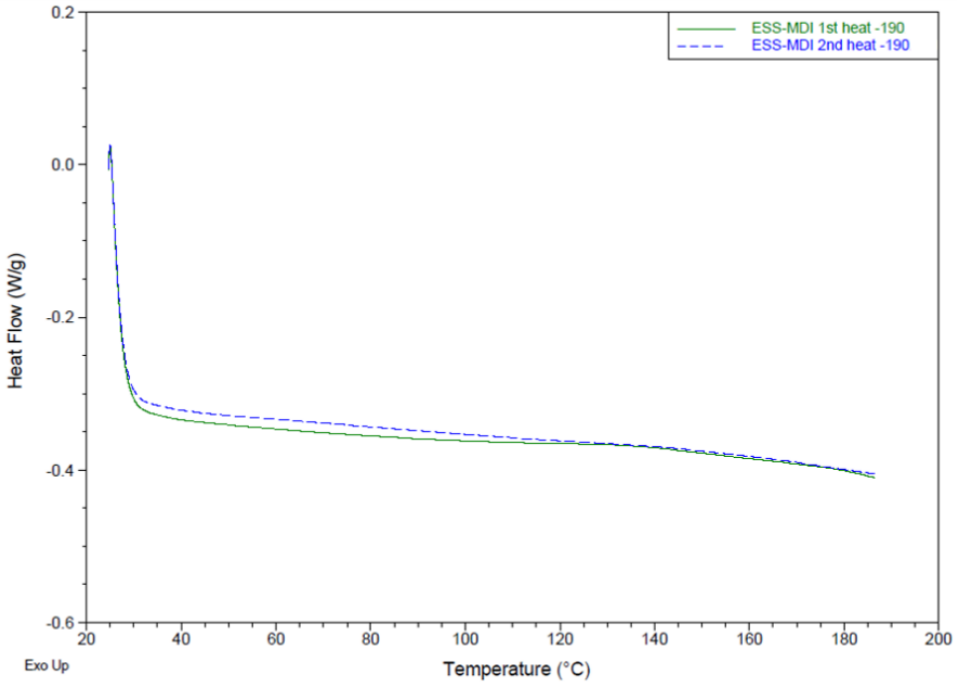

Figure 36. DSC Thermogram for ESS-MDI up to 190 ˚C

From the thermogram it can be seen that there was not a peak heat flow observed in either the 1st or 2nd heating cycles, indicating that the optimal curing temperature for ESS-MDI samples should be above 190 ºC. Heat flow did steadily increase from 25 ºC to 190 ºC indicating that some curing is occuring. The thermogram in Figure 37 shows the 1st heat and 2nd heat for MDI when using the 25 ºC to 300 ºC temperature range.

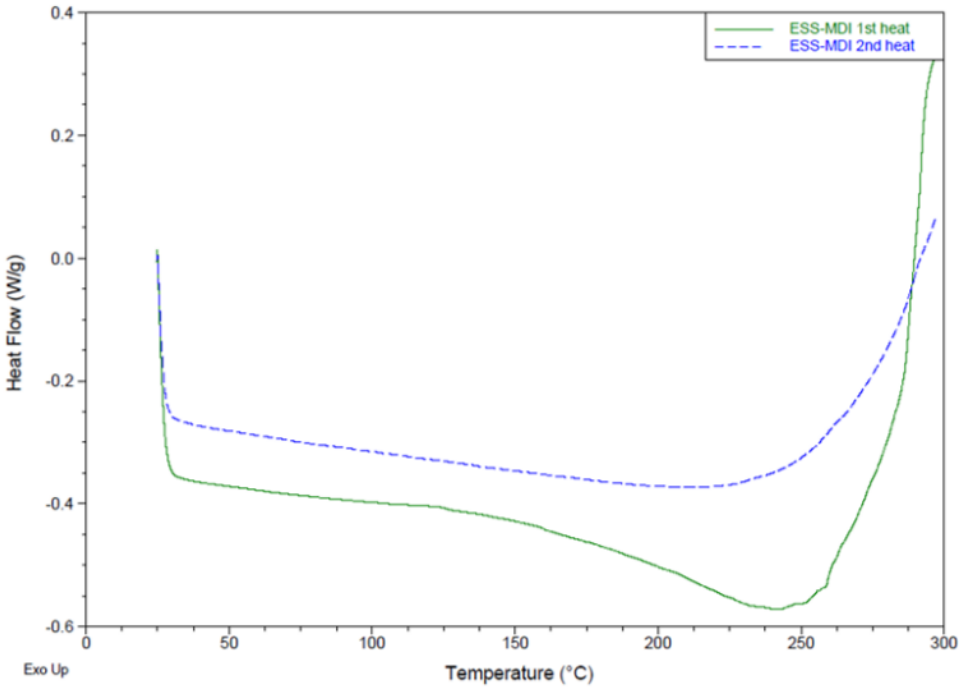

Figure 37. DSC Thermogram for ESS-MDI up to 300 ˚C

From the thermogram it can be seen that there was a peak endothermic heat flow observed in the 1st heating cycle, with an onset temperature of 150 ºC and a peak termperature at 241 ºC. The 2nd heat cycle had limited heat flow indicating that most of the sample was cured during the 1st heat cycle and that 241 ºC is an optimal heating level to induce curing. The endothermic peak is not as pronounced as the peak in the MDI sample, indicating that curing occurred on a more limited basis for the ESS-MDI mixtures. The DSC thermogram for the catalyzed reaction between phenyl glycidyl ether and MDI indicates that the two large exothermic peaks should occur, on at 175°C to indicate trimerisation of isocyanate to form isocyanurate and a second peak at 251°C to indicate formation of oxazolidone rings [34]. The reaction temperature peaks for oxazolidone and isocyanurate are not present, thus it cannot be confirmed that either reaction occurred. Also, there was no significant shift in the heat flow or

the peak temperatures from MDI to ESS-MDI samples indicating no clear evidence of a characteristic reaction between the two resins.

5.1.4. Fourier Transform Infrared Spectroscopy Results

Fourier transform infrared spectroscopy was used to determine what the functional groups of both MDI and ESS resins are and to determine if reactions occurred when they were mixed and cured and how that affected the chemical structure. The spectra collected included the wavenumbers from 500 cm^{-1} to 4000 cm^{-1}. Figure 38 shows the results for the MDI spectra.

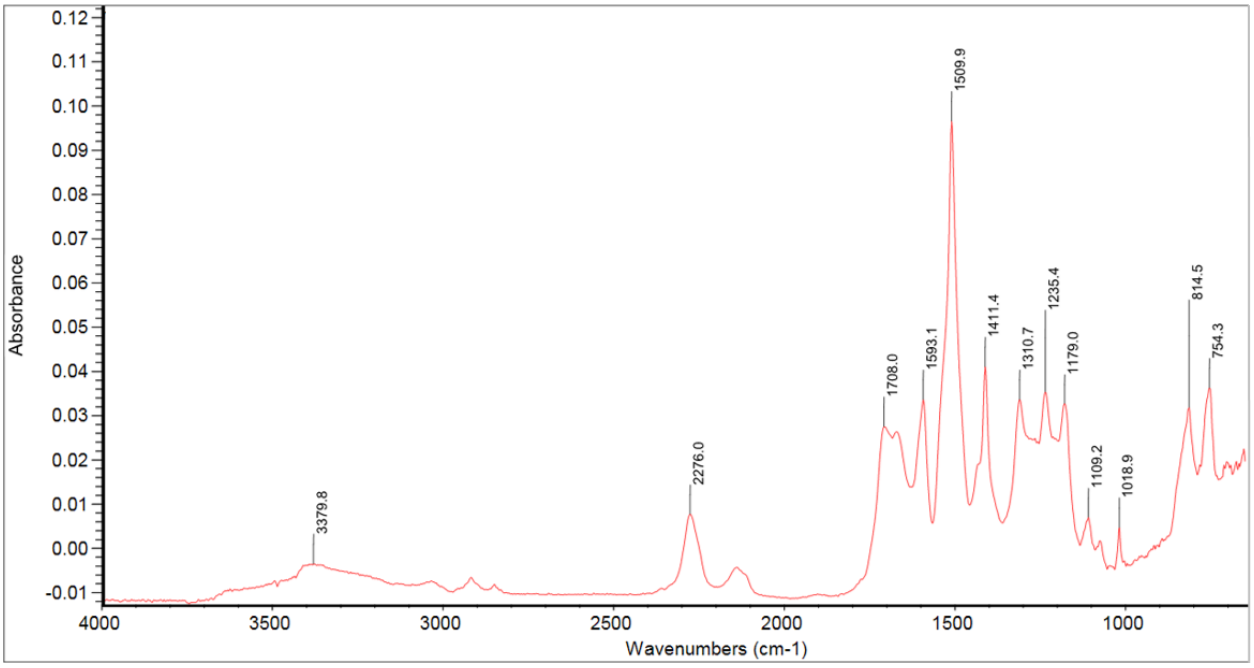

Figure 38. FTIR Spectra for Uncured MDI

The first notable peaks for the MDI resin at 2276 cm^{-1}, which is indicative of the functional isocyanate group (NCO). The peaks identified at 3050 cm^{-1}, 2200 cm^{-1}, and 1509 cm^{-1} are indicative of a para substituted aromatic hydrocarbon as identified by Nicolet's built in analysis software. The unmarked and low intensity peaks at approximately 2920 cm^{-1} and 2850

cm^{-1} correspond to methylene ($-CH_2-$). This analysis agrees with what MDI's chemical structure is, as it is a para substituted phenyl ring with isocyanate and methylene on opposite ends of the ring. Figure 39 shows the results for the FTIR spectra analysis for ESS.

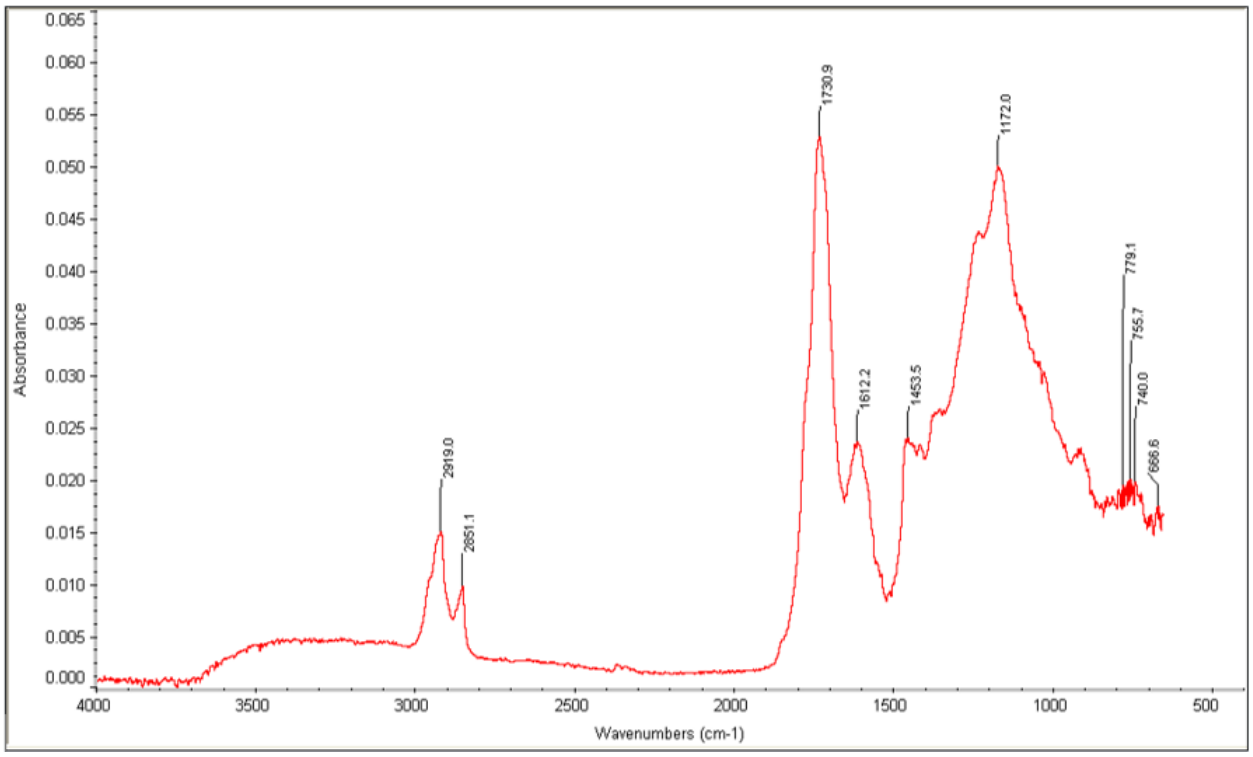

Figure 39. FTIR Spectra for Uncured ESS

The unmarked peak at 910 cm^{-1} is corresponds to an epoxide groups. The peak at 1730 cm^{-1} corresponds to sucrose esters (C=O stretch). The peak at 1172 cm^{-1} corresponds to C-O stretching inherent to esters as well. The peaks at 2919 cm^{-1} and 2851 cm^{-1} correspond to C-H stretching .Figure 40 shows the FTIR spectra obtained for the cured ESS-MDI samples.

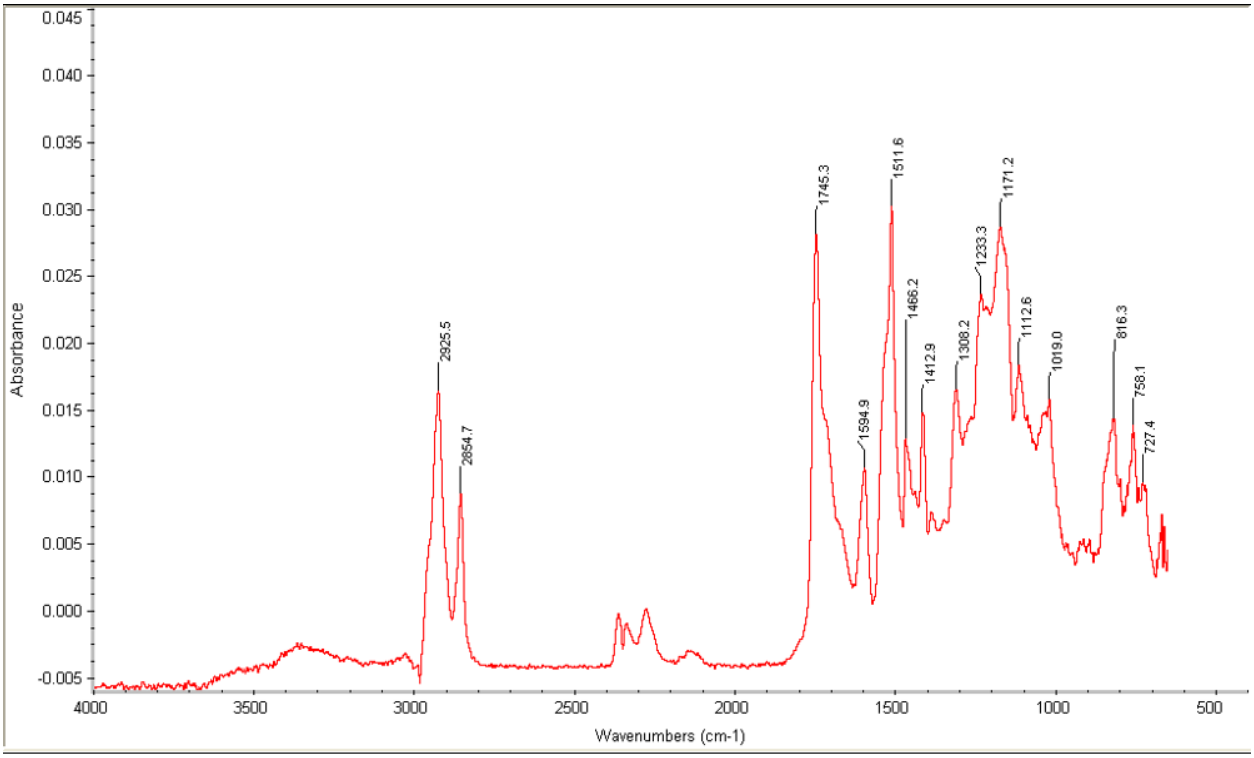

Figure 40. FTIR Spectra for ESS-MDI Resin at a 25:75 wt% Ratio

The ESS-MDI spectra's most important potential peaks would be for the isocyanurate and oxazolidone. Isocyanurate has a peak corresponding to 1710 cm^{-1} and oxazolidone has a peak corresponding to 1760 cm^{-1}. No distinct peaks were observed for oxazolidone or isocyanurate, with the peak at 1745 cm^{-1} likely corresponding to an ester peak (sucrose ester C=O stretch) and the peaks between 1000 cm^{-1} and 1300 cm^{-1} corresponding to C-O stretching inherent in esters, indicating the presence of unreacted ESS. Overall the reaction between the isocyanate and epoxide groups appears to be minimal if at all existent. The peak at 1594 cm^{-1} is for a primary alkyl amide ($-NH_2$), which is would indicate the presence of a urea structure, and the peak at 1511 cm^{-1} is indicative of N-O seen often in polyurethane structures, indicating that the MDI resin likely reacted with the hydroxyl groups of the ESS if any reaction between the two

resins did occur. Figure 41 shows the overlayed FTIR spectra for all of the five formulations tested.

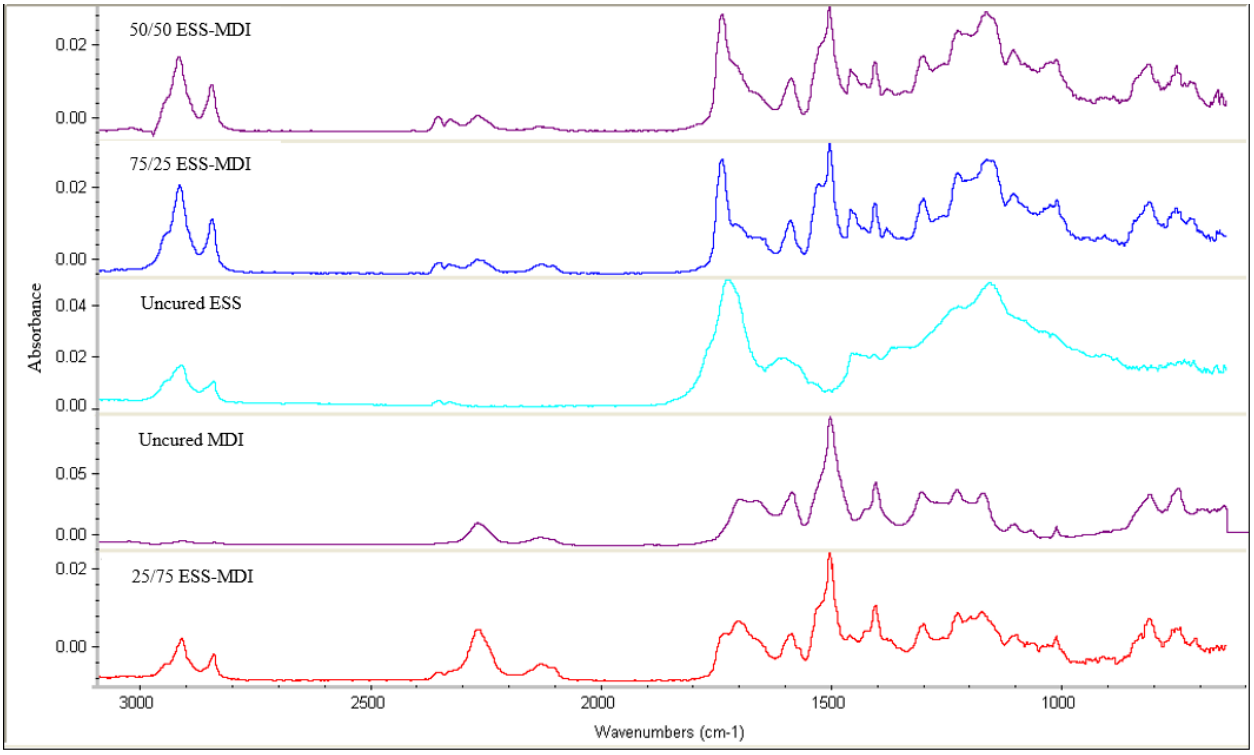

Figure 41. Combined FTIR Spectra

5.1.5. Soxhlet Extraction Results

The results of the soxhlet extraction can be summarized by the sol content calculated for the samples and the observed FTIR spectrum results. For the MDI samples, the sol percentage was found to be 1.2 ± 0.1%, indicating a high degree of stable curing occurred for the sample. The corollary to these results is that 98.8% of the sample remained in a solid state after extraction. FTIR was not performed for the MDI samples as the results are trivial to evaluation of the reaction and performance of the resin for this research. For the ESS-MDI samples, the sol percentage was found to be 7.3 ± 4.8%, indicating a relatively large percentage (92.7%) of the samples remained solid. However, the baseline MDI sol percentage must be taken into account

and the occurrence of trimerisation and formation of urea structures must be considered. The ESS-MDI mixture was created at 1:2 wt% ratio; assuming that at least 98.8% of the MDI would not be affected by the solvent extraction through formation of stable bonds, it can be calculated that only 81.5% of the ESS formed stable bonding. This is still a relatively high amount, but the FTIR results in Figure 42 provide greater clarity on unstable products of the reaction.

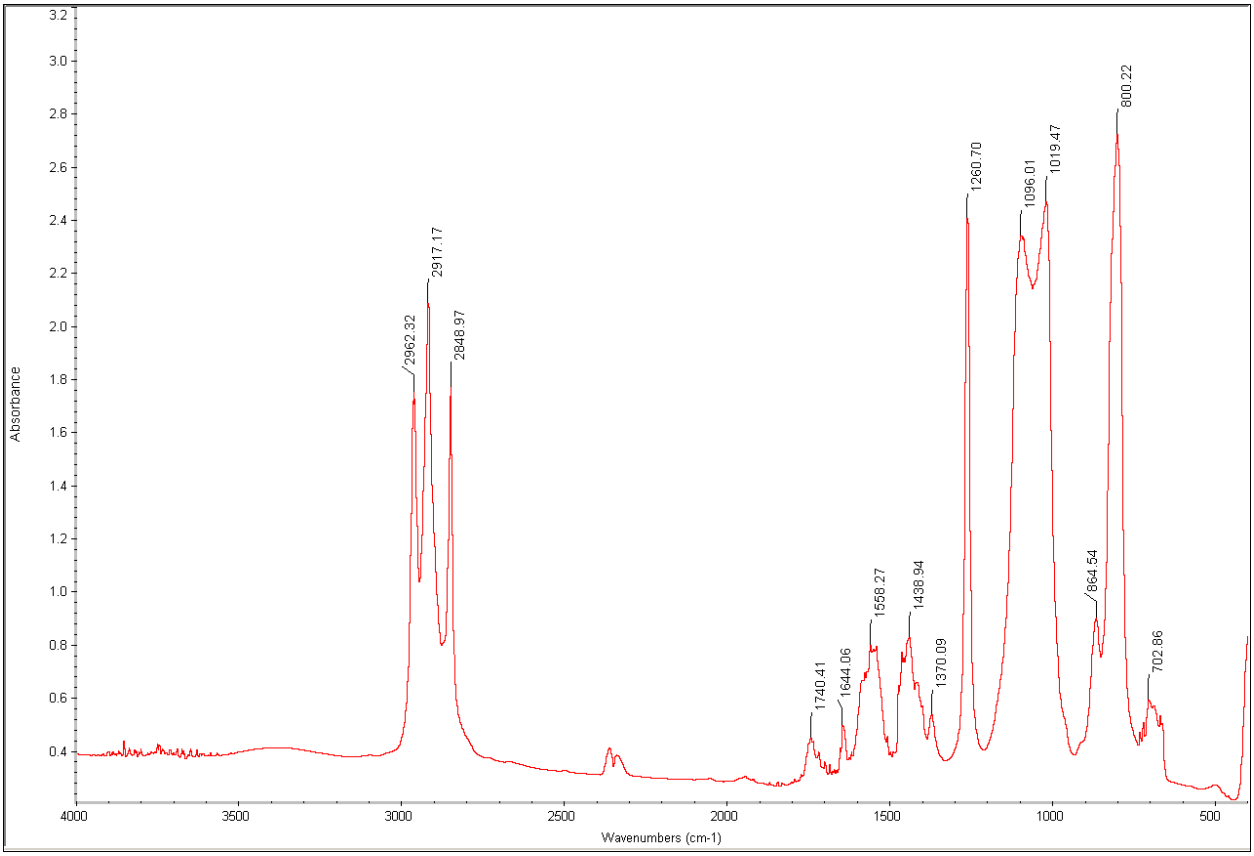

Figure 42. FTIR Spectra for ESS-MDI Gel

No isocyanate peaks remain at 2270 cm^{-1} indicating that all available functional isocyanate groups were consumed in reaction with epoxides, moisture, or through trimerisation. The peak at 2917 cm^{-1} corresponds to Methylene – CH_2 aliphatic compounds and the peak at 2962 cm^{-1} corresponds to Methyl – CH_3 aliphatic compound. The peak at 1260 cm^{-1} corresponds

to C-O-C in esters (C – O – C antisymmetric stretching). The peaks present indicate that little components of the MDI were present in the sol while several components of the ESS portion of the sample became soluble and are contained in the sol.

5.2. Mechanical and Physical Testing of Processed Boards Results and Analysis

This section includes the results obtained from the mechanical and physical testing of the lab-pressed boards. Tests performed and results found were for static bending, linear expansion, density, tension perpendicular to surface (internal bond), water absorption, direct screw withdrawal, and hardness. The main effects of the resin and fiber change were desired, but other effects were accounted for aside from those listed in the initial design of experiment, including what board was used to make the sample, whether the sample came from the edge or the center, and if testing samples post linear expansion samples caused detrimental effects. If post linear expansion proved to be significant, then the data obtained from this method was removed. Test results were measured against the results obtained for the wheat straw boards made using MDI resin that acted as the control value due to its use commercially with Masonite products.

5.2.1. Density Measurement Results

Density testing was conducted to determine the effect of resin choice and fiber choice on the density values. Boards do not need to meet a specific density value to be termed as a medium density board, but should ideally conform to ANSI A208.2 definitions for medium density fiberboard, where medium density boards are typically between 500 kg/m^3 and 1000 kg/m^3. ANSI 208.1 grade M boards typically have densities between 640 kg/m^3 and 800 kg/m^3. Six samples from each board were tested for density with an average density value determined

for each formulation. ANOVA analysis was used to determine significant factors in influencing the density with a 95% confidence interval used. A boxplot was constructed showing the average values for the linear expansion and the general spread of the data for each formulation. Figure 43 shows the boxplot.

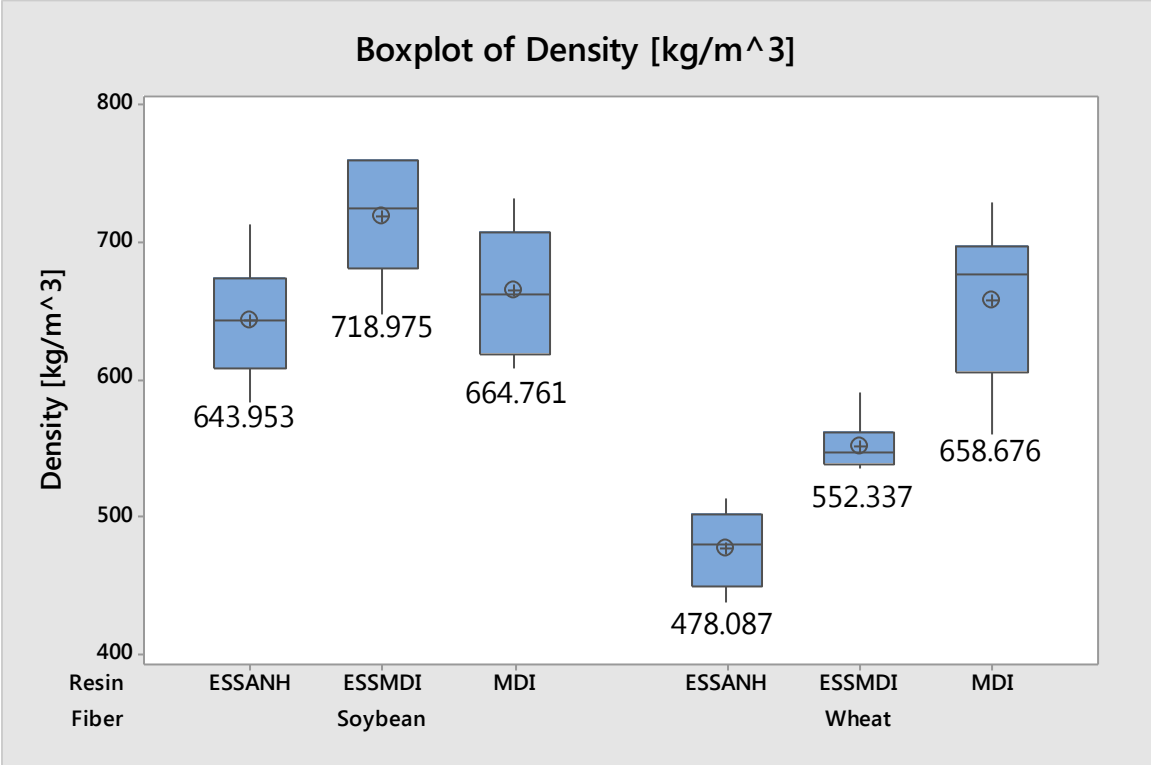

Figure 43. Boxplot of Density Data

The boxplot shows that most formulations were able to conform to the ANSI A208.2 and ANSI 208.1 grade M definitions for medium density boards. However, Wheat with ESS-MHHPA-DBU binder and Wheat with ESS-MDI binder boards were below standards and showed a sizable difference between other formulations in terms of density. These effects are likely due to previously unaccounted for compressibility issues or issues with maintaining mass or moisture content consistency between boards. Overall, no effects were observed in properties

due solely to the change in density between boards, thus no considerations were made to account for the difference in the analysis.

5.2.2. Water Absorption Results

Water absorption tests were conducted using four samples from each formulation to show the boards' resistance to taking on moisture. Properties of mass absorption and thickness absorption were measured at 2 and 24 hour periods to determine how the board weight and geometry would be altered at short uptake and long uptake periods. The samples should conform to the values obtained for the control wheat and MDI resin fiberboards. ANOVA analysis was used to determine significant factors in influencing the mass absorption and thickness swelling properties with a 95% confidence interval used.

5.2.2.1. Two Hour Mass Absorption Results

As part of method A for the water absorption testing in ASTM D1037, the water absorbed by the board samples should be measured at a two hour interval to determine initial water uptake values. A boxplot of the collected data can be seen in Figure 44. It should be noted that the wheat with ESS-MHHPA-DBU binder was excluded from the data as the samples became immeasurable due to water damage.

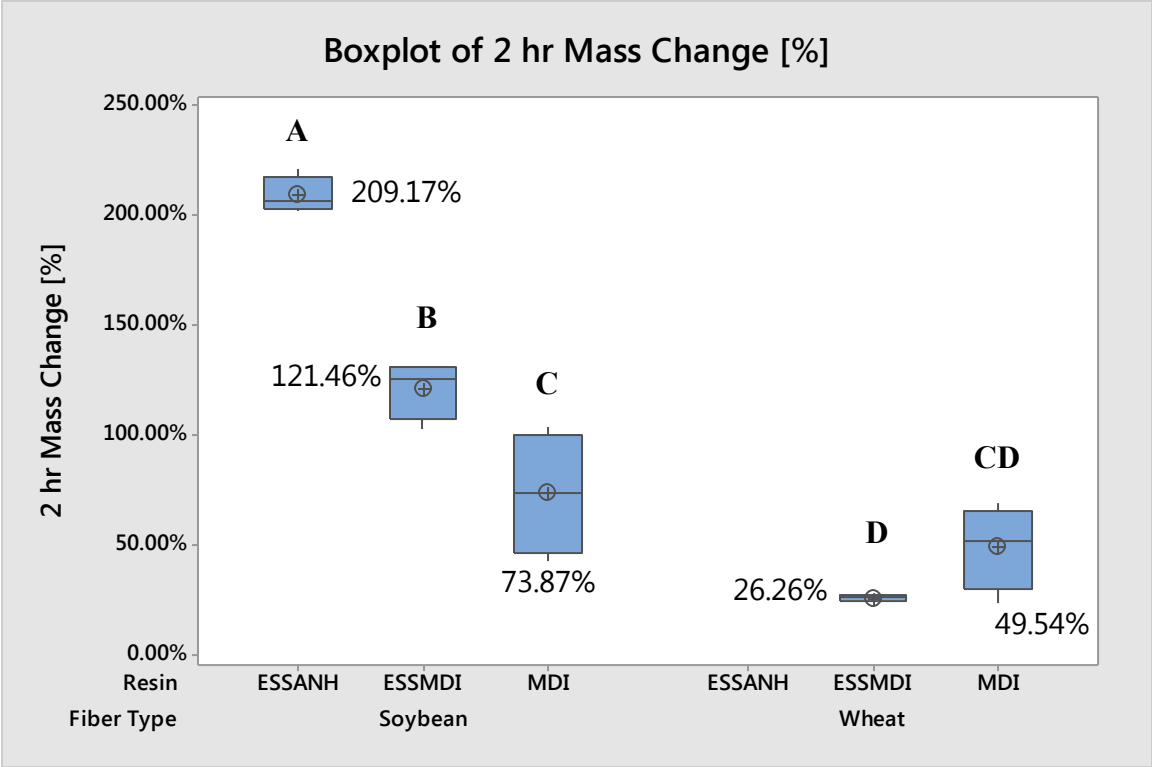

Figure 44. Boxplot of 2 Hour Mass Absorption Data

The boxplot shows significant changes between formulations, with Wheat ESS-MDI formulations showing the greatest performance. The Fisher's test grouping shown in Table A1 in the appendix shows that there are several groupings due to performance changes, with ESS-MHHPA-DBU blends causing significant decreases in properties observed. Overall, the only formulations that were in the same grouping as the control were the soybean and MDI boards and the wheat and ESS-MDI boards.

ANOVA analysis was conducted to determine the significant factors affecting the initial water absorption by mass observed in the boards. The board that the samples were cut from was included as a factor along with the type of fiber and resin as specified in the original design. The results of the ANOVA can be seen in Table A2 in the appendix. The initial ANOVA analysis shows that the resin choice and fiber choices were significant factors in affecting the initial water

absorption. The model accuracy was given by R^2 = 90.86%, with adjusted R^2 = 78.30%, indicating a good estimator of the variability in the initial mass absorption properties. A second ANOVA analysis was performed with the board factor removed to discount its effect and give a more accurate value for the R^2 and adjusted R^2 values. The revised ANOVA can be seen in Table A3 in the appendix. The revised ANOVA shows that the resin choice and fiber choices were the only significant factors affecting the water absorption. The model accuracy was given by R^2 = 89.59%, with adjusted R^2 = 87.63%, indicating the model has good adequacy in determining the variability in water absorption properties.

5.2.2.2. 24 Hour Mass Absorption Results

Water absorption for the 24 hour period was also measured for each formulation. A boxplot of the collected data can be seen in Figure 45. It should be noted that the Wheat with ESS-MHHPA-DBU binder was excluded from the data as the samples became immeasurable due to water damage.

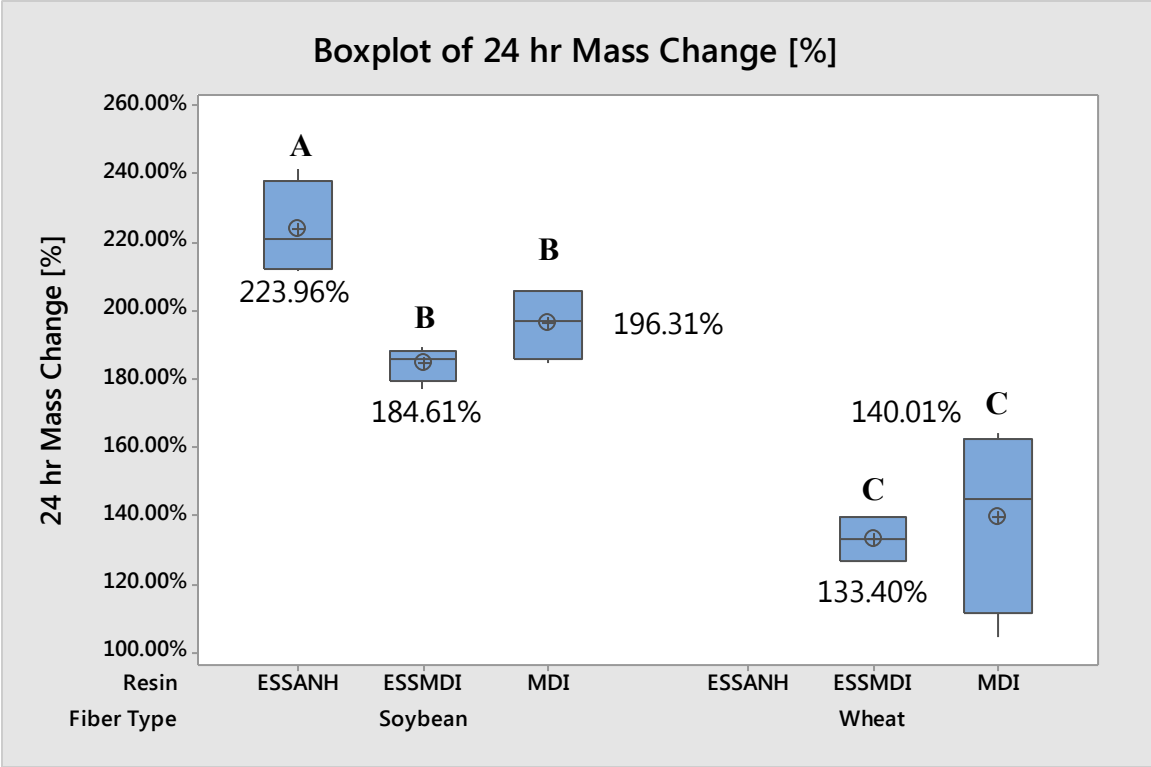

Figure 45. Boxplot of 24 Hour Mass Absorption Data

The boxplot shows significant changes between formulations, with Wheat ESS-MDI and Wheat MDI formulations showing the greatest performance. The Fisher's test grouping shown in Table A4 in the appendix shows that there are several groupings due to performance changes, with ESS-MHHPA-DBU blends causing significant decreases in properties observed. Only the wheat and ESS-MDI boards were able to meet the same performance standard as the control wheat and MDI boards.

ANOVA analysis was conducted to determine the significant factors affecting the equilibrated water absorption by mass observed in the boards. The board that the samples were cut from was included as a factor along with the type of fiber and resin as specified in the original design. The results of the ANOVA can be seen in Table A5 in the appendix. The initial ANOVA analysis shows that the resin choice and fiber choices were significant factors in

affecting the internal bond strength. The model accuracy was given by $R^2 = 94.01\%$, with adjusted $R^2 = 85.76\%$, indicating a good estimator of the variability in the equilibrated mass absorption properties. A second ANOVA analysis was performed with the board factor removed to discount its effect and give a more accurate value for the R^2 and adjusted R^2 values. The revised ANOVA can be seen in Table A6 in the appendix. The revised ANOVA shows that the resin choice and fiber choices were the only significant factors affecting the water absorption. The model accuracy was given by $R^2 = 87.50\%$, with adjusted $R^2 = 85.16\%$, indicating the model has good adequacy in determining the variability in water absorption properties.

5.2.2.3. Two Hour Thickness Swelling Results

Thickness swelling for the two hour period was measured for each formulation. A boxplot of the collected data can be seen in Figure 46. It should be noted that the Wheat with ESS-MHHPA-DBU binder was excluded from the data as the samples became immeasurable due to water damage.

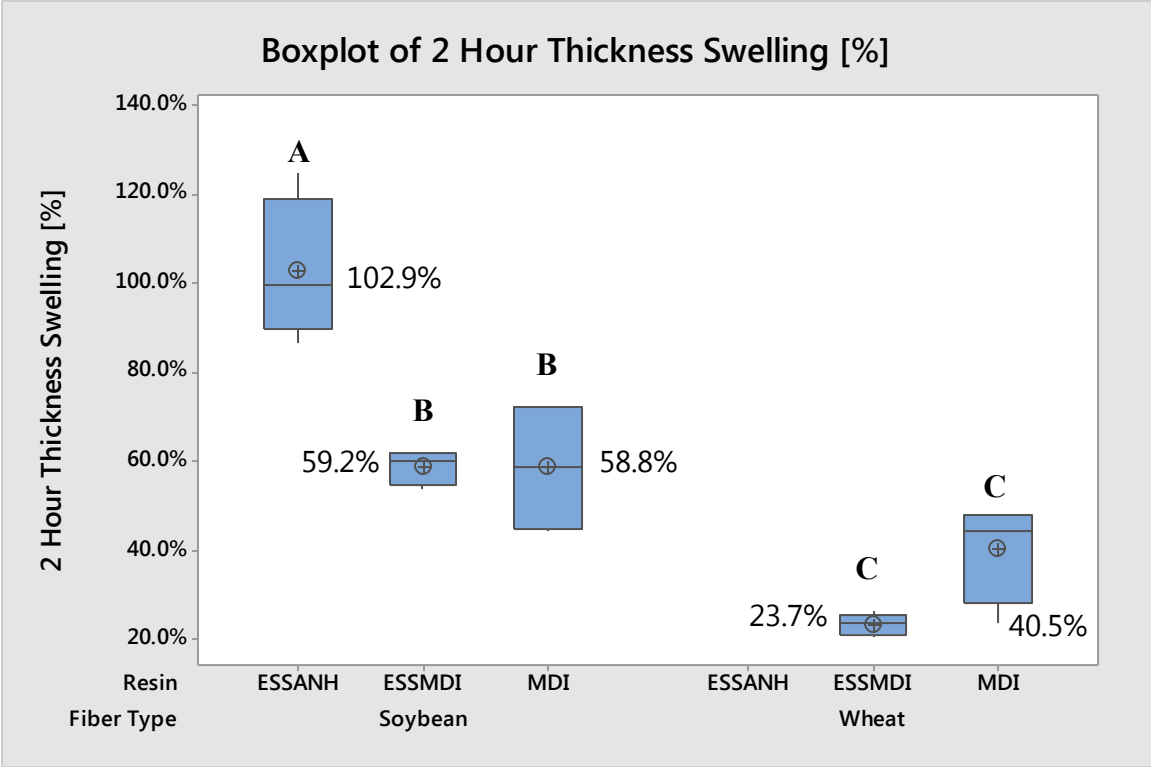

Figure 46. Boxplot of 2 Hour Thickness Swelling Data

The boxplot shows significant changes between formulations, with Wheat ESS-MDI and Wheat MDI formulations showing the greatest performance. The Fisher's test grouping shown in Table A7 in the appendix shows that there are several groupings due to performance changes, with ESS-MHHPA-DBU blends causing significant decreases in properties observed. Again the only formulation that was able to meet the performance of the control was the wheat and ESS-MDI boards.

ANOVA analysis was conducted to determine the significant factors affecting the thickness swelling observed in the boards. The board that the samples were cut from was included as a factor along with the type of fiber and resin as specified in the original design. The results of the ANOVA can be seen in Table A8 in the appendix. The initial ANOVA analysis shows that the resin choice and fiber choices were significant factors in affecting the internal

bond strength. The model accuracy was given by R^2 = 94.19%, with adjusted R^2 = 86.20%, indicating a good estimator of the variability in the equilibrated mass absorption properties. A second ANOVA analysis was performed with the board factor removed to discount its effect and give a more accurate value for the R^2 and adjusted R^2 values. The revised ANOVA can be seen in Table A9 in the appendix. The revised ANOVA shows that the resin choice and fiber choices were the only significant factors affecting the water absorption. The model accuracy was given by R^2 = 86.04%, with adjusted R^2 = 83.42%, indicating the model has good adequacy in determining the variability in water absorption properties.

5.2.2.4. 24 Hour Thickness Swelling Results

Thickness swelling for the 24 hour period was measured for each formulation. A boxplot of the collected data can be seen in Figure 47. It should be noted that the Wheat with ESS-MHHPA-DBU binder was excluded from the data as the samples became immeasurable due to water damage.

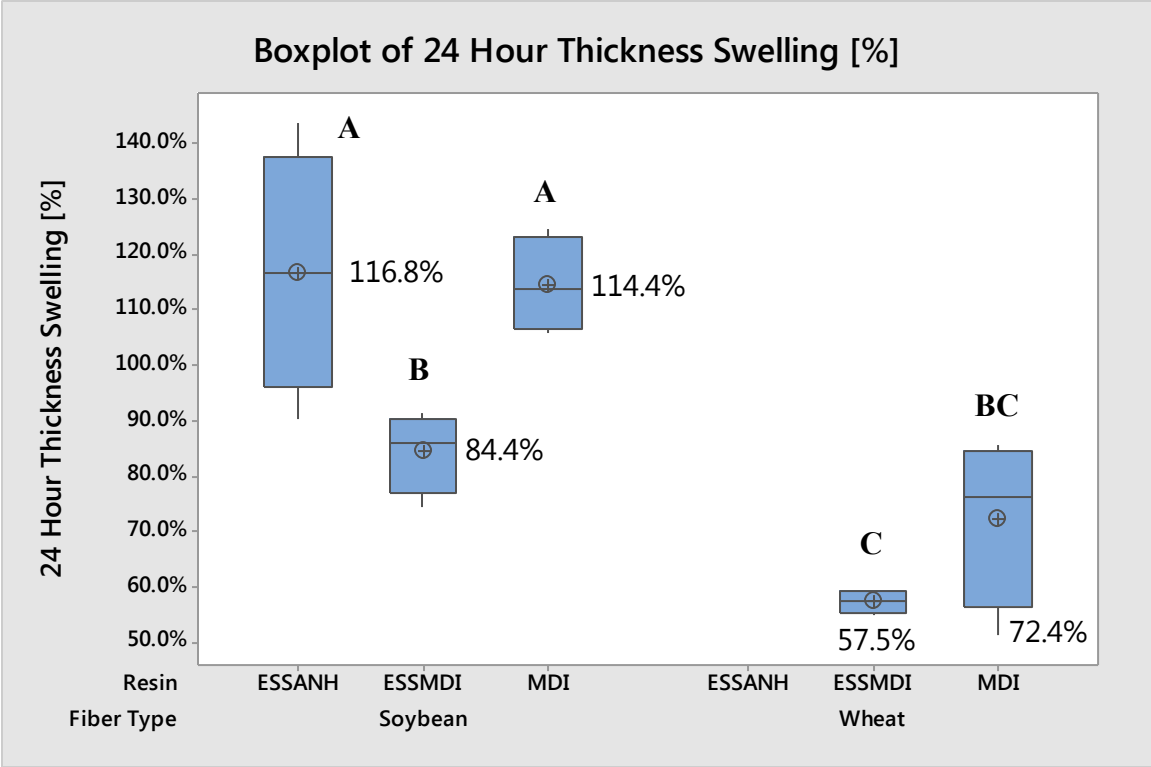

Figure 47. Boxplot of 24 Hour Thickness Swelling Data

The boxplot shows significant changes between formulations, with Wheat ESS-MDI formulations showing the greatest performance. The Fisher's test grouping shown in Table A10 in the appendix shows that there are several groupings due to performance changes, with the soybean fiber boards exhibiting significant decreases in properties observed. Overall, only the wheat and ESS-MDI boards and the soybean and ESS-MDI boards were able to remain in the same statistical grouping as the control wheat with MDI binder boards.

ANOVA analysis was conducted to determine the significant factors affecting the thickness swelling observed in the boards. The board that the samples were cut from was included as a factor along with the type of fiber and resin as specified in the original design. The results of the ANOVA can be seen in Table A11 in the appendix. The initial ANOVA analysis shows that the resin choice and fiber choices were significant factors in affecting the internal

bond strength. The model accuracy was given by R^2 = 92.70%, with adjusted R^2 = 82.67%, indicating a good estimator of the variability in the equilibrated mass absorption properties. A second ANOVA analysis was performed with the board factor removed to discount its effect and give a more accurate value for the R^2 and adjusted R^2 values. The revised ANOVA can be seen in Table A12 in the appendix. The revised ANOVA shows that the resin choice and fiber choices were the only significant factors affecting the thickness swelling. The model accuracy was given by R^2 = 79.47%, with adjusted R^2 = 75.62%, indicating the model has moderate adequacy in determining the variability in water absorption properties.

5.2.3. Linear Expansion Results

Linear expansion testing was conducted to determine the effect of resin choice and fiber choice on the relative expansion of boards in the linear dimension. Boards should ideally conform to the linear expansion experienced by the control wheat with MDI resin boards. Linear expansion testing shows the resistance to expansion under high humidity. Five samples from each board were tested for the linear expansion with an average linear expansion value determined for each formulation. ANOVA analysis was used to determine significant factors in influencing the linear expansion with a 95% confidence interval used. A boxplot was constructed showing the average values for the linear expansion and the general spread of the data for each formulation. Figure 48 shows the boxplot.

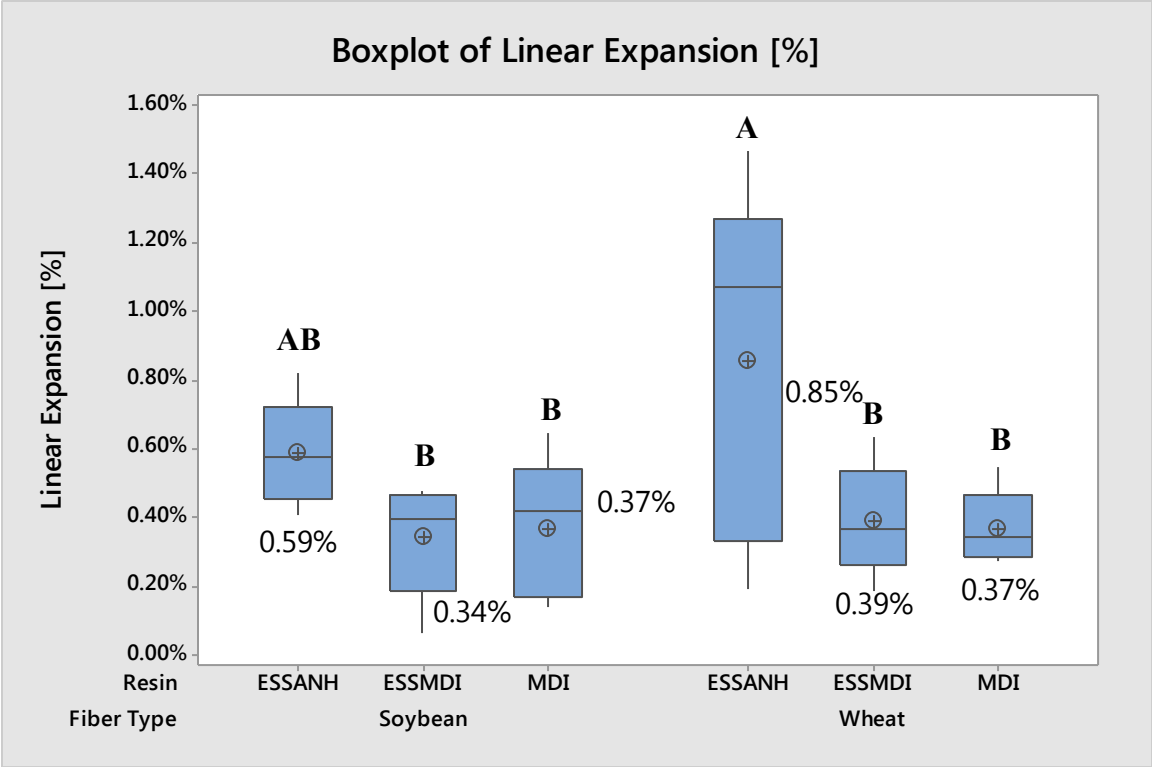

Figure 48. Boxplot of Linear Expansion Data

The boxplot shows minimal change between formulations, with the ESS-ANH resin boards showing relatively poor results. The Fisher's test grouping shown in Table A13 in the appendix shows that there are several groupings due to performance changes, with ESS-MHHPA-DBU blends causing significant decreases in properties observed. Only the wheat with ESS-MHHPA-DBU binder was not able to meet the same performance standards as that of the wheat with MDI resin boards.

ANOVA analysis was conducted to determine the significant factors affecting the linear expansion observed in the boards. Several testing factors beyond the initial factors considered for the design of experiment were included to determine if separation of panels affected properties. The board that the sample was cut from and whether the sample was cut from the edge or center of the board were included factors along with the type of fiber and resin as

specified in the original design. The results of the ANOVA can be seen in Table A14 in the appendix. The initial ANOVA analysis shows that there were no significant factor affecting the linear expansion. The model accuracy was given by $R^2 = 78.79\%$, with adjusted $R^2 = 20.37\%$, indicating a relatively poor estimator of the variability in the linear expansion properties. A second ANOVA analysis was performed with the board and edge or center factors removed to discount their effects and give a more accurate value for the R^2 and adjusted R^2 values. The revised ANOVA can be seen in Table A15 in the appendix. The revised ANOVA shows that the resin was the most influential factor, while fiber choice does not have a significant effect. The model accuracy was given by $R^2 = 39.17\%$, with adjusted $R^2 = 26.50\%$, indicating the model has poor accuracy in determining the variability in linear expansion properties. Based on these results, more factors affect the linear expansion than were accounted for in the initial design of experiment, indicating more variables may need to be controlled to produce the desired linear expansion.

5.2.4. Static Bending Results

Static Bending tests were conducted to determine the effect of resin choice and fiber choice on the modulus of rupture (MOR) and the modulus of elasticity (MOE) of the pressed boards. Boards should ideal conform to the same performance as that found for the wheat with MDI resin boards. Ten samples from each board formulation were tested with the MOE and MOR determined as an average value for each formulation. ANOVA analysis was used to determine significant factors in influencing the MOE and MOR with a 95% confidence interval used.

5.2.4.1. Modulus of Rupture

The modulus of rupture represents the maximum flexure strength that the board can experience before failure. A boxplot was constructed showing the average values for the MOR and the general spread of the data for each formulation. Figure 49 shows the boxplot.

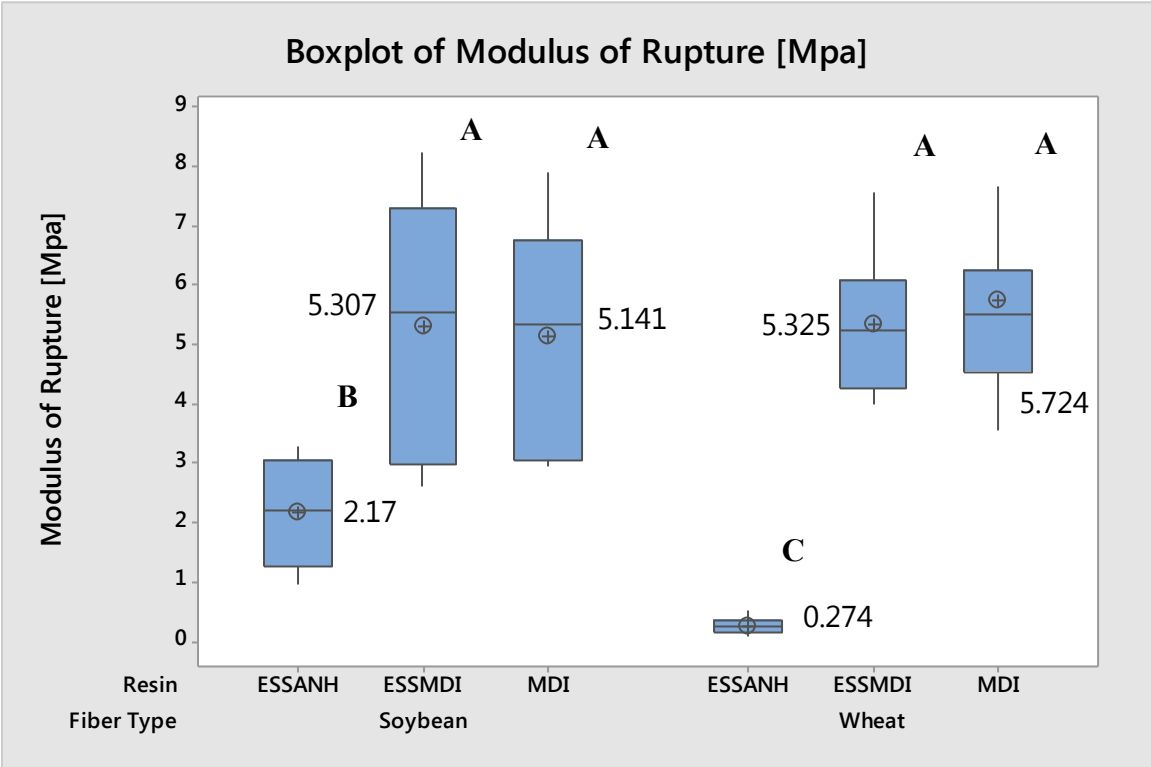

Figure 49. Boxplot of Modulus of Rupture Data

The boxplot shows that change in fiber and the differences experienced between EES-MDI and pure MDI binders were small. The Fisher's test grouping shown in Table A16 in the appendix shows that there was little change in performance between the formulations except for those formulations where ESS-MHHPA-DBU blends were implemented, were significant decreases in properties were observed. Only the two formulations that utilized the ESS-MHHPA-DBU binder system were not able to perform to the same standards as those of the wheat with MDI resin boards.

ANOVA analysis was conducted to determine the significant factors affecting the modulus of rupture values observed in the boards. Several testing factors beyond the initial factors considered for the design of experiment were included to determine if separation of panels affected properties. The board that the sample was cut from, whether the sample was cut from the edge or center of the board, and whether the board was tested after linear expansion or not were included factors along with the type of fiber and resin as specified in the original design. The results of the ANOVA can be seen in Table A17 in the appendix. The initial ANOVA analysis shows that the resin choice and the interaction between the fiber and resin choice and the fiber type and edge or center were significant factors in affecting the MOR. The model accuracy was given by $R^2 = 85.42\%$, with adjusted $R^2 = 71.33\%$, indicating a relatively good estimator of the variability in the MOR properties. A second ANOVA analysis was performed with the board and post linear expansion factors removed to discount their effects and give a more accurate value for the R^2 and adjusted R^2 values. The revised ANOVA can be seen in Table A18 in the appendix. The revised ANOVA shows that the resin and fiber type and the interaction between the fiber choice and the edge or center sample position were the most influential factors. The model accuracy was given by $R^2 = 75.06\%$, with adjusted $R^2 = 70.57\%$, indicating the model has moderate accuracy in determining the variability in MOR properties. The presence of the sample's position within the board having an effect on board properties indicates that there is inherent variability in the board manufacturing process implemented that affects the consistency of properties within each board.

5.2.4.2. Modulus of Elasticity

The modulus of elasticity represents the stiffness that the board has during initial loading before unrecoverable deformation occurs. A boxplot was constructed showing the average values for the MOE and the general spread of the data for each formulation. Figure 50 shows the boxplot.

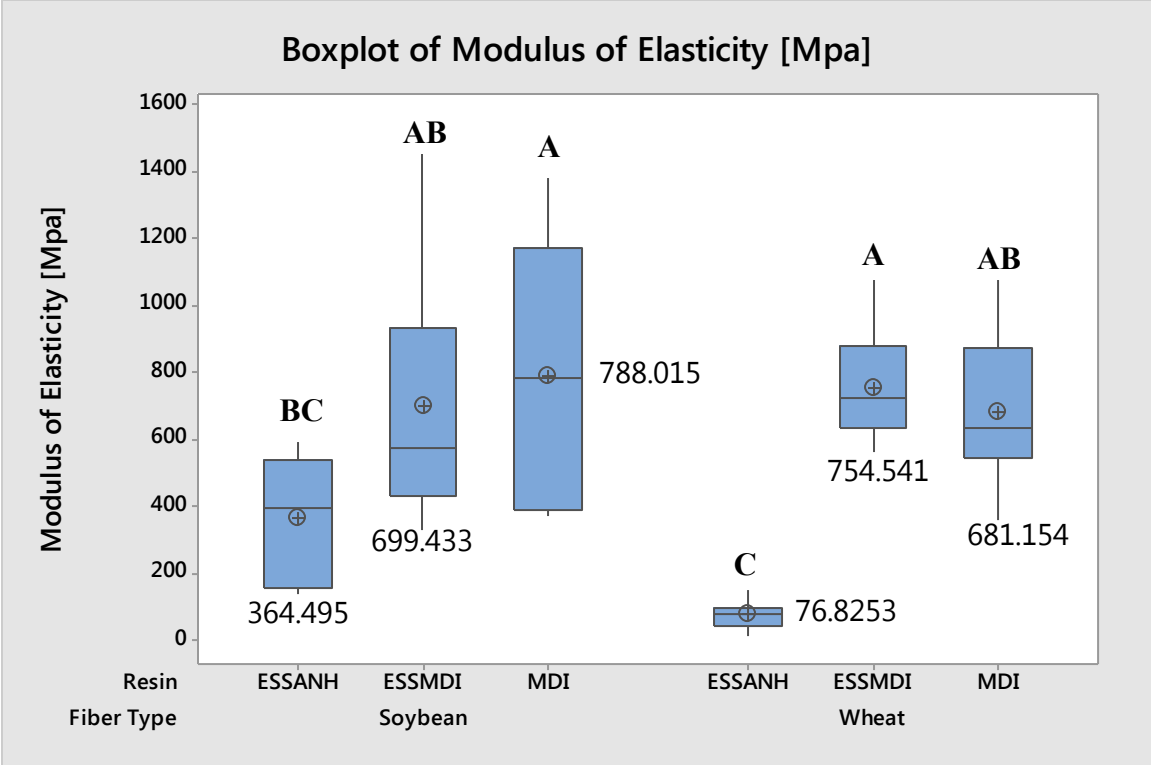

Figure 50. Boxplot of Modulus of Elasticity Data

The boxplot shows that changes were caused mostly by resin choice. The Tukey's test grouping shown in Table A19 in the appendix shows that there are several groupings due to performance changes, with ESS-MHHPA-DBU blends causing significant decreases in properties observed. The only formulation that was not able to conform to the performance standards of the wheat with MDI control was the wheat with ESS-MHHPA-DBU resin binder.

ANOVA analysis was conducted to determine the significant factors affecting the modulus of elasticity values observed in the boards. Several testing factors beyond the initial factors considered for the design of experiment were included to determine if separation of panels affected properties. The board that the sample was cut from, whether the sample was cut from the edge or center of the board, and whether the board was tested after linear expansion or not were included factors along with the type of fiber and resin as specified in the original design. The results of the ANOVA can be seen in Table A20 in the appendix. The initial ANOVA analysis shows that the resin choice was the only significant factor in affecting the MOR. The model accuracy was given by $R^2 = 73.79\%$, with adjusted $R^2 = 48.45\%$, indicating a relatively poor estimator of the variability in the MOE properties. A second ANOVA analysis was performed with the board, edge or center, and post linear expansion factors removed to discount their effects and give a more accurate value for the R^2 and adjusted R^2 values. The revised ANOVA can be seen in Table A21 in the appendix. The revised ANOVA shows that the resin was the most influential factor, while fiber choice does not have a significant effect. The model accuracy was given by $R^2 = 52.76\%$, with adjusted $R^2 = 48.38\%$, indicating the model has poor accuracy in determining the variability in MOE properties. Based on these results, more factors affect the modulus of elasticity than were accounted for in the initial design of experiment, indicating more variables may need to be controlled to produce the desired modulus of elasticity.

5.2.5. Tension Perpendicular to Surface (Internal Bond) Results

Tension perpendicular to surface or internal bond testing was conducted to determine the effect of resin choice and fiber choice on the board's resistance to internal failure. The samples

from each formulation should ideally perform to the same standard or greater than that of the control wheat with MDI resin formulation. The internal bond test shows the internal adhesion of fibers within the boards. Six samples from each board were tested for the internal bond strength with an average strength determined for each formulation. ANOVA analysis was used to determine significant factors in influencing the hardness with a 95% confidence interval used. A boxplot was constructed showing the average values for the internal bond strength and the general spread of the data for each formulation. Figure 51 shows the boxplot.

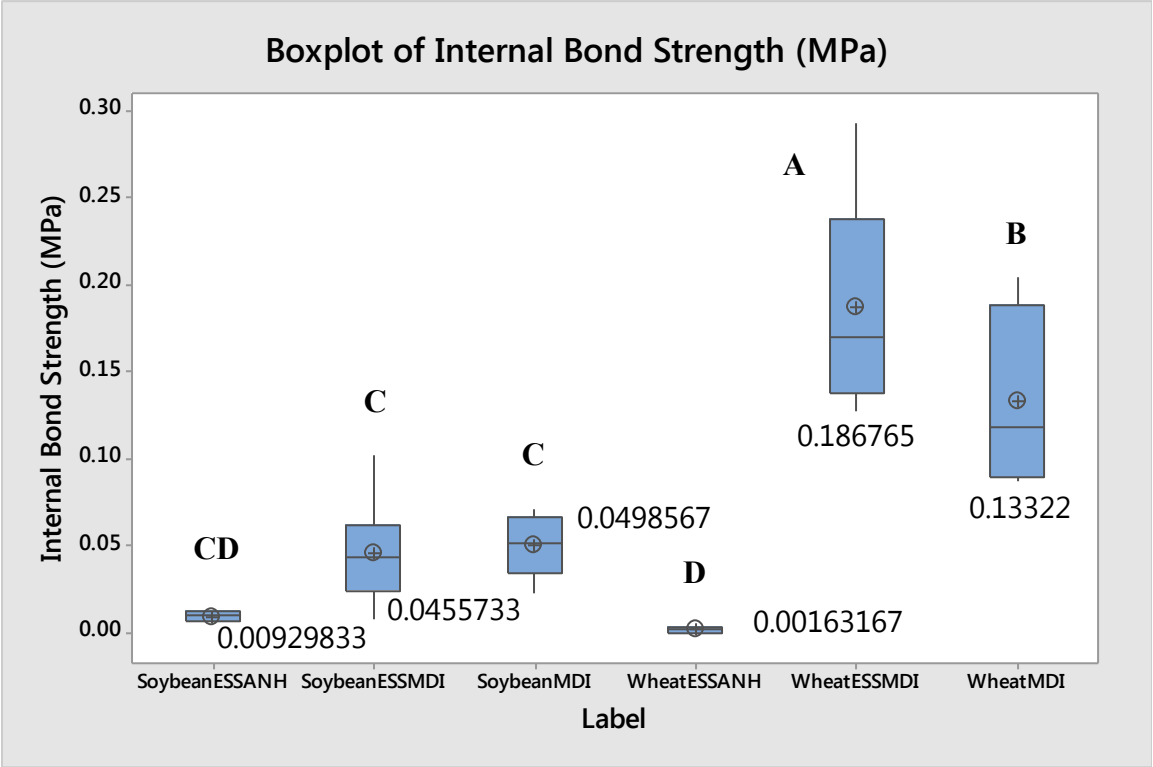

Figure 51. Boxplot of Internal Bond Data

The boxplot shows significant changes between formulations, with Wheat ESS-MDI formulations showing the greatest performance. The Fisher's test grouping shown in Table A22 in the appendix shows that there are several groupings due to performance changes, with ESS-

MHHPA-DBU blends causing significant decreases in properties observed. Only the wheat with ESS-MDI binder was able to perform to the same level as the control, even falling into its own category based on Fisher's grouping. None of the soy straw fiber formulations were able to perform up to the control level, indicating that poor bonding between fibers occurred for those formulations.

ANOVA analysis was conducted to determine the significant factors affecting the internal bond strength observed in the boards. The board that the samples were cut from was included as a factor along with the type of fiber and resin as specified in the original design. The results of the ANOVA can be seen in Table A23 in the appendix. The initial ANOVA analysis shows that the resin choice and fiber choices as well as their interaction were significant factors in affecting the internal bond strength. The model accuracy was given by $R^2 = 84.24\%$, with adjusted $R^2 = 78.78\%$, indicating a moderate estimator of the variability in the internal bond properties. A second ANOVA analysis was performed with the board factor removed to discount its effect and give a more accurate value for the R^2 and adjusted R^2 values. The revised ANOVA can be seen in Table A24 in the appendix. The revised ANOVA shows that the resin choice and fiber choices as well as their interaction were significant factors in affecting the internal bond strength. The model accuracy was given by $R^2 = 81.15\%$, with adjusted $R^2 = 78.00\%$, indicating the model has moderate adequacy in determining the variability in internal bonding properties.

5.2.6. Direct Screw Withdrawal

Direct screw withdrawal testing was conducted to determine the effect of resin choice and fiber choice on the screw withdrawal resistance. Boards should ideally perform at the same

level as the wheat with MDI binder control formulation. The direct screw withdrawal test shows the resistance to fastener withdrawal for the face of the board. Ten samples from each board were tested for the screw withdrawal load with an average load determined for each formulation. ANOVA analysis was used to determine significant factors in influencing the screw withdrawal resistance with a 95% confidence interval used. A boxplot was constructed showing the average values for the direct screw withdrawal load and the general spread of the data for each formulation. Figure 52 shows the boxplot.

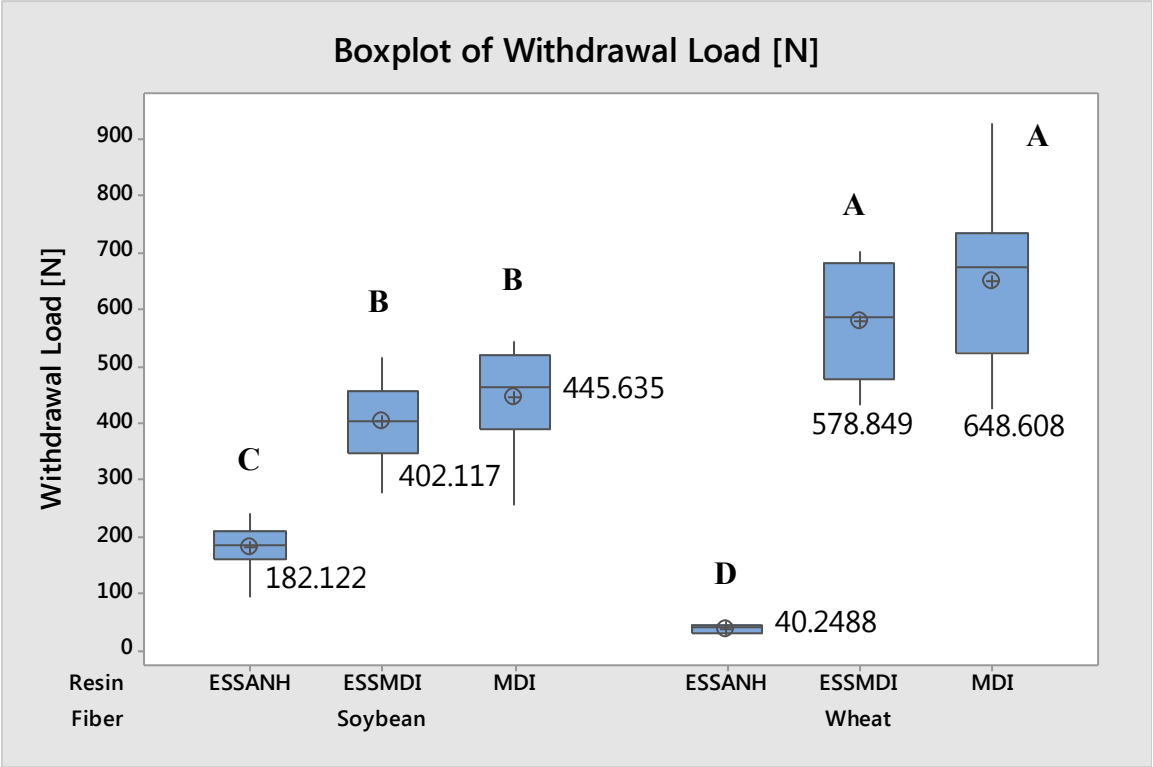

Figure 52. Boxplot of Direct Screw Withdrawal Data

The boxplot shows that wheat fibers improved the performance while ESS-MHHPA-DBU resin significantly decreased performance. The Tukey's test grouping shown in Table A25 in the appendix shows that ESS-MHHPA-DBU blends yielded a significant decrease in

properties, while using wheat as the fiber instead of soybean improved screw withdrawal resistance. The wheat with ESS-MDI binder was able to perform to the same level as the wheat with MDI control while all other formulations had lower performance values. Again this indicates poor bonding between fibers for the soy straw formulations.

ANOVA analysis was conducted to determine the significant factors affecting the direct screw withdrawal load observed in the boards. Several testing factors beyond the initial factors considered for the design of experiment were included to determine if separation of panels affected properties. The board that the sample was cut from, whether the sample was cut from the edge or center of the board, and whether the board was tested after linear expansion or not were included factors along with the type of fiber and resin as specified in the original design. The results of the ANOVA can be seen in Table A26 in the appendix. The initial ANOVA analysis shows that the fiber choice, resin choice, the sample's location in the board, and the interaction between the fiber and resin choice and the fiber type and edge or center were significant factors in affecting the MOR. The model accuracy was given by $R^2 = 94.50\%$, with adjusted $R^2 = 89.18\%$, indicating a relatively good estimator of the variability in the screw withdrawal resistance properties. A second ANOVA analysis was performed with the board and post linear expansion factors removed to discount their effects and give a more accurate value for the R^2 and adjusted R^2 values. The revised ANOVA can be seen in Table A27 in the appendix. The revised ANOVA shows that the resin, fiber type, the sample's position within the board and the interaction between the fiber choice and the resin choice were the most influential factors. The model accuracy was given by $R^2 = 88.69\%$, with adjusted $R^2 = 86.98\%$, indicating the model has good accuracy in determining the variability in the screw withdrawal properties. The presence of the sample's position within the board having an effect on board properties indicates

that there is inherent variability in the board manufacturing process implemented that affects the consistency of properties within each board.

5.2.7. Hardness Testing Results

Hardness testing was conducted to determine the effect of resin choice and fiber choice on the board's resistance to deformation. Boards should ideally perform to the same level as the control wheat with MDI binder formulation. The hardness test shows the local resistance to deformation for the face of the board. Eight samples from each board were tested for the hardness load with an average load determined for each formulation. ANOVA analysis was used to determine significant factors in influencing the hardness with a 95% confidence interval used. A boxplot was constructed showing the average values for the hardness load and the general spread of the data for each formulation. Figure 53 shows the boxplot.

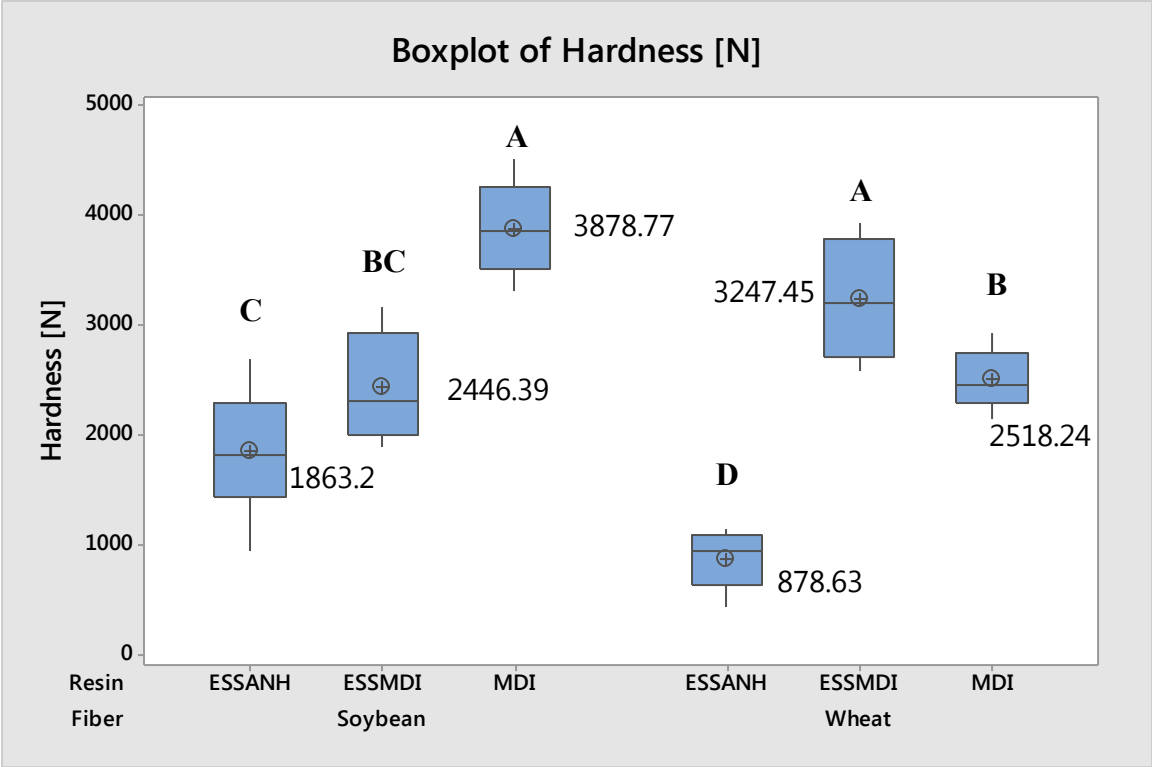

Figure 53. Boxplot of Hardness Testing Data

The boxplot shows that the resin choice and fiber choice had significant effects, with complex combinations of both having an effect on the hardness properties. The Tukey's test grouping shown in Table A28 in the appendix shows that ESS-MHHPA-DBU blends yielded a significant decrease in properties, while MDI was the best choice for soybean fiberboards and an ESS-MDI blend performed best for wheat fiberboards. The only formulations that were not able to meet or outperform the control formulation were the formulations that utilized the ESS-MHHPA-DBU binder. The soy straw with MDI binder and the wheat straw with ESS-MDI formulations were able to outperform the wheat with MDI control formulation.

ANOVA analysis was conducted to determine the significant factors affecting the hardness load observed in the boards. Several testing factors beyond the initial factors considered for the design of experiment were included to determine if separation of panels

affected properties. The board that the sample was cut from, whether the sample was cut from the edge or center of the board, and whether the board surface was the top or bottom were included factors along with the type of fiber and resin as specified in the original design. The results of the ANOVA can be seen in Table A29 in the appendix. The initial ANOVA analysis shows that the fiber choice, resin choice, the board number chosen, and the interaction between the resin and board and the fiber and resin were significant factors in affecting the hardness. The model accuracy was given by $R^2 = 91.11\%$, with adjusted $R^2 = 87.33\%$, indicating a relatively good estimator of the variability in the surface hardness properties. A second ANOVA analysis was performed with the top or bottom surface factor removed to discount its effects and give a more accurate value for the R^2 and adjusted R^2 values. The revised ANOVA can be seen in Table A30 in the appendix. The revised ANOVA shows that the resin, fiber type, the board and the interaction between the resin and board and the fiber and resin remained significant factors in affecting the hardness. The model accuracy was given by $R^2 = 90.24\%$, with adjusted $R^2 = 87.93\%$, indicating the model has good accuracy in determining the variability in the screw withdrawal properties. The presence of the board used to make the sample being a significant factor in affecting hardness indicates variability in the board manufacturing process that affects the properties of the boards, which is an undesirable factor.

5.3. Hammer Milling of Straw Fibers Results and Analysis

This section covers the results of the hammer milling of soybean and wheat straw at various conditions. The most notable results obtained for each condition were that of the fines content and viable fraction.

The average fiber distribution for each formulation was obtained by averaging the distributions observed in three replications at each setting level. The average distribution was *found* by separating the fibers into five distinct mesh ranges: <20 mesh, 21-40 mesh, 41-60 mesh, 61-80 mesh, and >80 mesh. The average wt% for each of these mesh ranges was found by averaging the wt% at each level from each of the replications, with the standard deviation also calculated and included. Fines content was considered to be the wt% of the >80 mesh range. The viable fraction was also calculated as the sum of the average wt% of the 21-40 mesh, 41-60 mesh, and 61-80 mesh ranges with a standard deviation also calculated and included. Tables were created to represent the distributions found for all of the settings described in the design of experiment, where the various settings were: soybean or wheat straw; 3/8" or 1" circular hole screens; hammer tip speed of 26.9 m/s, 35.9 m/s, or 44.9 m/s; and moisture content levels of 5 wt%, 15 wt%, or 25 wt%. The combinations of factor settings produced 36 unique combinations for the design. Fiber distribution data for each settings is shown in the following tables, with the each table showing distributions for both soybean and wheat. The comprehensive tables have been included in the appendix to reduce the amount of information devoted to the main body. Table A31 in the appendix shows the fiber distribution for 3/8" screen and 5% moisture settings for all tip speeds. Table A32 in the appendix shows the fiber distribution for 1" screen and 5% moisture settings for all tip speeds. Table A33 in the appendix shows the fiber distribution for 3/8" screen and 15% moisture settings for all tip speeds. Table A34 in the appendix shows the fiber distribution for 1" screen and 15% moisture settings for all tip speeds. Table A35 in the appendix shows the fiber distribution for 3/8" screen and 25% moisture settings for all tip speeds. Table A36 in the appendix shows the fiber distribution for 1" screen and 25% moisture settings for all tip speeds.

From the tables the optimal settings for reducing fines content and maximizing the viable fraction can be observed. The lowest fines content fraction observed occurred for several conditions, with the lowest finest content being 0.30% ± 0.04% for soybean at 15% moisture using a 44.9 m/s hammer tip speed and 1" round holes screen. The highest fines content was found to be 2.63% ± 0.61% for wheat at 25% moisture using a 35.9 m/s hammer tip speed and 3/8" round holes screen. The highest viable fraction content was 32.62% ± 2.51% for soybean at 5% moisture using a 44.9 m/s hammer tip speed and 3/8" round holes. The lowest viable fraction was 4.77% ± 1.16% for wheat at 15% moisture using a 26.9 m/s hammer tip speed and 1" round holes.

Though the tables for fiber distribution are comprehensive in providing data, they are not particularly useful in observing the main effects that each factor had on fines content and viable fraction content. Thus, ANOVA was performed on the data sets to find the significant factors affecting fines content and the viable fraction. Table A37 in the appendix shows the ANOVA performed for the fines content using the factors of fiber, screen size, moisture content, and hammer tip speed. From the ANOVA it can be seen that all four main factors had a significant effect on the fines content, and the fines content was significantly influenced by several higher order interactions between factors. The model proved that have moderately good accuracy in defining the variability of the fines content, with an $R^2 = 83.37\%$, with adjusted $R^2 = 75.28\%$. ANOVA was performed to determine significant factors affecting the viable fraction content as well, with the ANOVA table shown in Table A38 in the appendix. From the ANOVA it can be seen that again all four main factors had a significant effect on the viable fraction, with higher order interactions between factors significantly affecting the response. The model proved that

have exceptionally good accuracy in defining the variability of the fines content, with an R^2 = 95.35%, with adjusted R^2 = 93.08%.

Main effects plots were generated to show the general effect on the fines content and viable fraction content, with the main effects plot for fines content shown in Figure 54. The main effects plot for the viable fraction is shown in Figure 55.

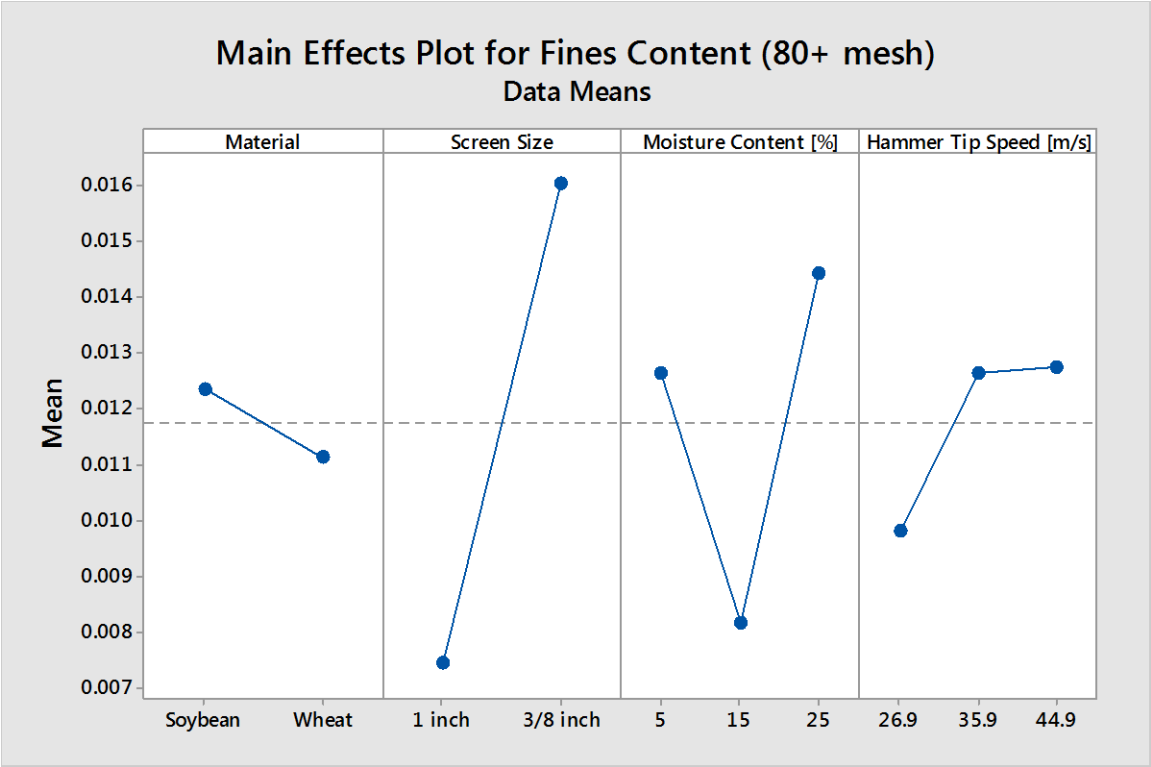

Figure 54. Main Effects Plot for Fines Content

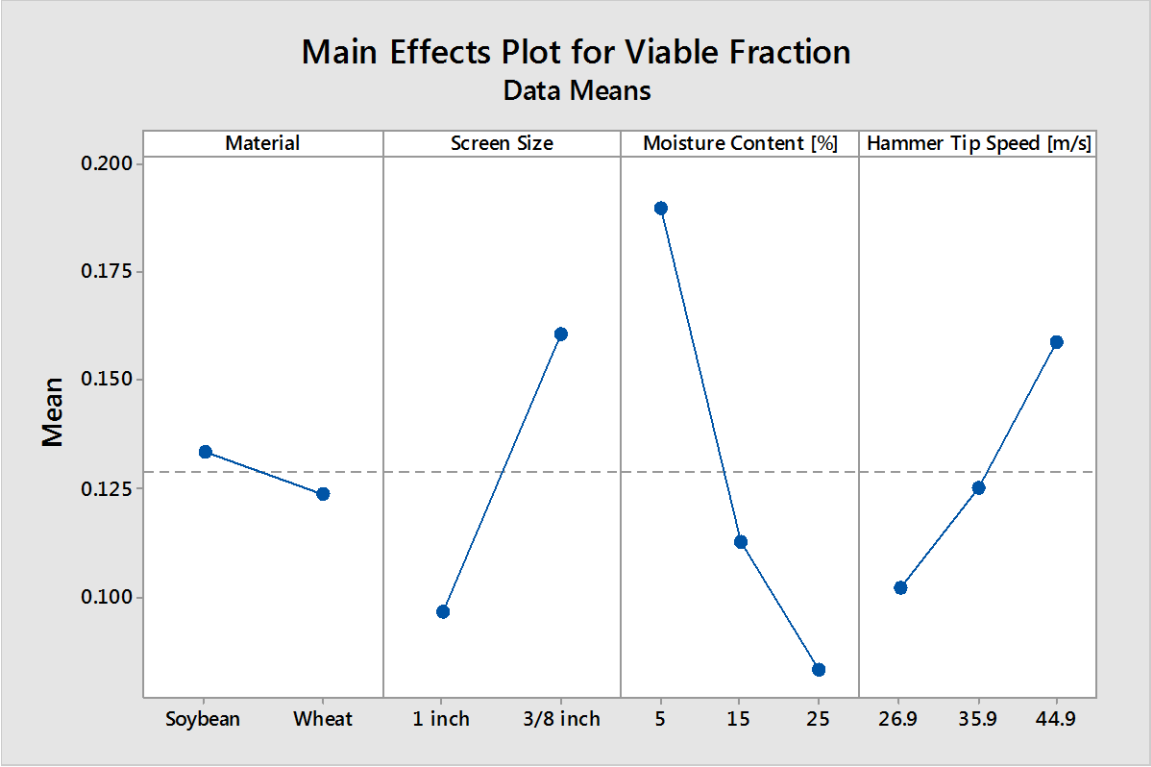

Figure 55. Main Effects Plot for Viable Fraction

From the main effects plots, it can be seen that the greatest effect on fines is the chosen screen size, with average fines going from 0.75% to 1.62% based only on changing the screen size. The fines content was also affected by a nonlinear relation between moisture content and fines content. The viable fraction content was heavily affected by the change in screen size, moisture content, and the hammer tip speed. The largest effect on the fines content was caused by the moisture content, with the viable fraction decreasing from 19.10% to 7.90% when moisture content is increased from 5% to 25%.

5.3.1. Hammer Milling Results for Soy Straw

Because both models had several high-order interactions affecting the fines content and viable fraction, the optimal levels for each factor cannot be fully determined by just looking at

the initial ANOVA. The data was broken up by fiber and then ANOVA performed again to account for the high order interactions. Table A39 in the appendix shows the ANOVA table for fines content for only soybean fibers.

From the ANOVA it can be seen that only the main factors of screen size and moisture had a significant effect on the fines content, with higher order interactions between factors also significantly affecting the response. The hammer tip speed has no significant effect except at higher order interactions. The model proved to have moderately good accuracy in defining the variability of the fines content, with an $R^2 = 81.48\%$ and adjusted $R^2 = 72.74\%$. Figure 56 shows the main effects plot for the fines content for soybean fibers. Figure 57 shows the interaction plot between fibers to give a clearer idea of how the factors interact with each other and the optimal levels that should be chosen to minimize the fines content.

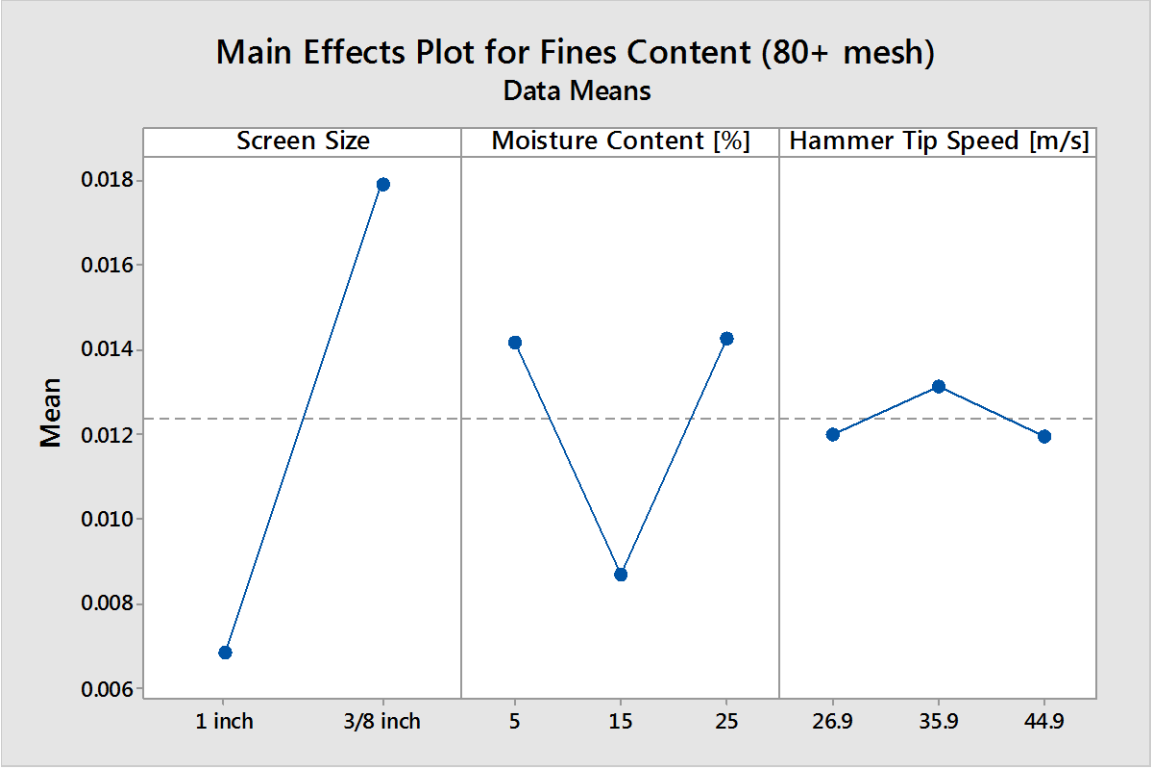

Figure 56. Main Effects Plot for Fines Content for Soybean

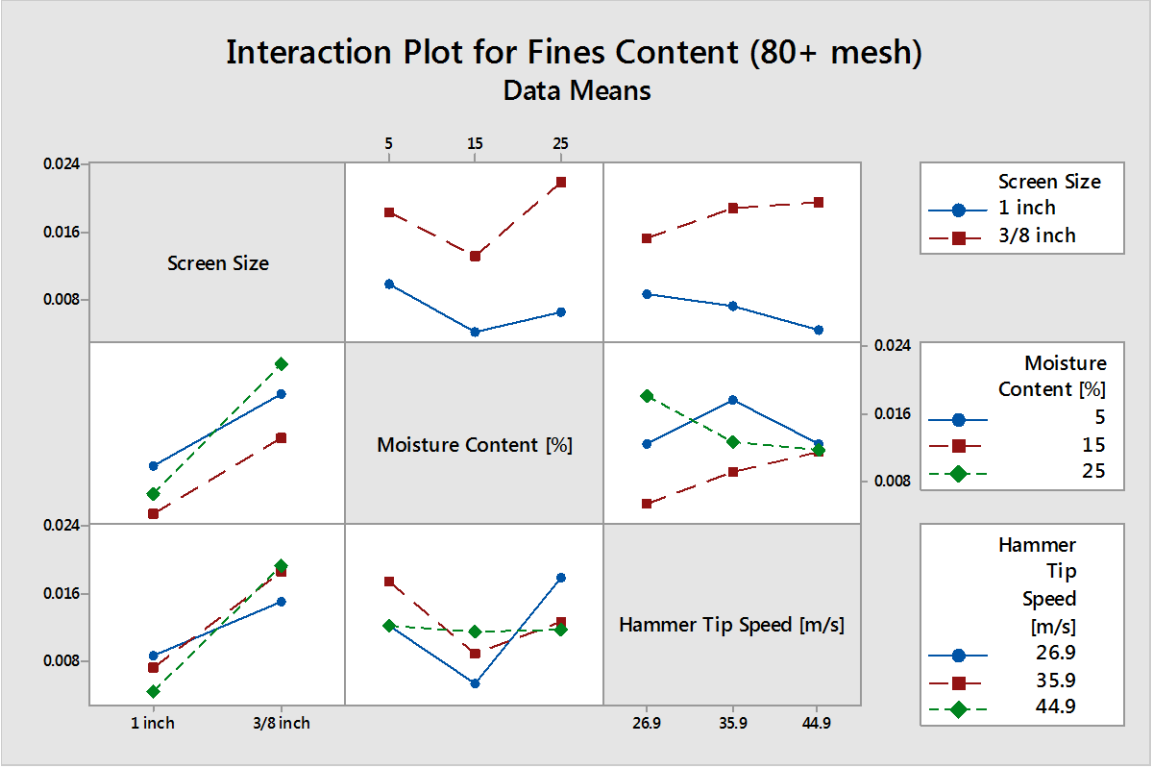

Figure 57. Interaction Plot for Fines Content for Soybean

From the main effects plot it can be seen that the change in screen size has the greatest impact on the fines content, with the fines content increasing from 0.68% to 17.97% as the screen hole size is changed from 3/8" to 1" holes. It is also relevent that the fines content has little change as the hammer tip speed increases, with the average fines content remaining near 1.23%. From the main effects plot the general optimal settings are to use 1" screens, 15% moisture content, and any hammer tip speed. From the interaction plot it is more clear what the optimal setting is for minimizing fines at all levels. All fines values are reduced at the 1" screen hole level regardless of the levels of the other factors. For the hammer tip speeds: at 26.9 m/s the minimum fines are generated when moisture content is at 15%; at 35.9 m/s the minmum fines are generated when moisture is at 15%; at 44.9 m/s the fines generation does not change with variation in the moisture content. The hammer tip speed of 26.9 m/s is the most susceptible to

changes in moisture content but produces the lowest fines content, thus it can be used as the optimal setting to reduce fines but requires careful monitering of the moisture content. 15% moisture content is the optimal setting for the moisture content.

ANOVA was also performed for the viable fraction generated for the soy straw. Table A40 in the appendix shows the ANOVA results for the viable fraction for the soy straw. From the ANOVA it can be seen that all of the main factors of screen size, moisture content, and hammer tip speed had a significant effect on the viable fraction, with higher order interactions between factors also significantly affecting the response. The model has exceptionally good accuracy in defining the variability of the viable fraction, with an $R^2 = 96.28\%$ and adjusted $R^2 = 94.52\%$. Figure 58 shows the main effects plot for the viable fraction for the soy straw fibers. Figure 59 shows the interaction plot between fibers to give a clearer idea of how the factors interact with each other and the optimal levels that should be chosen to maximize the viable fraction.

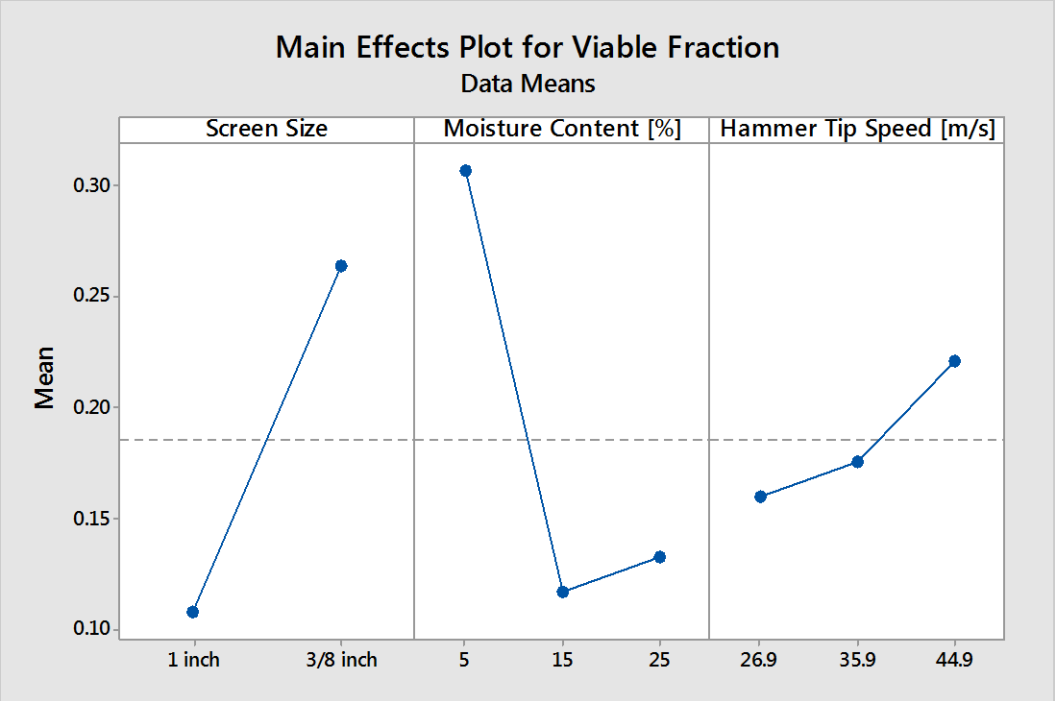

Figure 58. Main Effects Plot for Viable Fraction for Soybean

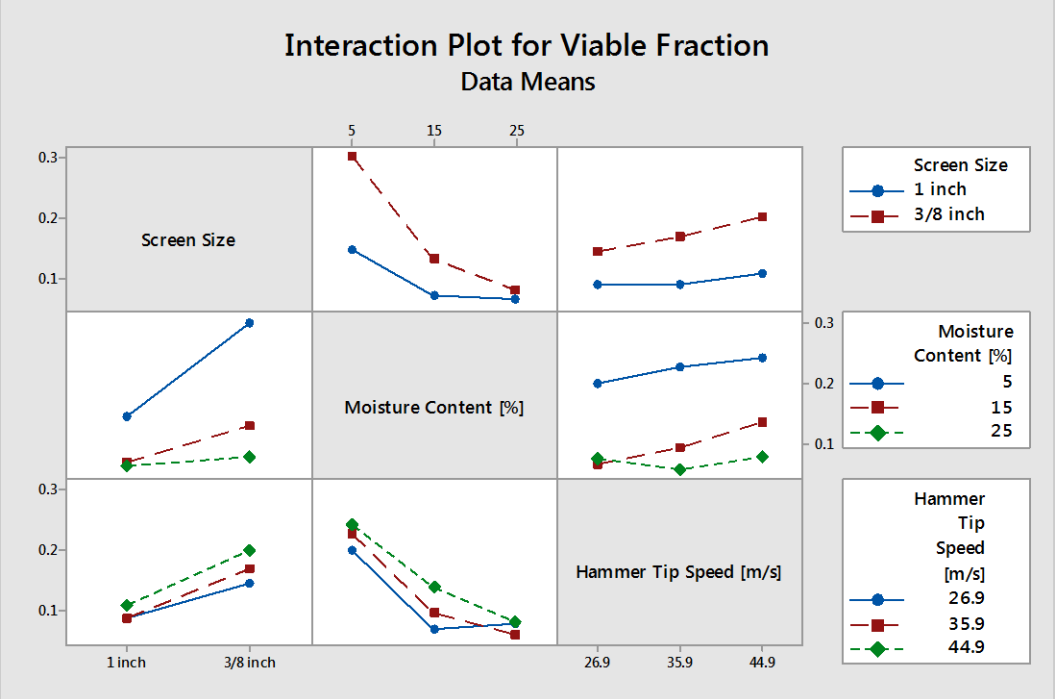

Figure 59. Interaction Plot for Viable Fraction for Soybean

From the main effects plot it can be seen that the change in moisture content has the greatest impact on the viable fractoin, with the viable fraction decreasing from 30.6% to 11.8% as the moisture content is changed from 5% to 15%. The general optimal factor levels determined from the main effects plot indicate the viable fraction will be maximized when using a 3/8" hole screen, 5% moisture content, and 44.9 m/s hammer tip speed. From the interaction plot it is more clear what the optimal setting is for maximizing the viable fraction. It is clear that the 3/8" hole screen produces the greatest viable fraction at all levels of moisture content and hammer tip speed, with a notable improvement when selecting the 5% moisture content level. For the hammer tip speed the viable fraction is maximum when using a 44.9 m/s tip speed and 5% moisture levels but there is little variation between tip speeds at the 5% moisture level. Overall the interaction plot is in agreement with the main effects plot in terms of optimal factor levels, with the 3/8" hole screen, 5% moisture content, and 44.9 m/s levels proving to maximize the viable fraction. Moreover when using the 5% moisture content level little control is needed for the hammer tip speed to produce near optimal levels.

5.3.2. Hammer Milling Results for Wheat Straw

ANOVA was performed for the fines content generated for wheat straw as well to determine how it differs from the characteristic results seen in the soy straw. Table A41 in the appendix shows the ANOVA results for the fines content in the wheat straw. From the ANOVA it can be seen that all of the main factors of screen size, moisture content, and hammer tip speed had a significant effect on the fines content, with higher order interactions between factors also significantly affecting the response. The model has moderate accuracy in defining the variability of the fines content, with an $R^2 = 85.37\%$ and adjusted $R^2 = 78.46\%$. Figure 60 shows the main effects plot for the viable fraction for the soy straw fibers. Figure 61 shows the interaction plot

between fibers to give a clearer idea of how the factors interact with each other and the optimal levels that should be chosen to minimize the fines content.

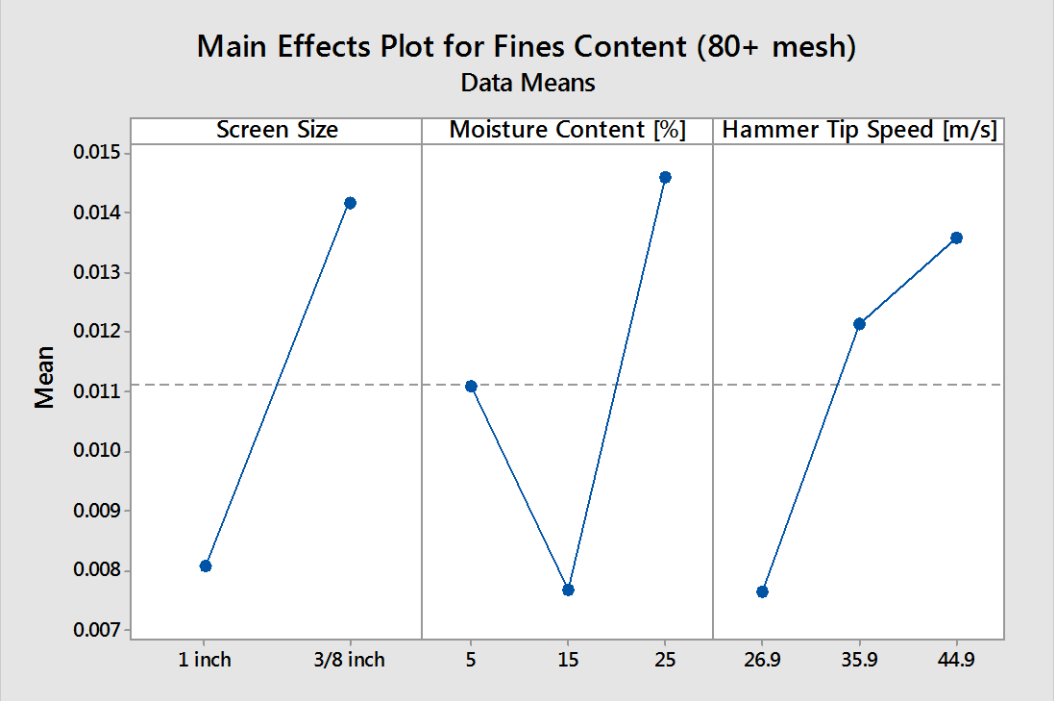

Figure 60. Main Effects Plot for Fines Content for Wheat

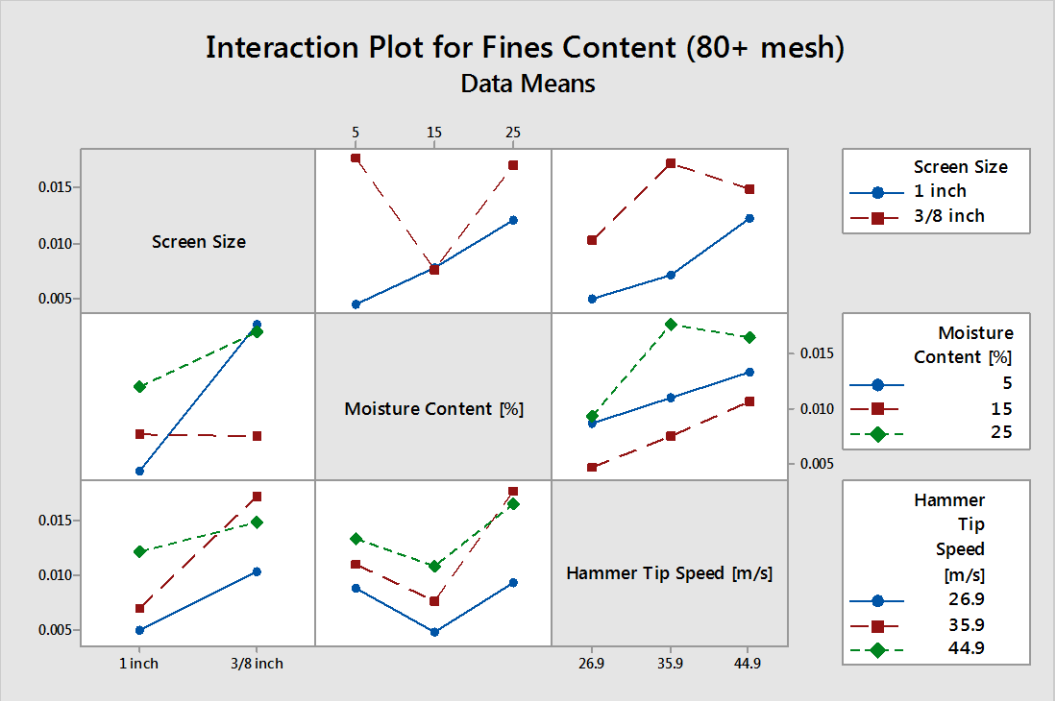

Figure 61. Interaction Plot for Fines Content for Wheat

The main effects plot shows that variability in the fines content is affected nearly equally by changing factors to the settings corresponding with their extreme response. From the main effects plot the general optimal levels for minimizing the fines content would be to use a 1" hole screen, 15% moisture content, and 26.9 m/s hammer tip speed. The interaction plot also gives some insight into selecting the optimal setting is for minimizing the fines content. All fines values are reduced at the 1" screen hole level except for the 15% moisture content level where fines generation remains the same regardless of changes in the screen size. For the hammer tip speed the optimal setting is 26.9 m/s for all moisture content values, with the 15% moisture content having the greatest variability as the hammer tip speed changes and the 15% moisture content level producing the lowest fines with no interaction between the 5% and 25% moisture content curves. Based on this interaction, the optimal setting to minimize fines is at the 26.9 m/s hammer tip speed and the 15% moisture content levels, again with close monitoring of moisture

levels required. ANOVA was also performed for the viable fraction generated for the wheat straw. Table A42 shows the ANOVA results for the viable fraction for wheat straw. From the ANOVA it can be seen that all of the main factors of screen size, moisture content, and hammer tip speed had a significant effect on the viable fraction, with higher order interactions between factors also significantly affecting the response. The model has exceptionally good accuracy in defining the variability of the viable fraction, with an $R^2 = 93.02\%$ and adjusted $R^2 = 89.73\%$. Figure 62 shows the main effects plot for the viable fraction for the soy straw fibers. Figure 63 shows the interaction plot between fibers to give a clearer idea of how the factors interact with each other and the optimal levels that should be chosen to maximize the viable fraction.

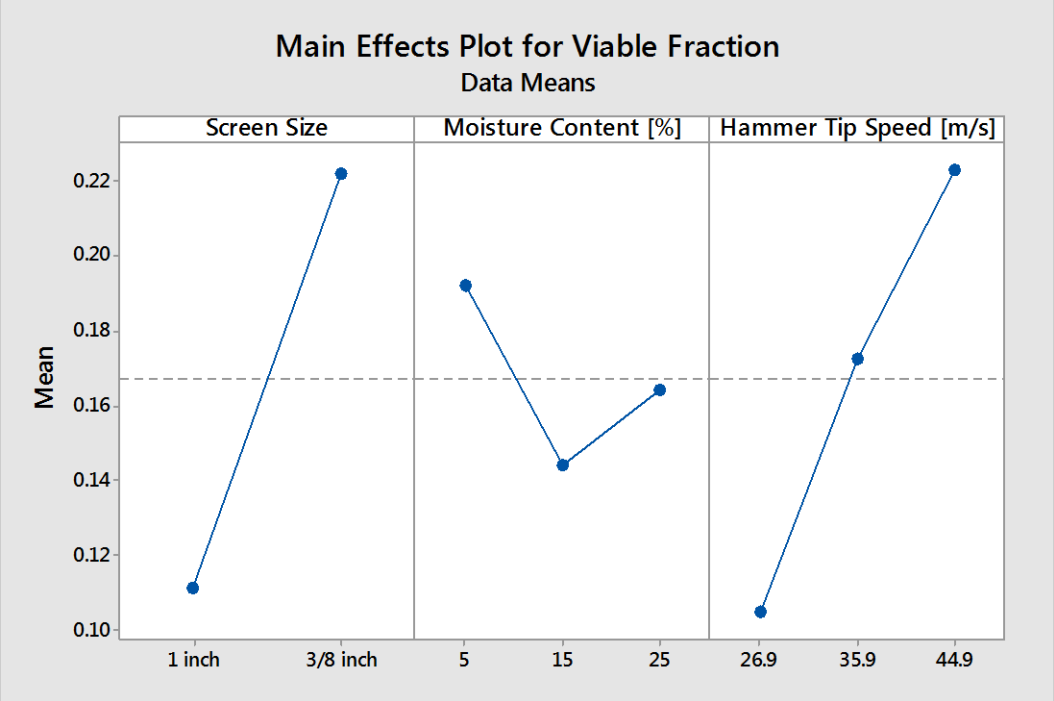

Figure 62. Main Effects Plot for Viable Fraction for Wheat

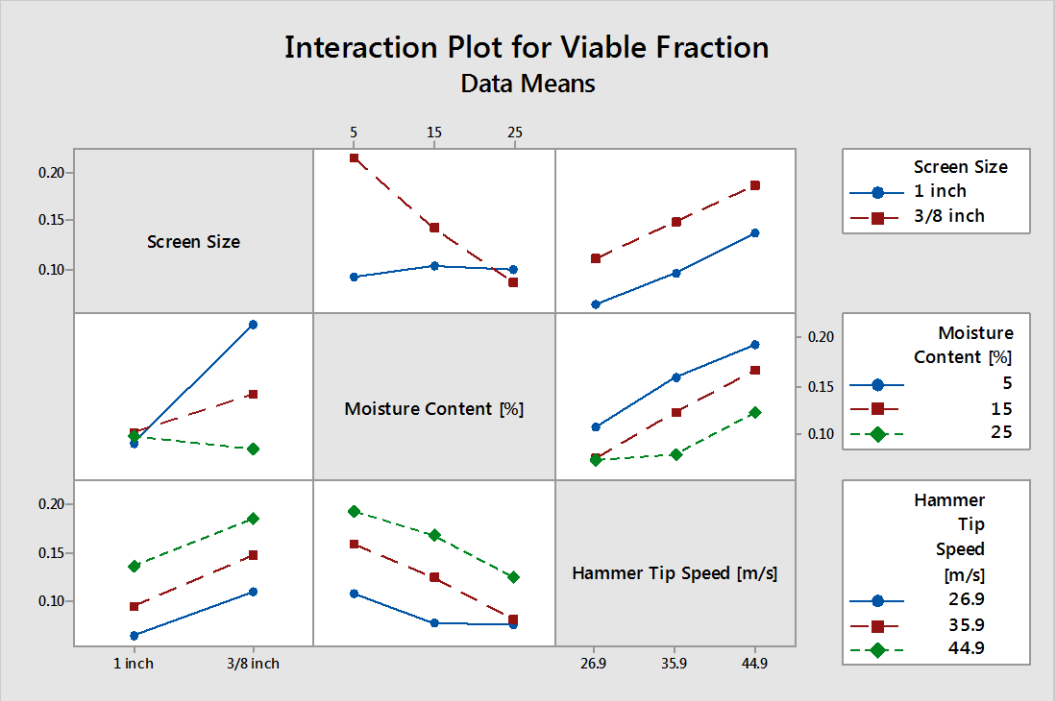

Figure 63. Interaction Plot for Viable Fraction for Wheat

From the main effects plot it can be seen that the change screen hole size and hammer tip speed have the greatest impact in the viable fraction content. The viable fraction changes from 11.1% to 22.5% as the screen hole size is decreased from 1" to 3/8". The viable fraction also greatly increased from 10.6% to 22.7% as the hammer tip speed increases from 26.9 m/s to 44.9 m/s. The general optimal levels from the main effects plot to maximize the viable fraction would then be a 3/8" hole screen, 5% moisture content, and 44.9 m/s hammer tip speed. The interaction plot it is more clear in defining the optimal settings for maximizing the viable fraction for various combinations of factors. From the interaction plot it can be seen that there is no interaction between screen size and hammer tip speed in the viable fraction, but there is a significant interaction and interesting grouping in the screen size and moisture content plots. For the 1" screens moisture content has no effect on the viable fraction level, while at the 3/8" screen

the viable fraction increases signifcantly from 9.5% to 22.3% as the moisture content level decreases from 25% to 5%. No other notable interactions occur between levels, with the factors showing linear relationships between each other in terms of viable fraction produced. Based on the interaction plot the optimal level for maximizing the viable fraction would be to use a 3/8" hole screen, 44.9 m/s hammer tip speed, and 5% moisture content which is in agreement with the main effects plot results.

6. CONCLUSIONS AND RECOMMENDATIONS

The overarching goals for this thesis project were: evaluate the properties of fiberboard made with wheat and soybean fibers with various binders, evaluate ESS as a resin for use in fiberboards, and determine optimal milling conditions to reduce the production of fines and maximize the production of viable fibers for board production. The results of this research can be summarized by evaluating each hypothesis individually and determining if it cannot be rejected or must be rejected based on the set criteria.

Hypothesis H1 must be rejected based on the testing results. Boards made with soy straw fibers performed well for the modulus of rupture, modulus of elasticity, and surface hardness tests and were able to meet or exceed the performance values established in the testing. However, the soy straw boards exhibited poor water absorption properties and poor properties for the mechanical testing that required good interfacial bonding between fibers. The internal bond and screw withdrawal testing showed significant drops in performance for the soy straw boards made with ESS-MDI and only MDI binders when compared to their wheat straw counterparts. These results indicate that soy straw cannot be used as a ready replacement for wheat straw fiberboards. This does not completely eliminate soy straw as a viable option for fiberboard however; using additional resin and/or adding a wax emulsion to the fibers before pressing the boards could potentially bring the properties of the soy straw boards up to that of the wheat straw boards. The obvious downside to this practice would be increased production costs, but it could be offset in markets where soy straw is noticeably cheaper to source than wheat straw.

Hypothesis H2 must be rejected based on the testing results. The mechanical and physical properties observed for both soybean and wheat straw boards were categorically

lessened when ESS was used as the sole resin binder. Based on results from the resin characterization and performance of board properties it is not suggested that a sole ESS resin system be implemented in producing fiberboard panels. The poor properties exhibited by the boards indicate poor interfacial bonding between fibers when ESS-MHHPA-DBU resin was used, indicating poor chemical and physical bonding between the fibers and resin. The excellent performance of the ESS-MHHPA-DBU resin in lap shear testing and the subsequent poor performance in the fiberboard application indicate that the cycle times and temperatures implemented could have also been a factor in decreasing the properties. Considering that the cycle time is of utmost importance in fiberboard manufacture, the ESS-MHHPA-DBU mixture cannot be used economically in fiberboard, but it can and should see application as a high-performance coating and adhesive when implemented in the correct applications.

Hypothesis H3 cannot be rejected based on the testing results. Resin characterization indicates some limited bonding occurred between the MDI and ESS resins, whether that be through the proposed isocyanate-epoxide reaction or some other reaction such as a reaction between the hydroxyl groups of the ESS and isocyanate. The boards also performed similarly in terms of mechanical performance, even with an improvement of internal bond strength and surface hardness observed in the wheat with ESS-MDI formulation. Regardless of these results, it cannot be recommended that ESS be implemented as a resin binder system with fiberboard or particleboard due to the current lack of commercial availability as well as the terminal epoxides in ESS making it too difficult to react with the isocyanate [46]. Vegetable oil based materials could still potentially be implemented in board manufacture, with possible resin formulations including MDI and opened epoxide vegetable oils. MDI has also shown to react with polyols of vegetable oils, which react with hydroxyl groups in the polyols to form polyurethanes, with

linseed oil showing high crosslinking density and superior mechanical properties compared to other vegetable oil based polyols [47]. Soy proteins have also shown moderate success as a potential alternative resin source, but have generally poor water absorption properties and are difficult to implement into production [28] [29].

Hypothesis H4 cannot be rejected based on the testing results. The wheat straw's fines content and viable fraction were both significantly affected by the fiber's moisture content, the screen's hole sizes, and hammer tip speeds. Optimal levels were found for both minimizing fines production and maximizing the viable fraction. For minimization of fines, a 1" hole screen, 15% moisture content, and 26.9 m/s hammer tip speed should be used. For maximizing the viable fraction, a 3/8" screen, 5% moisture content, and 44.9 m/s hammer tip speed should be used.

Hypothesis H5 must be rejected based on the testing results. The soy straw's viable fraction was significantly affected by the fiber's moisture content, the screen's hole sizes, and hammer tip speeds. However, it was found that for the fines content, the hammer tip speed has negligible effect on the fines content, while the screen size and moisture content proved to be significant effects. Optimal levels for fines minimization and viable fraction maximization were also found for soy straw. For minimization of fines, a 1" hole screen, 15% moisture content, and any hammer tip speed could be used, with 26.9 m/s having the lowest variability when interacting with other factor levels. For maximizing the viable fraction, a 3/8" screen, 5% moisture content, and 44.9 m/s hammer tip speed should be used.

For both wheat and soy straw, the optimal levels to be used in an industrial application are wholly dependent on the cost of production. Reduction of fines helps to keep retention of fibers high, as the fines are unrecoverable for usage in board production. However, it is also

possible that the increase in the viable fraction and subsequently smaller amount of material that needs to be further processed could outweigh the financial loss of the fines. Further economic analysis of the production with material costs and processing costs could potentially be performed to find what conditions induce the least cost solution, but no claims can be made in that regards based solely on this research. In addition, because this only shows one cycle of refinement, further processing will be needed to reach an optimal amount of fibers in the viable range. Because of this, the desired properties of the boards will also come into play, meaning optimal milling properties and refinement iterations will be a part of the overall board properties function.

From this research, it cannot be suggested that wheat or soybean boards be used in high load-bearing medium density fiberboard or particleboard applications due to not meeting ANSI 208.1 or 208.2 requirements. However, because a select few of the property requirements were achieved, it is feasible that boards could still be used in low load applications that do not require the standards of ANSI boards. One way that the boards could potentially be improved by refining the aspect ratio of the straw fibers used in the boards. Changing milling parameters such that smaller fibers with better aspect ratios would be produced could potentially improve the mechanical property values to the point of meeting ANSI standards. The obvious downside to this practice would be the significant increase in the generation of fines, which may make this solution unviable due to economics. The fiber distribution and aspect ratio of fibers also appears to play a much bigger role than anticipated and could be the main controlling factor in determining properties [13], with the control of what distribution to use based on costs of milling fibers to the desired distribution. Results from water absorption testing especially show the need for some type of added moisture resistance for the boards, with chemical treatment of the fibers

showing some promise [13]. Adding additional wax additive to the fibers before pressing can improve water resistance, but it can also potentially cause worse bonding between the fibers [48].

REFERENCES

[1] *ASTM D1554: Standard Terminology Relating to Wood-Base Fiber and Particle Panel Materials,* West Conshohocken, PA: ASTM International, 2010.

[2] Food and Agriculture Organization, "FAO: State of the World's Forests 2009," United Nations, Rome, 2009.

[3] Composite Panel Association, *ANSI 208.2 Medium Density Fiberboard (MDF) for Interior Applications,* Gaithersburg, MD, 2002.

[4] American National Standard, *ANSI Standard 208.1 Particleboard,* Gaithersburg, MD, 2009.

[5] Environmental Protection Agency, "Hardboard and Fiberboard Manufacturing," in *Wood Product Industry*, Environmental Protection Agency, 2002, pp. 10.6.4-1--10.6.4-38.

[6] Healthy Building Network, "Alternative Resin Binders," Global Health & Safety Initiative, 2008.

[7] Forest Products Laboratory, Wood Handbook: Wood as an Engineering Material, United States Department of Agriculture, 2010.

[8] California Air Resource Board, *Airborne Toxic Control Measure to Reduce Formaldehyde Emissions from Composite Wood Products,* California Environmental Protection Agency, 2007.

[9] H. Lei and C. E. Frazier, "Curing behavior of melamine-urea-formaldehyde (MUF) resin adhesive," *International Journal of Adhesion and Adhesives,* vol. 62, pp. 40-44, 2015.

[10] *ASTM E1757: Standard Practice for Preparation of Biomass for Compositional Analysis,* West Conshohocken, PA: ASTM International, 2007.

[11] L. Sangyeob, T. Shupe and C. Hse, "Properties of Bio-Based Medium Density Fiberboard," *Recent Developments in Wood Composites,* pp. 51-58, 2006.

[12] L. Morrison, "Ag Innovation News," *Soy-straw start-up,* vol. 21, pp. 4-5, April-June 2012.

[13] S. Halvarsson, H. Edlund and M. Norgren, "Wheat straw as raw material for manufacture of medium density fiberboard (MDF)," *BioResources,* vol. 5, no. 2, pp. 1215-1231, 2010.

[14] E. Sjostrom, Wood Chemistry Fundamentals and Applications, 2nd ed., San Diego, CA: Academic Press, 1993.

[15] R. M. Rowell, Paper and Composites from Agro-Based Resources, Boca Raton, FL: CRC Press, 1996.

[16] Z. Liu, "The Utilization of Soybean Straw Fiber Morphology and Chemical Characteristics," *BioResources,* vol. 10, pp. 2266-2280, 2015.

[17] N. Reddy and Y. Yang, "Biofibers from agricultural byproducts for industrial applications," *Trends in Biotechnology,* vol. 23, no. 1, pp. 22-27, 2005.

[18] G. Iñiguez-Covarrubias, S. Lange and R. Rowell, "Utilization of byproducts from the tequila industry: part 1: agave bagasse as a raw material for animal feeding and fiberboard production," *Bioresource Technology,* vol. 77, no. 1, pp. 25-31, 2001.

[19] P. Evon, J. Vinet, L. L and R. L, "Influence of thermo-pressing conditions on the mechanical propertiesof biodegradable fiberboards made from a deoiled sunflower cake," *Industrial Crops and Products,* vol. 65, pp. 117-126, 2015.

[20] X. Ye, J. Julson, M. Kuo, A. Womac and D. Myers, "Properties of medium density fiberboards made from renewable biomass," *Bioresource Technology,* vol. 98, no. 5, pp. 1077-1084, 2007.

[21] National Agricultural Statistics Service, "Crop Production 2014 Sumary," United States Department of Agriculture, 2015.

[22] J. Rossi, "Feeding Straw to Beef Cattle," University of Georgia College of Agricultural and Environmental Sciences.

[23] M. Ando and M. Sato, "Manufacture of plywood bonded with kenaf core powder," *Journal of Wood Science,* vol. 55, no. 4, pp. 283-288, 2009.

[24] T. Tabarasa, J. S and A. Ashori, "Mechanical and physical properties of wheat straw boards bonded with a tannin modified phenol-formaldehyde adhesive," *Composites Part B: Engineering,* vol. 42, no. 2, pp. 176-180, 2011.

[25] "The Influences of Drying Temperature of Wood Particles on the Quality Properties of Particleboard Composite," *Drying Technology: An International Journal,* vol. 31, no. 1, pp. 17-23, 2013.

[26] J. Xu, R. Widyornin, H. Yamauchi and S. Kawai, "Development of binderless fiberboard from kenaf core,"," *Journal of Wood Science,* vol. 52, no. 3, pp. 236-243, 2006.

[27] A. W. Christiansen, "How Overdrying Wood Reduces Its Bonding to Phenol-Formaldehyde Adhesives," *Wood and Fiber Science,* vol. 22, pp. 441-459, 1990.

[28] Y. Liu, *Formaldehyde-free Wood Adhesives from Soybean Proteins and Lignin: Development and Characterization,* Corvallis: Oregon State University, 2005.

[29] M. Kuo, D. Adams, D. Myers, D. Curry and e. al, "Properties of wood/agricultural fiberboard bonded with soybean-based adhesives," *Forest Products Journal,* vol. 48, pp. 71-75, 1998.

[30] D. Sundquist, *Dried Distillers Grains with Solubles as a Multifunctional Filler in Wood Particleboards,* Fargo: North Dakota State University, 2015.

[31] X. Pan, P. Sengupta and D. Webster, "High Biobased Content Epoxy — Anhydride Thermosets from Epoxidized Sucrose Esters of Fatty Acids," *BioMacromolecules,* vol. 12, no. 6, p. 2416–2428, 2011.

[32] X. Pan, P. Sengupta and D. Webster, "Novel biobased epoxy compounds: epoxidized sucrose esters of fatty acids," *Green Chemistry,* vol. 13, pp. 965-975, 2011.

[33] E. Monono, *Pilot Scale Production, Characterization, and Optimization of Epoxidized Vegetable Oil-Based Resin,* Fargo: North Dakota State University, 2015.

[34] M. Uribe and K. Hodd, "The catalysed reaction of isocyanate and epoxide groups: A study using differential scanning calorimetry," *Thermochimica Acta,* vol. 77, no. 1-3, pp. 367-373, 1984.

[35] D. Caille, J. Pascault and L. Tighzert, "Reaction of a diepoxide with a diisocyanate in bulk," *Polymer Bulletin,* vol. 24, pp. 23-30, 1990.

[36] E. M. Monono, "Pilot Scale (10 kg) production and characterization of epoxidized sucrose soyate," *Industrial Crops and Products,* vol. 74, pp. 987-997, 2015.

[37] S. Lee, T. Shupe and C. Hse, "Properties of Bio-Based Medium Density Fiberboard," Forest Products Society, Madison, WI.

[38] Z. Kadar, "Enhanced ethanol production by removal of cutin and epicuticular waxes of wheat straw by plasma assisted pretreatment," *Biomass and Bioenergy,* vol. 81, pp. 26-30, 2015.

[39] Z. Liu and e. al., "Surface Structure and Dynamic Adhesive Wettability of Wheat Straw," *Wood and Fiber Science,* vol. 36, pp. 239-249, 2004.

[40] S. Goodman, Handbook of Thermoset Plastics, Westwood, NJ: Noyes Publications, 1998.

[41] *ASTM D2339: Standard Test Method for Strength Properties of Adhesives in Two-Ply Wood Constructoin in Shear by Tension Loading,* West Conshohocken, PA: ASTM International, 2011.

[42] *ASTM D1037: Standard Test Methods for Evaluating Properties of Wood-Base Fiber and Particle Panel Materials,* West Conshohocken, PA: ASTM International, 2012.

[43] *ASTM D2395: Standard Test Methods for Density and Specific Gravity (Relative Density) of Wood and Wood-Based Materials,* West Conshohocken: ASTM International, 2014.

[44] ASTM International, *ASTM D75/75M Standard Practice for Sampling Aggregates,* ASTM International, 2014.

[45] D. C. Montgomery, Design and Analysis of Experiments, New York: Wiley, 2013.

[46] D. Radojclc, "Study on the reaction of amines with internal epoxides," *Eur. J. Lipid Sci. Technology,* vol. 118, pp. 1-5, 2016.

[47] A. Zlatanic, C. Lava, W. Zhang and Z. Petrovic, "Effect of Structure on Properties of Polyols and Polyurethanes Based on Different Vegetable Oils," *Journal of Polymer Science,* vol. 42, pp. 809-819, 2004.

[48] E. Sitz and D. Bajwa, "The mechanical properties of soybean straw and wheat straw blended medium density fiberboards made with methylene diphenyl diisocyanate binder," *Industrial Crops and Products,* vol. 75, pp. 200-205, 2015.

APPENDIX

Table A1. Fisher's Test Table for 2 Hour Mass Absorption

Labels	Samples	Mean	Grouping
SoybeanESSANH	4	209.17%	A
SoybeanESSMDI	4	121.46%	B
SoybeanMDI	4	73.87%	C
WheatMDI	4	49.54%	CD
WheatESSMDI	4	26.26%	D

Table A2. Initial ANOVA Table for 2 Hour Mass Absorption

Source	DF	Adj SS	Adj MS	F-Value	P-Value
Model	11	7.99728	0.72703	7.23	0.005
Linear	5	7.74532	1.54906	15.41	0.001
Fiber Type	1	1.34526	1.34526	13.38	0.006
Board Number	2	0.00121	0.0006	0.01	0.994
Resin	2	3.09077	1.54538	15.37	0.002
2-Way Interaction	6	0.10448	0.01741	0.17	0.977
Fiber Type*Board Number	2	0.05342	0.02671	0.27	0.773
Board Number*Resin	4	0.03266	0.00816	0.08	0.986
Error	8	0.80438	0.10055		
Lack-of-Fit	3	0.67506	0.22502	8.7	0.020
Pure Error	5	0.12932	0.02586		
Total	19	8.80166			

Table A3. Revised ANOVA Table for 2 Hour Mass Absorption

Source	DF	Adj SS	Adj MS	F-Value	P-Value
Model	3	7.885	2.62833	45.88	0.000
Linear	3	7.885	2.62833	45.88	0.000
Fiber Type	1	1.4286	1.42863	24.94	0.000
Resin	2	3.375	1.68748	29.45	0.000
Error	16	0.9167	0.05729		
Lack-of-Fit	11	0.7874	0.07158	2.77	0.136
Pure Error	5	0.1293	0.02586		
Total	19	8.8017			

Table A4. Fisher's Test Table for 24 Hour Mass Absorption

Labels	Samples	Mean	Grouping
SoybeanESSANH	4	223.96%	A
SoybeanMDI	4	196.31%	B
SoybeanESSMDI	4	184.61%	B
WheatMDI	4	140.01%	C
WheatESSMDI	4	133.40%	C

Table A5. Initial ANOVA Table for 24 Hour Mass Absorption

Source	DF	Adj SS	Adj MS	F-Value	P-Value
Model	11	2.53115	0.2301	11.41	0.001
Linear	5	2.43913	0.48783	24.18	0.000
Fiber Type	1	1.13229	1.13229	56.13	0.000
Board Number	2	0.00667	0.00334	0.17	0.850
Resin	2	0.32043	0.16022	7.94	0.013
2-Way Interaction	6	0.1612	0.02687	1.33	0.344
Fiber Type*Board Number	2	0.06434	0.03217	1.59	0.261
Board Number*Resin	4	0.04156	0.01039	0.51	0.728
Error	8	0.16139	0.02017		
Lack-of-Fit	3	0.08528	0.02843	1.87	0.253
Pure Error	5	0.07611	0.01522		
Total	19	2.69254			

Table A6. Revised ANOVA Table for 24 Hour Mass Absorption

Source	DF	Adj SS	Adj MS	F-Value	P-Value
Model	3	2.35607	0.78536	37.35	0.000
Linear	3	2.35607	0.78536	37.35	0.000
Fiber Type	1	1.15581	1.15581	54.96	0.000
Resin	2	0.33288	0.16644	7.91	0.004
Error	16	0.33647	0.02103		
Lack-of-Fit	11	0.26036	0.02367	1.55	0.328
Pure Error	5	0.07611	0.01522		
Total	19	2.69254			

Table A7. Fisher's Test Table for 2 Hour Thickness Swelling

Labels	Samples	Mean	Grouping
SoybeanESSANH	4	102.91%	A
SoybeanESSMDI	4	59.19%	B
SoybeanMDI	4	58.83%	B
WheatMDI	4	40.46%	C
WheatESSMDI	4	23.69%	C

Table A8. Initial ANOVA Table for 2 Hour Thickness Swelling

Source	DF	Adj SS	Adj MS	F-Value	P-Value
Model	11	1.49991	0.136355	11.79	0.001
Linear	5	1.42285	0.28457	24.6	0.000
Fiber Type	1	0.29583	0.295827	25.58	0.001
Board Number	2	0.01238	0.006192	0.54	0.605
Resin	2	0.49559	0.247794	21.42	0.001
2-Way Interaction	6	0.11812	0.019687	1.7	0.238
Fiber Type*Board Number	2	0.04063	0.020316	1.76	0.233
Board Number*Resin	4	0.04013	0.010031	0.87	0.523
Error	8	0.09253	0.011566		
Lack-of-Fit	3	0.04853	0.016176	1.84	0.257
Pure Error	5	0.044	0.0088		
Total	19	1.59244			

Table A9. Revised ANOVA Table for 2 Hour Thickness Swelling

Source	DF	Adj SS	Adj MS	F-Value	P-Value
Model	3	1.37016	0.456719	32.88	0.000
Linear	3	1.37016	0.456719	32.88	0.000
Fiber Type	1	0.29013	0.290131	20.88	0.000
Resin	2	0.54087	0.270437	19.47	0.000
Error	16	0.22228	0.013893		
Lack-of-Fit	11	0.17828	0.016207	1.84	0.259
Pure Error	5	0.044	0.0088		
Total	19	1.59244			

Table A10. Fisher's Test Table for 24 Hour Thickness Swelling

Labels	Samples	Mean	Grouping
SoybeanESSANH	4	116.8%	A
SoybeanMDI	4	114.4%	A
SoybeanESSMDI	4	84.4%	B
WheatMDI	4	72.4%	BC
WheatESSMDI	4	57.5%	C

Table A11. Initial ANOVA Table for 24 Hour Thickness Swelling

Source	DF	Adj SS	Adj MS	F-Value	P-Value
Model	11	1.23554	0.112322	9.24	0.002
Linear	5	1.09286	0.218573	17.98	0.000
Fiber Type	1	0.43204	0.432039	35.53	0.000
Board Number	2	0.02794	0.013972	1.15	0.364
Resin	2	0.25158	0.125791	10.35	0.006
2-Way Interaction	6	0.17634	0.029389	2.42	0.124
Fiber Type*Board Number	2	0.00838	0.004189	0.34	0.719
Board Number*Resin	4	0.13037	0.032592	2.68	0.110
Error	8	0.09727	0.012159		
Lack-of-Fit	3	0.0708	0.0236	4.46	0.071
Pure Error	5	0.02647	0.005295		
Total	19	1.33282			

Table A12. Revised ANOVA Table for 24 Hour Thickness Swelling

Source	DF	Adj SS	Adj MS	F-Value	P-Value
Model	3	1.05914	0.353046	20.64	0.000
Linear	3	1.05914	0.353046	20.64	0.000
Fiber Type	1	0.47486	0.474861	27.76	0.000
Resin	2	0.28206	0.141032	8.25	0.003
Error	16	0.27368	0.017105		
Lack-of-Fit	11	0.24721	0.022473	4.24	0.061
Pure Error	5	0.02647	0.005295		
Total	19	1.33282			

Table A13. Fisher's Test Table for Linear Expansion

Labels	Samples	Mean	Grouping
WheatESSANH	5	0.00855	A
SoybeanESSANH	5	0.005865	AB
WheatESSMDI	5	0.003915	B
SoybeanMDI	5	0.003697	B
WheatMDI	5	0.003682	B
SoybeanESSMDI	5	0.003411	B

Table A14. Initial ANOVA Table for Linear Expansion

Source	DF	Adj SS	Adj MS	F-Value	P-Value
Model	21	0.000202	0.000010	1.35	0.343
Linear	7	0.000050	0.000007	1.00	0.492
Fiber Type	1	0.000000	0.000000	0.00	0.969
Board Number	3	0.000028	0.000009	1.33	0.332
Edge or Center	1	0.000006	0.000006	0.84	0.385
Resin	2	0.000021	0.000010	1.47	0.286
2-Way Interaction	14	0.000082	0.000006	0.82	0.643
Fiber Type*Board Number	3	0.000015	0.000005	0.68	0.587
Fiber Type*Edge or Center	1	0.000002	0.000002	0.30	0.596
Fiber Type*Resin	2	0.000010	0.000005	0.72	0.517
Board Number*Resin	6	0.000052	0.000009	1.21	0.389
Edge or Center*Resin	2	0.000008	0.000004	0.53	0.608
Error	8	0.000057	0.000007		
Total	29	0.000259			

Table A15. Revised ANOVA Table for Linear Expansion

Source	DF	Adj SS	Adj MS	F-Value	P-Value
Model	5	0.000102	0.000020	3.09	0.027
Linear	3	0.000091	0.000030	4.63	0.011
Fiber Type	1	0.000008	0.000008	1.27	0.270
Resin	2	0.000083	0.000042	6.31	0.006
2-Way Interaction	2	0.000010	0.000005	0.78	0.471
Fiber Type*Resin	2	0.000010	0.000005	0.78	0.471
Error	24	0.000158	0.000007		
Total	29	0.000259			

Table A16. Fisher's Test Table for Modulus of Rupture

Labels	Samples	Mean	Grouping
WheatMDI	10	5.724	A
WheatESSMDI	10	5.325	A
SoybeanESSMDI	10	5.307	A
SoybeanMDI	10	5.141	A
SoybeanESSANH	10	2.170	B
WheatESSANH	10	0.274	C

Table A17. Initial ANOVA Table for Modulus of Rupture

Source	DF	Adj SS	Adj MS	F-Value	P-Value
Model	29	313.389	10.8065	6.06	0.000
Linear	8	127.325	15.9156	8.93	0.000
Fiber Type	1	5.907	5.9073	3.31	0.079
Board Number	3	5.668	1.8893	1.06	0.381
Edge or Center	1	3.377	3.377	1.89	0.179
Resin	2	106.07	53.0351	29.75	0.000
Post Linear Exp.	1	0.415	0.415	0.23	0.633
2-Way Interaction	21	70.079	3.3371	1.87	0.057
Fiber Type*Board Number	3	1.747	0.5824	0.33	0.806
Fiber Type*Edge or Center	1	7.876	7.8765	4.42	0.044
Fiber Type*Resin	2	13.498	6.749	3.79	0.034
Fiber Type*Post Linear Exp.	1	2.756	2.7563	1.55	0.223
Board Number*Resin	6	19.512	3.252	1.82	0.128
Board Number*Post Linear Exp.	3	4.403	1.4678	0.82	0.491
Edge or Center*Resin	2	2.26	1.1299	0.63	0.537
Edge or Center*Post Linear Expansion	1	0.292	0.2918	0.16	0.689
Resin*Post Linear Exp.	2	2.037	1.0183	0.57	0.571
Error	30	53.473	1.7824		
Lack-of-Fit	25	38.927	1.5571	0.54	0.864
Pure Error	5	14.546	2.9092		
Total	59	366.862			

Table A18. Revised ANOVA Table for Modulus of Rupture

Source	DF	Adj SS	Adj MS	F-Value	P-Value
Model	9	275.35	30.594	16.72	0.000
Linear	4	191.303	47.826	26.13	0.000
Fiber Type	1	15.266	15.266	8.34	0.006
Edge or Center	1	4.786	4.786	2.61	0.112
Resin	2	171.252	85.626	46.78	0.000
2-Way Interaction	5	37.751	7.55	4.13	0.003
Fiber Type*Edge or Center	1	18.343	18.343	10.02	0.003
Fiber Type*Resin	2	16.88	8.44	4.61	0.015
Edge or Center*Resin	2	2.528	1.264	0.69	0.506
Error	50	91.513	1.83		
Lack-of-Fit	45	76.967	1.71	0.59	0.846
Pure Error	5	14.546	2.909		
Total	59	366.862			

Table A19. Tukey's Test Table for Modulus of Elasticity

Labels	Samples	Mean	Grouping
SoybeanMDI	10	788	A
WheatESSMDI	10	754.5	A
SoybeanESSMDI	10	699	AB
WheatMDI	10	681.2	AB
SoybeanESSANH	10	364.5	BC
WheatESSANH	10	76.8	C

Table A20. Initial ANOVA Table for Modulus of Elasticity

Source	DF	Adj SS	Adj MS	F-Value	P-Value
Model	29	5533442	190808	2.91	0.002
Linear	8	1516685	189586	2.89	0.016
Fiber Type	1	196032	196032	2.99	0.094
Board Number	3	19819	6606	0.1	0.959
Edge or Center	1	73163	73163	1.12	0.299
Resin	2	1036659	518330	7.91	0.002
Post Linear Exp.	1	68178	68178	1.04	0.316
2-Way Interaction	21	1647043	78431	1.2	0.32
Fiber Type*Board Number	3	196799	65600	1	0.406
Fiber Type*Edge or Center	1	220113	220113	3.36	0.077
Fiber Type*Resin	2	329476	164738	2.51	0.098
Fiber Type*Post Linear Exp.	1	185102	185102	2.83	0.103
Board Number*Resin	6	328132	54689	0.83	0.553
Board Number*Post Linear Exp.	3	116588	38863	0.59	0.624
Edge or Center*Resin	2	89502	44751	0.68	0.513
Edge or Center*Post Linear Expansion	1	5083	5083	0.08	0.783
Resin*Post Linear Exp.	2	49635	24817	0.38	0.688
Error	30	1965661	65522		
Lack-of-Fit	25	1081890	43276	0.24	0.992
Pure Error	5	883771	176754		
Total	59	7499104			

Table A21. Revised ANOVA Table for Modulus of Elasticity

Source	DF	Adj SS	Adj MS	F-Value	P-Value
Model	5	3956334	791267	12.06	0.000
Linear	3	3662296	1220765	18.61	0.000
Fiber Type	1	192013	192013	2.93	0.093
Resin	2	3470283	1735141	26.45	0.000
2-Way Interaction	2	294038	147019	2.24	0.116
Fiber Type*Resin	2	294038	147019	2.24	0.116
Error	54	3542770	65607		
Lack-of-Fit	49	2658999	54265	0.31	0.987
Pure Error	5	883771	176754		
Total	59	7499104			

Table A22. Fisher's Test Table for Internal Bond

Labels	Samples	Mean	Grouping
WheatESSMDI	6	0.1868	A
WheatMDI	6	0.1332	B
SoybeanMDI	6	0.04986	C
SoybeanESSMDI	6	0.0456	C
SoybeanESSANH	6	0.0093	CD
WheatESSANH	6	0.001632	D

Table A23. Initial ANOVA Table for Internal Bond

Source	DF	Adj SS	Adj MS	F-Value	P-Value
Model	9	0.168078	0.018675	15.44	0.000
Linear	4	0.128269	0.032067	26.5	0.000
Fiber	1	0.047041	0.047041	38.88	0.000
Resin	2	0.081083	0.040541	33.51	0.000
Board	1	0.000146	0.000146	0.12	0.731
2-Way Interaction	5	0.039809	0.007962	6.58	0.000
Fiber*Resin	2	0.033789	0.016895	13.96	0.000
Fiber*Board	1	0.00007	0.00007	0.06	0.811
Resin*Board	2	0.005949	0.002975	2.46	0.105
Error	26	0.031456	0.00121		
Lack-of-Fit	2	0.000438	0.000219	0.17	0.845
Pure Error	24	0.031019	0.001292		
Total	35	0.199535			

Table A24. Revised ANOVA Table for Internal Bond

Source	**DF**	**Adj SS**	**Adj MS**	**F-Value**	**P-Value**
Model	5	0.161913	0.032383	25.82	0.000
Linear	3	0.128123	0.042708	34.06	0.000
Fiber	1	0.047041	0.047041	37.51	0.000
Resin	2	0.081083	0.040541	32.33	0.000
2-Way Interaction	2	0.033789	0.016895	13.47	0.000
Fiber*Resin	2	0.033789	0.016895	13.47	0.000
Error	30	0.037622	0.001254		
Lack-of-Fit	6	0.006603	0.001101	0.85	0.544
Pure Error	24	0.031019	0.001292		
Total	35	0.199535			

Table A25. Tukey's Test Table for Direct Screw Withdrawal

Formulation Name	**Samples**	**Average Screw Withdrawal Load [N]**	**Grouping**
WheatMDI	10	648.6	A
WheatESSMDI	10	578.8	A
SoybeanMDI	10	445.6	B
SoybeanESSMDI	10	402.1	B
SoybeanESSANH	10	182.1	C
WheatESSANH	10	39.16	D

Table A26. Initial ANOVA Table for Direct Screw Withdrawal

Source	DF	Adj SS	Adj MS	F-Value	P-Value
Model	29	2929077	101003	17.77	0.000
Linear	8	1049157	131145	23.07	0.000
Board	3	41580	13860	2.44	0.084
Fiber	1	93339	93339	16.42	0.000
Resin	2	882791	441395	77.64	0.000
Edge or Center	1	45008	45008	7.92	0.009
Post Linear Expansion	1	1955	1955	0.34	0.562
2-Way Interaction	21	519065	24717	4.35	0.000
Board*Fiber	3	42456	14152	2.49	0.079
Board*Resin	6	30165	5028	0.88	0.518
Board*Post Linear Expansion	3	7837	2612	0.46	0.713
Fiber*Resin	2	348427	174214	30.64	0.000
Fiber*Edge or Center	1	30083	30083	5.29	0.029
Fiber*Post Linear Expansion	1	13820	13820	2.43	0.129
Resin*Edge or Center	2	11721	5861	1.03	0.369
Resin*Post Linear Expansion	2	9608	4804	0.85	0.440
Edge or Center*Post Linear Expansion	1	2665	2665	0.47	0.499
Error	30	170554	5685		
Lack-of-Fit	27	143648	5320	0.59	0.806
Pure Error	3	26906	8969		
Total	59	3099631			

Table A27. Revised ANOVA Table for Direct Screw Withdrawal

Source	DF	Adj SS	Adj MS	F-Value	P-Value
Model	9	2757499	306389	44.78	0.000
Linear	4	1485570	371393	54.28	0.000
Fiber	1	89641	89641	13.1	0.001
Resin	2	1346729	673365	98.41	0.000
Edge or Center	1	39681	39681	5.8	0.020
2-Way Interaction	5	413929	82786	12.1	0.000
Fiber*Resin	2	368295	184147	26.91	0.000
Fiber*Edge or Center	1	18844	18844	2.75	0.103
Resin*Edge or Center	2	19849	9924	1.45	0.244
Error	50	342133	6843		
Lack-of-Fit	47	315226	6707	0.75	0.726
Pure Error	3	26906	8969		
Total	59	3099631			

Table A28. Tukey's Test Table for Hardness Testing

Formulation Name	Samples	Average Screw Withdrawal Load [N]	Grouping
SoybeanMDI	8	3879	A
WheatESSMDI	8	3247	A
WheatMDI	8	2518	B
SoybeanESSMDI	8	2446	BC
SoybeanESSANH	8	1863	C
WheatESSANH	8	878	D

Table A29. Initial ANOVA Table for Hardness Testing

Source	DF	Adj SS	Adj MS	F-Value	P-Value
Model	14	47234094	3373864	24.15	0.000
Linear	5	34448673	6889735	49.32	0.000
Board	1	1171896	1171896	8.39	0.007
Fiber	1	3178756	3178756	22.75	0.000
Resin	2	30092160	15046080	107.7	0.000
Top or Bottom	1	5861	5861	0.04	0.839
2-Way Interaction	9	12785420	1420602	10.17	0.000
Board*Fiber	1	5590	5590	0.04	0.843
Board*Resin	2	1665963	832981	5.96	0.006
Board*Top or Bottom	1	143635	143635	1.03	0.318
Fiber*Resin	2	10669657	5334828	38.19	0.000
Fiber*Top or Bottom	1	297970	297970	2.13	0.154
Resin*Top or Bottom	2	2606	1303	0.01	0.991
Error	33	4610304	139706		
Lack-of-Fit	9	2361472	262386	2.8	0.021
Pure Error	24	2248832	93701		
Total	47	51844398			

Table A30. Revised ANOVA Table for Hardness Testing

Source	DF	Adj SS	Adj MS	F-Value	P-Value
Model	9	46784022	5198225	39.04	0.000
Linear	4	34442812	8610703	64.66	0.000
Board	1	1171896	1171896	8.8	0.005
Fiber	1	3178756	3178756	23.87	0.000
Resin	2	30092160	15046080	112.99	0.000
2-Way Interaction	5	12341209	2468242	18.53	0.000
Board*Fiber	1	5590	5590	0.04	0.839
Board*Resin	2	1665963	832981	6.26	0.004
Fiber*Resin	2	10669657	5334828	40.06	0.000
Error	38	5060376	133168		
Lack-of-Fit	14	2811544	200825	2.14	0.049
Pure Error	24	2248832	93701		
Total	47	51844398			

Table A31. Fiber Distribution and Viable Fraction for the 3/8” Screen and 5% Moisture Settings

Soybean – 26.9 m/s, 3/8" Screen, 4.62% Moist				**Wheat – 26.9 m/s, 3/8" Screen, 3.86% Moist**			
Mesh Size	**Average**	**Std. Dev**	**Viable Fraction**	**Mesh Size**	**Average**	**Std. Dev**	**Viable Fraction**
< 20 mesh	70.53%	0.0430		< 20 mesh	84.46%	0.0172	
21-40 mesh	21.33%	0.0256	**Average**	21-40 mesh	11.29%	0.0017	**Average**
41-60 mesh	5.16%	0.0121	27.94%	41-60 mesh	2.14%	0.0137	14.33%
61-80 mesh	1.45%	0.0032	**Std. Dev**	61-80 mesh	0.90%	0.0015	**Std. Dev**
> 80 mesh	1.53%	0.0047	0.0404	> 80 mesh	1.21%	0.0034	0.0149
Soybean – 35.9 m/s, 3/8" Screen, 4.62% Moist				**Wheat – 35.9 m/s, 3/8" Screen, 3.86% Moist**			
Mesh Size	**Average**	**Std. Dev**	**Viable Fraction**	**Mesh Size**	**Average**	**Std. Dev**	**Viable Fraction**
< 20 mesh	67.08%	0.0095		< 20 mesh	75.92%	0.0129	
21-40 mesh	23.96%	0.0114	**Average**	21-40 mesh	15.61%	0.0068	**Average**
41-60 mesh	5.11%	0.0007	30.67%	41-60 mesh	5.13%	0.0039	22.27%
61-80 mesh	1.60%	0.0019	**Std. Dev**	61-80 mesh	1.54%	0.0018	**Std. Dev**
> 80 mesh	2.25%	0.0043	0.0110	> 80 mesh	1.80%	0.0018	0.0115
Soybean – 44.9 m/s, 3/8" Screen, 4.62% Moist				**Wheat – 44.9 m/s, 3/8" Screen, 3.86% Moist**			
Mesh Size	**Average**	**Std. Dev**	**Viable Fraction**	**Mesh Size**	**Average**	**Std. Dev**	**Viable Fraction**
< 20 mesh	65.60%	0.0307		< 20 mesh	69.64%	0.0098	
21-40 mesh	25.14%	0.0110	**Average**	21-40 mesh	19.87%	0.0068	**Average**
41-60 mesh	5.94%	0.0090	32.62%	41-60 mesh	6.39%	0.0051	28.04%
61-80 mesh	1.55%	0.0055	**Std. Dev**	61-80 mesh	1.79%	0.0012	**Std. Dev**
> 80 mesh	1.78%	0.0059	0.0251	> 80 mesh	2.32%	0.0017	0.0094

Table A32. Fiber Distribution and Viable Fraction for the 1” Screen and 5% Moisture Settings

Soybean – 26.9 m/s, 1" Screen, 4.62% Moist				Wheat – 26.9 m/s, 1" Screen, 4.86% Moist			
Mesh Size	**Average**	**Std. Dev**	**Viable Fraction**	**Mesh Size**	**Average**	**Std. Dev**	**Viable Fraction**
< 20 mesh	86.55%	0.0433		< 20 mesh	92.07%	0.0157	
21-40 mesh	9.43%	0.0226	**Average**	21-40 mesh	5.34%	0.0085	**Average**
41-60 mesh	2.42%	0.0119	12.50%	41-60 mesh	1.51%	0.0045	7.37%
61-80 mesh	0.65%	0.0044	**Std. Dev**	61-80 mesh	0.52%	0.0012	**Std. Dev**
> 80 mesh	0.96%	0.0046	0.0389	> 80 mesh	0.56%	0.0019	0.0140
Soybean – 35.9 m/s, 1" Screen, 4.62% Moist				**Wheat – 35.9 m/s, 1" Screen, 4.86% Moist**			
Mesh Size	**Average**	**Std. Dev**	**Viable Fraction**	**Mesh Size**	**Average**	**Std. Dev**	**Viable Fraction**
< 20 mesh	83.32%	0.0222		< 20 mesh	89.85%	0.0422	
21-40 mesh	11.50%	0.0133	**Average**	21-40 mesh	7.63%	0.0239	**Average**
41-60 mesh	3.13%	0.0071	15.41%	41-60 mesh	1.72%	0.0107	9.75%
61-80 mesh	0.78%	0.0017	**Std. Dev**	61-80 mesh	0.40%	0.0040	**Std. Dev**
> 80 mesh	1.27%	0.0014	0.0220	> 80 mesh	0.40%	0.0039	0.0384
Soybean – 44.9 m/s, 1" Screen, 4.62% Moist				**Wheat – 44.9 m/s, 1" Screen, 4.86% Moist**			
Mesh Size	**Average**	**Std. Dev**	**Viable Fraction**	**Mesh Size**	**Average**	**Std. Dev**	**Viable Fraction**
< 20 mesh	82.70%	0.0097		< 20 mesh	88.99%	0.0301	
21-40 mesh	13.54%	0.0058	**Average**	21-40 mesh	8.25%	0.0230	**Average**
41-60 mesh	2.55%	0.0025	16.57%	41-60 mesh	1.98%	0.0046	10.65%
61-80 mesh	0.48%	0.0007	**Std. Dev**	61-80 mesh	0.42%	0.0015	**Std. Dev**
> 80 mesh	0.72%	0.0010	0.0089	> 80 mesh	0.36%	0.0014	0.0288

Table A33. Fiber Distribution and Viable Fraction for the 3/8” Screen and 15% Moisture Settings

Soybean – 26.9 m/s, 3/8" Screen, 16.35% Moist				**Wheat – 26.9 m/s, 3/8" Screen, 16.42% Moist**			
Mesh Size	**Average**	**Std. Dev**	**Viable Fraction**	**Mesh Size**	**Average**	**Std. Dev**	**Viable Fraction**
< 20 mesh	91.58%	0.0104		< 20 mesh	88.66%	0.0109	
21-40 mesh	5.86%	0.0041	**Average**	21-40 mesh	8.18%	0.0130	**Average**
41-60 mesh	1.47%	0.0032	7.76%	41-60 mesh	1.93%	0.0018	10.69%
61-80 mesh	0.44%	0.0014	**Std. Dev**	61-80 mesh	0.57%	0.0019	**Std. Dev**
> 80 mesh	0.66%	0.0030	0.0079	> 80 mesh	0.65%	0.0013	0.0119
Soybean – 35.9 m/s, 3/8" Screen, 16.35% Moist				**Wheat – 35.9 m/s, 3/8" Screen, 16.42% Moist**			
Mesh Size	**Average**	**Std. Dev**	**Viable Fraction**	**Mesh Size**	**Average**	**Std. Dev**	**Viable Fraction**
< 20 mesh	85.51%	0.0367		< 20 mesh	85.04%	0.0134	
21-40 mesh	9.91%	0.0244	**Average**	21-40 mesh	10.72%	0.0091	**Average**
41-60 mesh	2.52%	0.0079	13.18%	41-60 mesh	2.68%	0.0050	14.21%
61-80 mesh	0.76%	0.0025	**Std. Dev**	61-80 mesh	0.80%	0.0013	**Std. Dev**
> 80 mesh	1.31%	0.0022	0.0346	> 80 mesh	0.75%	0.0017	0.0117
Soybean – 44.9 m/s, 3/8" Screen, 16.35% Moist				**Wheat – 44.9 m/s, 3/8" Screen, 16.42% Moist**			
Mesh Size	**Average**	**Std. Dev**	**Viable Fraction**	**Mesh Size**	**Average**	**Std. Dev**	**Viable Fraction**
< 20 mesh	79.36%	0.0394		< 20 mesh	80.86%	0.0127	
21-40 mesh	13.47%	0.0116	**Average**	21-40 mesh	14.57%	0.0082	**Average**
41-60 mesh	3.92%	0.0129	18.63%	41-60 mesh	2.88%	0.0050	18.25%
61-80 mesh	1.24%	0.0050	**Std. Dev**	61-80 mesh	0.80%	0.0015	**Std. Dev**
> 80 mesh	2.02%	0.0102	0.0295	> 80 mesh	0.89%	0.0015	0.0112

Table A34. Fiber Distribution and Viable Fraction for the 1” Screen and 15% Moisture Settings

Soybean – 26.9 m/s, 1" Screen, 13.86% Moist				**Wheat – 26.9 m/s, 1" Screen, 16.51% Moist**			
Mesh Size	**Average**	**Std. Dev**	**Viable Fraction**	**Mesh Size**	**Average**	**Std. Dev**	**Viable Fraction**
< 20 mesh	93.39%	0.0102		< 20 mesh	94.93%	0.0126	
21-40 mesh	4.73%	0.0062	**Average**	21-40 mesh	3.88%	0.0098	**Average**
41-60 mesh	1.16%	0.0026	6.19%	41-60 mesh	0.71%	0.0016	4.77%
61-80 mesh	0.30%	0.0005	**Std. Dev**	61-80 mesh	0.18%	0.0006	**Std. Dev**
> 80 mesh	0.42%	0.0013	0.0090	> 80 mesh	0.30%	0.0012	0.0116
Soybean – 35.9 m/s, 1" Screen, 13.86% Moist				**Wheat – 35.9 m/s, 1" Screen, 16.51% Moist**			
Mesh Size	**Average**	**Std. Dev**	**Viable Fraction**	**Mesh Size**	**Average**	**Std. Dev**	**Viable Fraction**
< 20 mesh	93.22%	0.0117		< 20 mesh	88.52%	0.0297	
21-40 mesh	5.03%	0.0083	**Average**	21-40 mesh	8.21%	0.0136	**Average**
41-60 mesh	0.94%	0.0011	6.28%	41-60 mesh	2.01%	0.0106	10.72%
61-80 mesh	0.31%	0.0008	**Std. Dev**	61-80 mesh	0.49%	0.0029	**Std. Dev**
> 80 mesh	0.50%	0.0020	0.0101	> 80 mesh	0.77%	0.0029	0.0269
Soybean – 44.9 m/s, 1" Screen, 13.86% Moist				**Wheat – 44.9 m/s, 1" Screen, 16.51% Moist**			
Mesh Size	Average	Std. Dev	**Viable Fraction**	**Mesh Size**	**Average**	**Std. Dev**	**Viable Fraction**
< 20 mesh	90.34%	0.0042		< 20 mesh	83.24%	0.0415	
21-40 mesh	7.61%	0.0056	**Average**	21-40 mesh	11.71%	0.0207	**Average**
41-60 mesh	1.39%	0.0022	9.35%	41-60 mesh	2.96%	0.0108	15.50%
61-80 mesh	0.36%	0.0001	**Std. Dev**	61-80 mesh	0.83%	0.0039	**Std. Dev**
> 80 mesh	0.30%	0.0004	0.0043	> 80 mesh	1.27%	0.0062	0.0354

Table A35. Fiber Distribution and Viable Fraction for the 3/8” Screen and 25% Moisture Settings

Soybean – 26.9 m/s, 3/8" Screen, 26.04% Moist				**Wheat – 26.9 m/s, 3/8" Screen, 23.02% Moist**			
Mesh Size	**Average**	**Std. Dev**	**Viable Fraction**	**Mesh Size**	**Average**	**Std. Dev**	**Viable Fraction**
< 20 mesh	81.59%	0.0155		< 20 mesh	86.64%	0.0264	
21-40 mesh	9.86%	0.0127	**Average**	21-40 mesh	8.47%	0.0141	**Average**
41-60 mesh	4.16%	0.0022	16.03%	41-60 mesh	2.78%	0.0088	12.12%
61-80 mesh	2.00%	0.0020	**Std. Dev**	61-80 mesh	0.86%	0.0032	**Std. Dev**
> 80 mesh	2.38%	0.0005	0.0151	> 80 mesh	1.24%	0.0060	0.0218
Soybean – 35.9 m/s, 3/8" Screen, 26.04% Moist				**Wheat – 35.9 m/s, 3/8" Screen, 23.02% Moist**			
Mesh Size	**Average**	**Std. Dev**	**Viable Fraction**	**Mesh Size**	**Average**	**Std. Dev**	**Viable Fraction**
< 20 mesh	84.05%	0.0194		< 20 mesh	76.48%	0.0297	
21-40 mesh	8.64%	0.0056	**Average**	21-40 mesh	14.05%	0.0084	**Average**
41-60 mesh	3.62%	0.0084	13.84%	41-60 mesh	5.05%	0.0108	20.89%
61-80 mesh	1.58%	0.0033	**Std. Dev**	61-80 mesh	1.79%	0.0063	**Std. Dev**
> 80 mesh	2.11%	0.0044	0.00157	> 80 mesh	2.63%	0.0061	0.0237
Soybean – 44.9 m/s, 3/8" Screen, 26.04% Moist				**Wheat – 44.9 m/s, 3/8" Screen, 23.02% Moist**			
Mesh Size	**Average**	**Std. Dev**	**Viable Fraction**	**Mesh Size**	**Average**	**Std. Dev**	**Viable Fraction**
< 20 mesh	78.79%	0.0253		< 20 mesh	79.08%	0.0304	
21-40 mesh	13.44%	0.0075	**Average**	21-40 mesh	13.79%	0.0223	**Average**
41-60 mesh	4.38%	0.0093	19.14%	41-60 mesh	4.43%	0.0078	19.65%
61-80 mesh	1.32%	0.0018	**Std. Dev**	61-80 mesh	1.44%	0.0056	**Std. Dev**
> 80 mesh	2.06%	0.0075	0.0181	> 80 mesh	1.26%	0.0018	0.0289

Table A36. Fiber Distribution and Viable Fraction for the 1” Screen and 25% Moisture Settings

Soybean – 26.9 m/s, 1" Screen, 24.30% Moist				**Wheat – 26.9 m/s, 1" Screen, 24.65% Moist**			
Mesh Size	**Average**	**Std. Dev**	**Viable Fraction**	**Mesh Size**	**Average**	**Std. Dev**	**Viable Fraction**
< 20 mesh	90.95%	0.0260		< 20 mesh	92.52%	0.0115	
21-40 mesh	5.37%	0.0149	**Average**	21-40 mesh	5.04%	0.0089	**Average**
41-60 mesh	1.80%	0.0054	7.79%	41-60 mesh	1.38%	0.0016	6.83%
61-80 mesh	0.62%	0.0035	**Std. Dev**	61-80 mesh	0.41%	0.0006	**Std. Dev**
> 80 mesh	1.26%	0.0030	0.0237	> 80 mesh	0.65%	0.0010	0.0107
Soybean – 35.9 m/s, 1" Screen, 24.30% Moist				**Wheat – 35.9 m/s, 1" Screen, 24.65% Moist**			
Mesh Size	**Average**	**Std. Dev**	**Viable Fraction**	**Mesh Size**	**Average**	**Std. Dev**	**Viable Fraction**
< 20 mesh	94.75%	0.0032		< 20 mesh	90.96%	0.0291	
21-40 mesh	3.65%	0.0029	**Average**	21-40 mesh	5.24%	0.0188	**Average**
41-60 mesh	0.87%	0.0008	4.81%	41-60 mesh	2.20%	0.0056	8.10%
61-80 mesh	0.29%	0.0007	**Std. Dev**	61-80 mesh	0.66%	0.0005	**Std. Dev**
> 80 mesh	0.44%	0.0008	0.0036	> 80 mesh	0.94%	0.0058	0.0240
Soybean – 44.9 m/s, 1" Screen, 24.30% Moist				**Wheat – 44.9 m/s, 1" Screen, 24.65% Moist**			
Mesh Size	**Average**	**Std. Dev**	**Viable Fraction**	**Mesh Size**	**Average**	**Std. Dev**	**Viable Fraction**
< 20 mesh	93.10%	0.0060		< 20 mesh	82.97%	0.0045	
21-40 mesh	4.97%	0.0023	**Average**	21-40 mesh	10.42%	0.0085	**Average**
41-60 mesh	1.31%	0.0022	6.61%	41-60 mesh	3.34%	0.0014	14.98%
61-80 mesh	0.32%	0.0011	**Std. Dev**	61-80 mesh	1.23%	0.0019	**Std. Dev**
> 80 mesh	0.30%	0.0005	0.0055	> 80 mesh	2.05%	0.0011	0.0055

Table A37. ANOVA for Fines Content Factors

Source	DF	Adj SS	Adj MS	F-Value	P-Value
Model	35	0.005154	0.000147	10.31	0.000
Linear	6	0.002959	0.000493	34.52	0.000
Material	1	0.000042	0.000042	2.93	0.091
Screen Size	1	0.001978	0.001978	138.51	0.000
Moisture Content [%]	2	0.00074	0.00037	25.91	0.000
Hammer Tip Speed [m/s]	2	0.000198	0.000099	6.93	0.002
2-Way Interaction	13	0.000843	0.000065	4.54	0.000
Material*Screen Size	1	0.000167	0.000167	11.73	0.001
Material*Moisture Content [%]	2	0.000054	0.000027	1.88	0.160
Material*Hammer Tip Speed	2	0.00016	0.00008	5.61	0.005
Screen Size*Moisture Content [%]	2	0.000223	0.000112	7.81	0.001
Screen Size*Hammer Tip Speed [m/s]	2	0.000114	0.000057	3.99	0.023
Moisture Content [%]*Hammer Tip Speed	4	0.000125	0.000031	2.19	0.079
3-Way Interaction	12	0.001059	0.000088	6.18	0.000
Material*Screen Size*Moisture Content [%]	2	0.000315	0.000158	11.04	0.000
Material*Screen Size*Hammer Tip Speed [m/s]	2	0.000189	0.000095	6.63	0.002
Material*Moisture Content [%]*Hammer Tip Speed	4	0.000301	0.000075	5.28	0.001
Screen Size*Moisture Content [%]*Hammer Tip Speed [m/s]	4	0.000253	0.000063	4.43	0.003
4-Way Interaaction	4	0.000293	0.000073	5.13	0.001
Material*Screen Size*Moisture Content [%]	4	0.000293	0.000073	5.13	0.001
Error	72	0.001028	0.000014		
Total	107	0.006182			

Table A38. ANOVA for Viable Fraction Factors

Source	DF	Adj SS	Adj MS	F-Value	P-Value
Model	35	0.572847	0.016367	42.14	0.000
Linear	6	0.39129	0.065215	167.91	0.000
Material	1	0.002766	0.002766	7.12	0.009
Screen Size	1	0.110308	0.110308	284.01	0.000
Moisture Content [%]	2	0.219376	0.109688	282.41	0.000
Hammer Tip Speed [m/s]	2	0.05884	0.02942	75.75	0.000
2-Way Interaction	13	0.164735	0.012672	32.63	0.000
Material*Screen Size	1	0.005015	0.005015	12.91	0.001
Material*Moisture Content [%]	2	0.051962	0.025981	66.89	0.000
Material*Hammer Tip Speed	2	0.006172	0.003086	7.94	0.001
Screen Size*Moisture Content [%]	2	0.086931	0.043466	111.91	0.000
Screen Size*Hammer Tip Speed [m/s]	2	0.001901	0.000951	2.45	0.094
Moisture Content [%]*Hammer Tip Speed	4	0.012753	0.003188	8.21	0.000
3-Way Interaction	12	0.006485	0.00054	1.39	0.190
Material*Screen Size*Moisture Content [%]	2	0.00026	0.00013	0.33	0.717
Material*Screen Size*Hammer Tip Speed [m/s]	2	0.001318	0.000659	1.7	0.190
Material*Moisture Content [%]*Hammer Tip Speed	4	0.000602	0.00015	0.39	0.817
Screen Size*Moisture Content [%]*Hammer Tip Speed [m/s]	4	0.004305	0.001076	2.77	0.034
4-Way Interaaction	4	0.010337	0.002584	6.65	0.000
Material*Screen Size*Moisture Content [%]	4	0.010337	0.002584	6.65	0.000
Error	72	0.027965	0.000388		
Total	107	0.600812			

Table A39. ANOVA Table for Fines Content for Soybean

Source	DF	Adj SS	Adj MS	F-Value	P-Value
Model	17	0.002723	0.00016	9.32	0.000
Linear	5	0.002031	0.000406	23.64	0.000
Screen Size	1	0.001649	0.001649	95.92	0.000
Moisture Content [%]	2	0.000366	0.000183	10.65	0.000
Hammer Tip Speed [m/s]	2	0.000016	0.000008	0.48	0.623
2-Way Interaction	8	0.00064	0.00008	4.65	0.001
Screen Size*Moisture Content [%]	2	0.000119	0.00006	3.47	0.042
Screen Size*Hammer Tip Speed [%]	2	0.00017	0.000085	4.95	0.013
Moisture Content [%]*Hammer Tip Speed	4	0.00035	0.000088	5.09	0.002
3-Way Interaction	4	0.000052	0.000013	0.75	0.563
Screen Size*Moisture Content [%]*Hammer Tip Speed [m/s]	4	0.000052	0.000013	0.75	0.563
Error	36	0.000619	0.000017		
Total	53	0.003341			

Table A40. ANOVA Table for Viable Fraction for Soybean

Source	DF	Adj SS	Adj MS	F-Value	P-Value
Model	17	0.392772	0.023104	54.77	0.000
Linear	5	0.333574	0.066715	158.15	0.000
Screen Size	1	0.081182	0.081182	192.45	0.000
Moisture Content [%]	2	0.238307	0.119154	282.46	0.000
Hammer Tip Speed [m/s]	2	0.014085	0.007042	16.69	0.000
2-Way Interaction	8	0.057021	0.007128	16.9	0.000
Screen Size*Moisture Content [%]	2	0.045253	0.022626	53.64	0.000
Screen Size*Hammer Tip Speed [%]	2	0.003132	0.001566	3.71	0.034
Moisture Content [%]*Hammer Tip Speed	4	0.008637	0.002159	5.12	0.002
3-Way Interaction	4	0.002176	0.000544	1.29	0.292
Screen Size*Moisture Content [%]*Hammer Tip Speed [m/s]	4	0.002176	0.000544	1.29	0.292
Error	36	0.015186	0.000422		
Total	53	0.407958			

Table A41. ANOVA Table for Fines Content for Wheat

Source	DF	Adj SS	Adj MS	F-Value	P-Value
Model	17	0.00239	0.000141	12.35	0.000
Linear	5	0.001267	0.000253	22.27	0.000
Screen Size	1	0.000497	0.000497	43.71	0.000
Moisture Content [%]	2	0.000428	0.000214	18.79	0.000
Hammer Tip Speed [m/s]	2	0.000342	0.000171	15.02	0.000
2-Way Interaction	8	0.000629	0.000079	6.9	0.000
Screen Size*Moisture Content [%]	2	0.000419	0.00021	18.42	0.000
Screen Size*Hammer Tip Speed [%]	2	0.000133	0.000067	5.85	0.006
Moisture Content [%]*Hammer Tip Speed	4	0.000076	0.000019	1.67	0.178
3-Way Interaction	4	0.000494	0.000124	10.86	0.000
Screen Size*Moisture Content [%]*Hammer Tip Speed [m/s]	4	0.000494	0.000124	10.86	0.000
Error	36	0.00041	0.000011		
Total	53	0.002799			

Table A42. ANOVA Table for Viable Fraction for Wheat

Source	DF	Adj SS	Adj MS	F-Value	P-Value
Model	17	0.390665	0.02298	28.23	0.000
Linear	5	0.314451	0.06289	77.27	0.000
Screen Size	1	0.166221	0.166221	204.22	0.000
Moisture Content [%]	2	0.020986	0.010493	12.89	0.000
Hammer Tip Speed [m/s]	2	0.127245	0.063622	78.17	0.000
2-Way Interaction	8	0.047887	0.005986	7.35	0.000
Screen Size*Moisture Content [%]	2	0.036801	0.018401	22.61	0.000
Screen Size*Hammer Tip Speed [%]	2	0.009286	0.004643	5.7	0.007
Moisture Content [%]*Hammer Tip Speed	4	0.0018	0.00045	0.55	0.698
3-Way Interaction	4	0.028327	0.007082	8.7	0.000
Screen Size*Moisture Content [%]*Hammer Tip Speed [m/s]	4	0.028327	0.007082	8.7	0.000
Error	36	0.029302	0.000814		
Total	53	0.419967			